Use of Affimers for Targeting *S. aureus* Biofilms

Fayez Fahad Alsulaimani

Submitted in accordance with the requirements for the degree of

Doctor of Philosophy

The University of Leeds
School of Molecular and Cellular Biology
Faculty of Biological Sciences

January 2021

The candidate confirms that the work submitted is his own and that appropriate credit has been given where reference has been made to the work of others.

This copy has been supplied on the understanding that it is copyright material and that no quotation from the thesis may be published without proper acknowledgement.

The right of Fayez Fahad Alsulaimani to be identified as Author of this work has been asserted by him in accordance with the Copyright, Designs and Patents Act 1988.

© 2021 The University of Leeds and Fayez Alsulaimani

Acknowledgements

First of all I thank Almighty Allah for his blessing and guidance and grace that he gave me to enable me to get to this point and without his guidance I would not have been able to get this degree. I would also like to thank my family for their love and support throughout my PhD and for putting up with me. Special thanks goes to my wife Ghada Shawli and my son Fahad for their unconditional love and support. Additionally, I would like to thank my supervisor Professor Kenneth Mcdowall for his guidance and support as well as all the members of my supervisory team.

Abstract

Staphylococcus aureus is an important cause of infective endocarditis, which is an infection of the lining of the native or prosthetic heart valves. These infections can be debilitating, even life-threatening, and are often difficult to diagnose clinically. *S. aureus* grows on the surfaces of medical devices and natural tissues as a biofilm. Bacteria in biofilms can be difficult to eradicate as they are less susceptible to antibiotics. Thus, biofilms associated with medical devices or chronic infections often require surgical removal or debridement, respectively. Thus, it would be clinically advantageous to be able to not only detect the presence of bacteria when a patient presents with clear signs of infection, but also to determine the source by a non-invasive method. Affimers were successfully raised against *S. aureus* strains SH1000, USA300 and UAMS-1 biofilms using phage display. Affimers are artificial proteins that can be used for targeting. Eleven Affimers were tested for *S. aureus* biofilm binding, two Affimers showed significant binding to *S. aureus* biofilm formed by strains SH1000, USA300 and UAMS-1. Affimers were also raised against *S. aureus* Proteins A and Clumping factor A, Affimer against Protein A was found to bind Protein A with K_D of 118 nM. Affimers against raised here have the potential to be incorporated with microbubbles to be used for imaging and detection of biofilms in Infective endocarditis.

Table of Contents

List of Tables

List of Figures

List of Abbreviations

aa	Amino Acid
Amp	Ampicillin
BAI	Biofilm associated infection
BSA	Bovine serum albumin
Carb	Carbenicillin
DMSO	dimethyl sulfoxide
EDTA	ethylene diamine tetra acetic acid
ELISA	Enzyme-linked immunosorbent assay
HRP	Horseradish peroxidase
IPTG	isopropyl β-D-1-thiogalactopyranoside
Kan	Kanamycin
LB	Luria Broth
Min	minute
Ni-NTA	nickel-nitrilotriacitic acid
ORF	Open reading frame
PCR	polymerase chain reaction
PEG	polyethylene glycol
PBS	Phosphate buffered saline
PBST	Phosphate buffered saline with Tween
RPM	revolution per minute
SDS	Sodium dodecyl sulphate
SDS-PAGE	sodium dodecyl sulphate polyacrylamide gel electrophoresis
Sec	seconds
SOC	super optimal broth with catabolite repression
TBE	Tris/borate/EDTA
TCEP	Tris (2-carboxyethyl)phosphine

TE	Tris-EDTA buffer
TEMED	N,N,N',N'-tetramethylethane-1,2-diamine
TMB	3,3’,5,5’-tetramethylbenzidine
Tris	tris(hydroxymethyl)aminomethane
Triton	4-(1,1,3,3-tetramethylbutyl)phenyl-polyethylene glycol

Chapter 1: Introduction

1.1 Overview of *Staphylococcus aureus* infection

Bacterial cells can colonise biological and non-biological surfaces by forming a complex community of cells, encased in a self-produced matrix, called a biofilm (Hall-Stoodley et al., 2012, Otto, 2018). Biofilm formation is a major contributor to the complications associated with chronic infections (Etter et al., 2020, Lister and Horswill, 2014). The spread of chronic infections, due to biofilm formation, is an ever-growing threat to humans especially among hospitalised patients, often resulting in prolonged hospitalisations and persistent infections (Reddy et al., 2017). Biofilm formation adds to the threat of chronic infections by providing infectious pathogens with a large armoury of virulence factors, such as enzymes, toxins, and adhesins, and can convey tolerance to antibiotics and resistance to phagocytosis, enabling the microbial population within the biofilm to survive in the host environment (Foster et al., 2014, Kong et al., 2018).

The most common nosocomial biofilm infections result from the colonisation of indwelling medical devices, such as catheters, prosthetic joints, and heart valves (Hall-Stoodley et al., 2004, Otto, 2013). *Staphylococcus aureus* is the most common pathogen associated with the colonisation of medical devices in hospitalised patients (Baddour et al., 2015). *S. aureus* is a Gram-positive bacterial species that normally belongs to the population of flora colonising the skin and nasal mucosal cavities in humans (Pendleton and Kocher, 2015). Approximately one-third of the nasal mucosal surfaces in the human population are thought to be colonised by *S. aureus* suggesting a strong correlation between the nasal carriage of *S. aureus* and the spread of infection (Tong et al., 2015). *S. aureus* is the leading cause of a variety of diseases, ranging from minor skin and soft tissue infections to life-threatening illnesses, such as endocarditis, bacteraemia, and osteomyelitis. Under normal conditions, *S. aureus* is a commensal organism; however, it can also act as

an opportunistic pathogen under conditions during which the skin or mucosal surfaces are damaged, thereby allowing *S. aureus* to cross the epithelial barrier and enter the bloodstream, causing life-threatening complications associated with pre-existing conditions (Murray, 2005). The high virulence and pathogenicity of *S. aureus* can be attributed to several factors including the development of antibiotic resistance and biofilm formation (Chatterjee et al., 2013). According to a recent study performed by (Neopane et al., 2018), examining *S. aureus* isolated from hospitalised patients, 70% of the tested isolates were biofilm-forming and exhibited much higher antibiotic resistance than non-biofilm-forming isolates. Furthermore, 86% of the biofilm-forming isolates were also multidrug-resistant (MDR), and 43% of them were methicillin-resistant *S. aureus* (MRSA) (Neopane et al., 2018), which suggests the presence of a direct relationship between biofilm formation and antibiotic resistance. The increasing number of cases in which the identified *S. aureus* isolates were MDR or MRSA is alarming and suggests that a necessity for closely monitoring the spreading of biofilm-forming isolates of *S. aureus*. Additionally, the presence of biofilms in chronic wounds has been extensively described and has been shown to be a factor associated with reduced healing rates (Hall-Stoodley et al., 2004). *S. aureus* is metabolically versatile, able to switch between aerobic and anaerobic respiration, depending on environmental oxygen concentrations during infection (Masalha et al., 2001).

An increase in the development of antibiotic resistant *S. aureus* strains has been reported over the last two decades, most notably MRSA and vancomycin-resistant *S. aureus* (VRSA) (Kirmusaolu, 2017, Mah and O'Toole, 2001). Hospital-acquired infections involving MRSA are associated with approximately 300 deaths each year in the UK. Although the number of deaths has gradually decreased in recent years, MRSA infections still account for 0.1% of all deaths and 0.2% of all hospital-related deaths, according to the most recent available data from the Office for National Statistics.

More importantly, the ability of *S. aureus* to form biofilms in the host can lead to complications, which become even more severe when caused by a resistant strain. Initially, planktonic bacteria can adhere to a surface and form

biofilms by utilising host proteins (Lister and Horswill, 2014a). For example, during infective endocarditis (IE), *S. aureus* binds to fibrinogen and other host-derived proteins that form a coating on implanted heart valves (Parsek and Fuqua, 2004). Moreover, biofilm formations are not confined to solid surfaces, as *P. aeruginosa* planktonic cells can form biofilms by aggregating around mucus within the airways of the lungs in cystic fibrosis patients (Archer et al., 2011, Otto, 2018).

1.2 Methicillin-resistant *S. aureus*

As indicated earlier, one of the major challenges associated with *S. aureus* infections is the increasing emergence of antibiotic-resistant *S. aureus* strains, such as MRSA and VRSA, among hospitalised patients (Johnson, 2011). According to a study by Hidron et al., (2008) MRSA is the most common pathogen associated with nosocomial infections of medical devices and bloodstream infections (Hidron et al., 2008). Infections involving MRSA strains have been associated with approximately 300 deaths each year (Johnson, 2011). Although the number of deaths has gradually decreased in recent years, MRSA infections still account for 0.1% of all deaths, and 0.2% of all hospital deaths in the UK, according to the most recent available data from the Office for National Statistics (ONS, 2013).

The introduction of antibiotics in clinical settings has resulted in the emergence of antibiotic resistance, such as penicillin-resistant *S. aureus*, which was first reported in 1942 (Rammelkamp and Maxon, 1942, Stryjewski and Corey, 2014). Subsequently, methicillin, a derivative of penicillin, was introduced in 1959 and used to treat penicillin-resistant *S. aureus* infections. However, *S. aureus* quickly developed resistance to methicillin, as the first case of MRSA was documented in 1961 (Jevons, 1961, Stryjewski and Corey, 2014). MRSA presents acquired resistance to the β-lactam class of antimicrobials, through the horizontal acquisition of the *mecA* gene, encoding penicillin-binding protein 2a (PBP2a), which has a low binding affinity for β-lactam antibiotics, enabling the activity of transpeptidase in the presence of the β-lactam antibiotics (Stryjewski and Corey, 2014). Due to the emergence

of antibiotic resistance, controlling and treating MRSA is difficult. As indicated earlier, MRSA infections can complicate minor infections, resulting in life-threatening diseases (Lister and Horswill, 2014b); minor diseases and infections caused by MRSA include staphylococcal-scalded skin syndrome, central nervous system infections, osteomyelitis, pneumonia and urinary tract infections; life-threatening diseases and infections caused by MRSA include endocarditis, chronic lung infections associated with cystic fibrosis, and toxic shock syndrome (Gill et al., 2005).

One of the major challenges in clinical practice is distinguishing between biofilm-associated infections (BAI) and acute infections, caused by circulating planktonic cells. Establishing clinically relevant criteria is essential for guiding clinicians to better diagnoses (Parsek and Singh, 2003) because microorganisms within surface-attached biofilms can be difficult to distinguish from planktonic cells when using currently available tests (Eggleston and Panizzi, 2014). Blood cultures are usually the first step during diagnosis, but these may be unreliable due to their inability to distinguish between planktonic cells and cells sloughed/detached from biofilms (Donlan, 2002). The presence of a biofilm often results in recurrent chronic infections, which should signal the presence of a biofilm to the clinician; however, recurrent infections are not direct evidence of a BAI (Hall-Stoodley et al., 2012a). Better diagnostic methods are necessary to allow clinicians to specifically identify the presence of a biofilm.

1.3 Introduction to bacterial biofilms

The ability of many bacteria to form biofilms has been frequently documented, and 99% of all bacteria are hypothesised to be found in nature as biofilms (Donlan and Costerton, 2002). Historically, biofilms have been found and reported on different biotic and abiotic surfaces including the lining of the lungs, heart valves and teeth as well as industrial water systems, deep ocean hydrothermal vents, and early fossils (Hall-Stoodley et al., 2004, Reysenbach and Cady, 2001, Taylor et al., 1999). The first reported observation of biofilm formation was associated with dental plaques, as noted by the Dutch scientist

Antonie van Leeuwenhoek, in 1684. The term “biofilm” was first used by Costerton in 1978 to describe the accumulation of sessile bacteria (Costerton et al., 1978). Planktonic cells are phenotypically different from cells within a biofilm, and the ability of bacteria to grow as biofilms represents an evolutionary adaptation to the environment, providing homeostasis in response to extreme changes in different environments, such as changes in temperature, pH, and nutrient availability (Davey and O'Toole G, 2000).

Biofilm formation provides several advantages to bacteria that enable the bacteria to prolong their survival in the host, such as protection from the host immune system and tolerance against antimicrobials (Otto, 2013). Biofilms also protect bacteria from being dislodged by shear forces and osmotic pressure (Otto, 2013). Biofilms are commonly implicated in many chronic infections, including urinary tract infections, IE, chronic wound infections, cystic fibrosis, and musculoskeletal infections (Bjarnsholt, 2013, Brouqui and Raoult, 2001, Gristina et al., 1985, Hall-Stoodley and Stoodley, 2009, Hall-Stoodley et al., 2012b). Furthermore, biofilms account for approximately 80% of all bacterial infections; despite this, the majority of methods utilised to study bacterial infections advocate experimentation using planktonic cultures (Del Pozo and Patel, 2007, Sharma et al., 2019).

1.3.1 Overview of *S. aureus* biofilm formation and structure

S. aureus biofilm formation is a progressive process that develops through five-stages. Attachment is divided into two stages, initial attachment and irreversible attachment, followed by two maturation stages, maturation I and maturation II, and finally dispersal (Monroe, 2007, Pinto et al., 2019). These steps are not restricted to *S. aureus*, as other bacteria share overall the same biofilm formation steps; however, the genetic factors involved may differ (Monroe, 2007, Pinto et al., 2019).

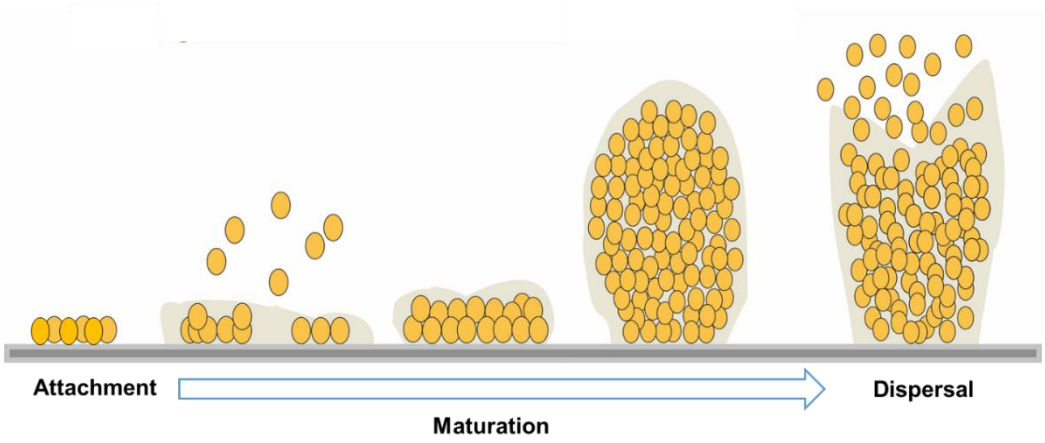

Figure 1.1 Biofilm formation stages. Attachment, planktonic cells attach to biotic or abiotic surfaces through interactions with host proteins or electrostatic forces. Maturation, attached bacteria colonise the surface by multiply, forming microcolonies, which results in the production of extracellular polysaccharides (EPS), leading to the stability of the biofilm. Biofilm Dispersal, once a certain cell density is reached, the cells become dislodged from the biofilm. Dislodged cells will then revert to the planktonic cell phenotype, to colonise other surfaces. Adapted from (Monroe, 2007).

1.3.2 Attachment

S. aureus colonisation of the host surface is influenced by several factors, including pH, surface tension, and host plasma components (Foster and Hook, 1998). *S. aureus* planktonic cells can adhere to abiotic and biotic surfaces; attachments to abiotic surfaces is usually dependent on hydrophobic and electrostatic interactions (Moormeier and Bayles, 2017), whereas attachments to biotic surfaces, such as skin and tissue, is primarily dependent on cell-to-cell interactions and the interaction of cells with host plasma proteins, including fibrinogen, fibronectin, collagen, vitronectin, or laminin (Mazmanian et al., 2001, Moormeier and Bayles, 2017, Otto, 2013). During infections, interactions with host proteins are facilitated by a specific group of cell-wall proteins, known as the microbial surface components recognising adhesive matrix molecules (MSCRAMMs) (Moormeier and Bayles, 2017). The MSCRAMMs are a family of proteins that are covalently anchored to peptidoglycans in the *S. aureus* cell wall (Mazmanian et al., 2001). These MSCRAMMs share a common secretion-dependent targeting motif referred to

as LPXTG (Leu-Pro-X-Thr-Gly), where X refers to any amino acid (Foster et al., 2014b)(Figure 1.2X). Some of the most well-described MSCRAMMs include: fibronectin-binding proteins (FnBPA and FnBPB) (O'Neill et al., 2008), iron-regulated surface determinants (IsdA, IsdB, IsdC, and IsdH) (Dryla et al., 2003, Morikawa et al., 2003), serine-aspartate repeat family proteins (SdrC, SdrD, and SdrE) (Corrigan et al., 2009), the clumping factors (ClfA and ClfB) (O'Brien et al., 2002, Zhu et al., 2019), collagen adhesin (Madani et al., 2017), and Protein A (SpA) (Zhu et al., 2019).

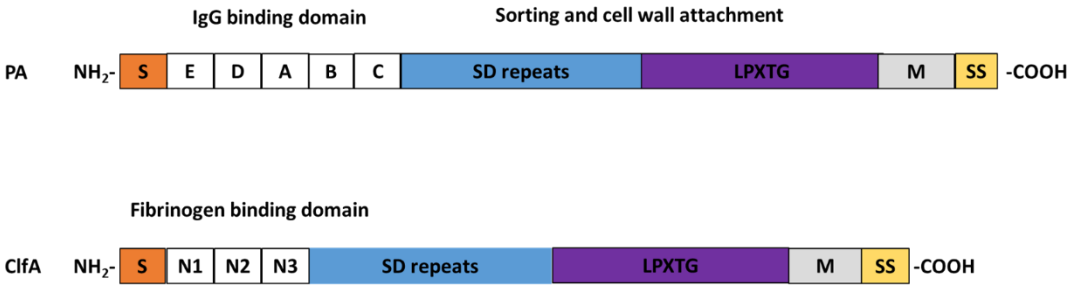

Figure 1.2 Schematic representation of SpA and ClfA binding domain. SpA and CLFA Both SpA and ClfA share structural similarity as they both have a Secretion signal sequence (S) at the *N*-terminal end and LPXTG motif at the sorting signal (SS) at the C-terminal end. They also consist of membrane anchor (M) and serine-aspartate (SD) repeats that links the *N*-terminal to the C-terminal. SpA has five conserved IgG binding domains E, D, A, B, C and ClfA consists of three conserved subdomains N1, N2, N3 located at the *N*-terminal. Figure adapted from (Foster et al., 2014).

The MSCRAMMs bind host components with different affinities; however, some share binding specificity against the same host components, such as ClfA, fnbA, and fnbB, which all bind fibrinogen and platelets (Foster et al., 2013). Although the primary functions of MSCRAMMs are to facilitate binding with host proteins and to trigger biofilm formation, some MSCRAMMs also play double roles in the pathogenicity of *S. aureus,* such as PA and ClfA, which interact with components of the host immune system, such as IgG and platelets, respectively (Foster et al., 2014b, Moormeier and Bayles, 2017). The utilisation of MSCRAMMs is not restricted to *S. aureus*, as other Gram-positive bacteria, such as *S. epidermis* (Arrecubieta et al., 2007), coagulase-negative staphylococci (Ponnuraj et al., 2003), and enterococci (Rich et al., 1999), also initiate biofilm formation through MSCRAMM-mediated attachments (Foster et al., 2014b, Moormeier, 2017). At this stage, attachment is not finalised, and cells can easily return to a planktonic cell state when faced

with conditions that favour growth in the planktonic state, such as nutrient availability (Wu and Outten, 2009).

In cases such as IE, in which the blood flow through the heart is strong, cells can be dislodged by hydrodynamic forces (Dunne, 2002, Goller and Seed, 2010). After the initial attachment and adherence of *S. aureus* cells to the surface, the cells begin to multiply and accumulate (Moormeier and Bayles, 2017). However, during this multiplication phase, the adhered cells are still vulnerable to removal, and the irreversible attachment to a surface relies on the ability of the bacteria to withstand shear forces to remain attached to the surface (Kostakioti et al., 2013, Moormeier and Bayles, 2017). To sustain the growth of the biofilm, *S. aureus* produces several stabilisers that strengthen the cell-to-cell interaction and promote intracellular binding (Moormeier and Bayles, 2017) . Amongst these stabilisers SpA and ClfA are the most characterised because of the multiple functions they contribute to biofilm formation, which include the promotion of cell accumulation and protection against host immune system (Speziale et al., 2014).

1.4.2.1 Protein A

SpA is a 42-kDa MSCRAMMs that is anchored to the cell wall of *S. aureus* cell wall. It is expressed by most if not all *S. aureus* isolates and some strains of *S. epidermidis* (Foster et al., 2014a, Silverman, 2001). SpA plays an important role in *S. aureus* virulence by interfering with the host immune system by binding IgG and preventing opsonisation or TNFR-1 receptor 1 causing release of cytokines and by promoting biofilm formation through attachment and aggregation by cell-cell interaction or binding to surfaces coated with Von Willebrand Factor (vWF) (Falugi et al., 2013) (Figure 1.3). SpA has five homologous immunoglobulin binding domains located at its *N*-terminus (Speziale et al., 2014).

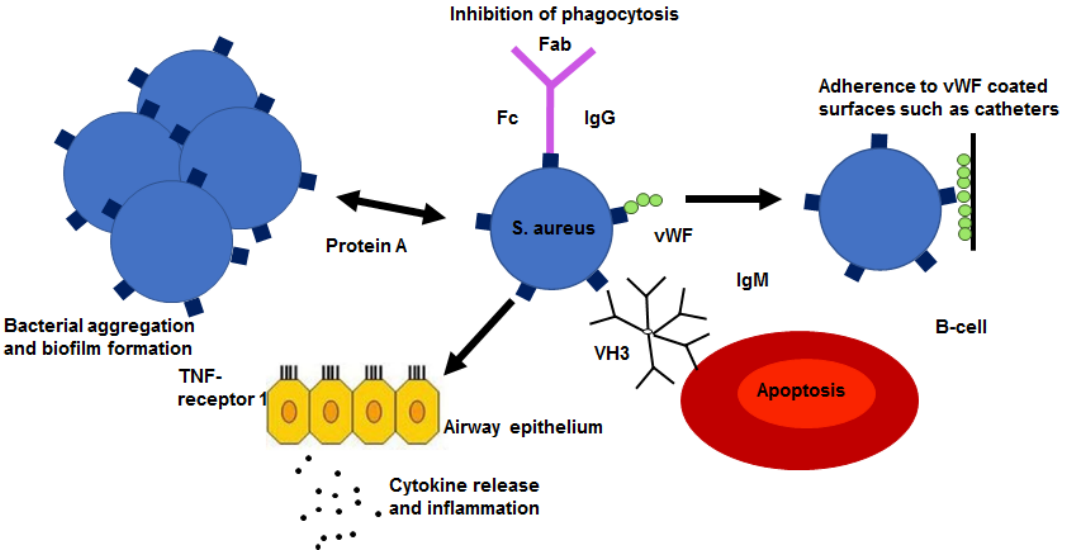

Figure 1.3 Schematic representation highlighting the multiple functions of *S. aureus* SpA function. SpA is involved in cytokine release via binding to tumour necrosis factor (TNF) receptor 1. SpA binds the fragment crystallizable region (FC region) of IgG to prevent phagocytosis. SpA attaches to surfaces by binding to vWF. SpA binds human Fab heavy chain (V_H3) region of antibodies expressed/bound on B-cells antigen receptor causing apoptosis. Clumps formed by cell-cell aggregation that causes accumulation and biofilm formation.

As mentioned previously, along with other MSCRAMMs, SpA facilitates adherence to surfaces by binding to host proteins such as vWF (Figure 1.3) (Falugi et al., 2013). Once the cells are attached to a surface via SpA or other MSCRAMMs, SpA promotes cell-cell adhesion causing *S. aureus* planktonic cells to aggregate to the surface (Gomez et al., 2004). As the cells are adhering in clumps to the surface, the cells already attached start production of polysaccharide intracellular adhesin (PIA) encoded within the *ica* operon (Cramton et al., 1999). This allows the cells to remain adhered to the surface and the formation of layer of cells that result in a mature biofilm.

Furthermore, SpA also plays an important role in evasion of the host immune system that results in failure of the host to develop an adaptive immune response, which leads to recurrent infections by *S. aureus* (Falugi et al., 2013). Due to its ability to affect the host immune response, SpA is considered to the have properties of a B-cell superantigen (Silverman and Goodyear,

2002). Furthermore, SpA binds the Fc region of IgG resulting in inhibition of phagocytosis by preverting opsonisation by phagocytic cells (Silverman and Goodyear, 2002). Also, SpA is able to interact with B cells via the V_H3 region of Fab of both IgG and IgM by forming a complex with Fab (Silverman and Goodyear, 2002). By binding the Fragment crystallizable (Fc) or Fragment antigen binding (Fab) fragments of antibodies, SpA prevents complement binding or interaction with cell receptors (Yang et al., 2003). In addition, SpA induces cytokine release by binding to TNFR1 receptor resulting in inflammation (Gomez et al., 2006) causing release of cytokines resulting in inflammation in the lungs and other tissue, which has been seen in cases of Staphylococcal pneumonia (Falugi et al., 2013).

1.4.2.1 Clumping Factor A

ClfA is a 52-kDa protein that is part of the MSCRAMMs group of cell wall anchored proteins expressed in *S. aureus* (Figure 1.2). Similar to SpA, ClfA contributes to the virulence of *S. aureus* in several ways such as delayed wound healing and biofilm formation (Foster and Hook, 1998). It is a well-known fact that *S. aureus* can form clumps in blood through several mechanisms one of which is interacting with fibrinogen via clumping factor A (Crosby et al., 2016). Fibrinogen which is found in blood plasma, plays a crucial role in wound healing and blood coagulation (Crosby et al., 2016). When fibrinogen is processed to fibrin that forms a fibrous clot that is connected together by crosslinking via clotting transglutaminase factor XIIIa (Crosby et al., 2016). *S. aureus* interacts directly with fibrinogen allowing the formation of a fibrous clot with attached cell causing clumping (Crosby et al., 2016). The main function of ClfA is binding fibrinogen, which serves as a bridging molecule to bind platelets. ClfA consists of a fibrinogen-binding domain which binds the C-terminus of fibrinogens γ-chain (Speziale et al., 2014b). In vascular injury, platelets attach to damaged surfaces and release substances that promote rapid wound healing by aggregating and adhering to a surface and forming a fibrin clot (Jung et al., 2012). Some studies also suggest that ClfA can bind platelets directly via platelet binding domain (Siboo et al., 2001). The ability to bind platelets leads to delayed wound healing resulting in complications and chronic infection by *S. aureus* (Jung et al.,

2012). This ability of ClfA to induce aggregation of platelets and binding to fibrinogen is not only used to interfere with wound healing but also contributes to biofilm formation and stability. Binding of host components facilitates the initial attachment to surfaces such as native or prosthetic heart valves in cases of IE during infection (Foster and Hook, 1998, Siboo et al., 2001). Aggregation of platelets is important for biofilm stability in which the fibrin clot formation is mixed with the polysaccharide matrix produced during biofilm formation and acts as a bridge that promotes stability between the microcolonies within the biofilm. Another important stabiliser is polysaccharide intercellular adhesin (PIA), also referred to as polymeric *N*-acetyl-glucosamine (PNAG), which is produced by the *icaADBC* operon (Foster et al., 2014b). The *icaADBC* locus is commonly found in *Staphylococcal spp.* (Namvar et al., 2013). Depending on the composition of the extracellular matrix (ECM), *S. aureus* biofilm formation can be classified as *ica*-dependent or *ica*-independent biofilm formation (Arciola et al., 2015). The *ica*-independent biofilm formation relies mostly on attachment by production of cell wall proteins (Arciola et al., 2015). Furthermore, a strong correlation between *ica*-independent biofilm formation and MRSA isolates has been noted (O'Neill et al., 2008). During *ica*-dependent biofilm formation, PIA is the primary component of the ECM, and the formed biofilms are generally more stable (Arciola et al., 2015).

1.3.3 Biofilm maturation and dispersal

As microcolonies grow, bacterial cells begin producing the ECM that forms the essential scaffold necessary to establish the three-dimensional architecture of biofilms (Moormeier and Bayles, 2017). The establishment of the ECM results in the formation of water channels, which allow the transport of nutrients and waste into and out of the biofilm (Otto, 2013). Biofilm structures can differ between species; however, the encapsulation of cells within the ECM is a shared feature among biofilms (Davey and O'Toole, 2000, Hall-Stoodley et al., 2004). The biofilm ECM is primarily composed of extracellular polysaccharides (EPS) but also contains proteins, lipids, extracellular DNA (eDNA), RNA, and nutrients (Dufour et al., 2010). EPS is the major component of the biofilm ECM, composing up to 80%–85% of the structure, whereas the cells make up the remaining 15%–20% (Dufour et al., 2010). The genomic

DNA released into the matrix, as a result of *S. aureus* programmed cell death (PCD), serves as an adhesin that holds the cells together with in the biofilm (Otto, 2013). Evidence suggests that the presence of eDNA in the matrix is a common feature among biofilms formed by several bacterial species, including *Pseudomonas aeruginosa, S. epidermidis* (Montanaro et al., 2011). *S. aureus* strains that do not possess the *ica* operon tend to rely on eDNA binding along with MSCRAMMs in biofilm stability (Montanaro et al., 2011).

Most biofilm research has focused on attachment and maturation, and only recently have any major contribution to biofilm dispersal mechanisms been described. Biofilm formation and dispersal in bacteria is regulated by quorum sensing (QS), which is a cell density driven response system to regulate gene expression by the release of auto-inducing molecules (Moormeier and Bayles, 2017). In *S. aureus*, QS is regulated by the *agr* operon, which regulates the secretion of auto-inducing peptide (AIP) (Figure 1.4) (Boles and Horswill, 2008). Upon reaching a specific cell density as determined by the accumulation of AIP, the cells switch to a planktonic phenotype and degradation of the ECM is initiated; ECM degradation is achieved through inducing the secretion of proteases, such as δ-haemolysin (hlD) (Otto, 2013). In addition, the expression of the *agr* operon results in the inhibition of production of cell-wall proteins involved in attachment such as SpA (Novick and Geisinger, 2008b). This results in the release of cells embedded within the biofilm, thereby allowing colonisation of other sites (Figure 1.4) (Moormeier and Bayles, 2017). Additionally, the *agr* operon mediates biofilm dispersal by regulating the production of phenol-soluble modulins (PSM), which act as surfactants and disrupt the interaction between the matrix and cell (Peschel and Otto, 2013). Although several studies have linked the production of PSM to biofilm dispersal, other studies suggest that PSM may also play a role in stabilising the biofilm structure (Schwartz et al., 2012).

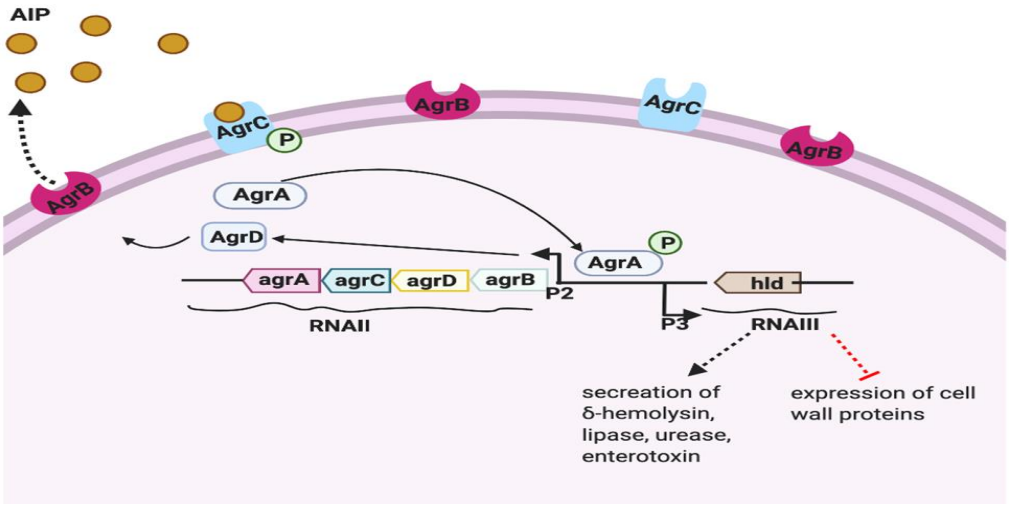

Figure 1.4 Mechanism of *agr* regulation of Quorum sensing in *S. aureus*. *S. aureus* biofilms reach maturation, the agr QS system induces production of AIP which is initiated by the transcription of agrD gene through the P2 promoter. AIP is then excreted outside the cell though AgrB and binds AgrC, which is the surface membrane histidine kinase that activates AgrA, the response regulator protein, by phosphorylation. Phosphorylated AgrA then activates the P2 and P3 promoters, activation of the P3 promotors results in the transcription of RNAIII, which regulates the production of ECM-degrading molecules such as δ-hemolysin, which is encoded by hld, which also down regulates the expression cell wall proteins involved in attachment. Figure adapted from (Novick and Geisinger, 2008a).

1.3.4 Biofilms provide tolerance against antibiotics

As described in Section 1.3, the severity of biofilm associated infections is intensified due to the ineffectiveness of antimicrobials against *S. aureus* biofilms. Antibiotics that are active against growing planktonic bacteria tend to be less effective against bacteria within biofilms (Mah and O'Toole, 2001), as current antibiotics tend to target processes required for cell growth. For example, penicillin and vancomycin inhibit cell wall synthesis, whereas gentamicin and tobramycin inhibit protein synthesis (Garrison et al., 2015). Biofilms provide antibiotic tolerance through several mechanisms, which contribute to treatment difficulties (Mah and O'Toole, 2001). Antibiotic tolerance, which is the result of a microorganism entering a dormant state, should not be confused with resistance, which results from a mutation or the acquisition of a resistance gene (e.g., *mecA*), through horizontal gene transfer (Lewis, 2007). The effectiveness of antimicrobials is also dependent on the position of the bacterial cells within the biofilm layers, as cells closer to the

ECM surface are more affected than cells deeper within the ECM. Biofilms both limit the diffusion of antimicrobials and cells at the centre grow more slowly, due to limits on the diffusion of nutrients, O_2, and CO_2 (Mah and O'Toole, 2001).

In addition, biofilms contain a population of non-proliferating small-colony cell variants, known as persister cells, which are in a state of dormancy (Lewis, 2007). Bacterial persistence results from variations in the cellular growth rates among the biofilm bacterial populations (Gerdes and Maisonneuve, 2012). Persistence has been defined by Gerdes as “a phenomenon that causes bacterial cells to tolerate multiple antibiotics and other environmental insults” by slowing their metabolic processes (Gerdes and Maisonneuve, 2012). Persister cells are generated by conditions that lead to the discontinuance of growth, such as stationary phases, biofilm formation, and nutrient limitations in response to stress (Balaban et al., 2004). Furthermore, the involvement of ubiquitous genetic elements, such as toxin-antitoxin (TA) systems, have been implicated during persistence (Balaban et al., 2004). TA systems are comprised of closely related genes that encode a stable protein or ‘toxin’, which inhibits cell growth, and a labile antitoxin, which regulates toxin activity (Maisonneuve and Gerdes, 2014).

1.3.5 Biofilms protect against the host immune system

Avoiding interaction with the host immune system is an important mechanism used by *S. aureus* and other organisms to ensure the continuation of infection. Biofilm formation allows *S. aureus* to fully utilise many virulence factors that protect against the host immune system. Among these virulence factors is the ECM, which acts as a physical barrier preventing access to the cells and protects against phagocytosis by polymorphic neutrophils (PMNs), through the production of PIA and toxins (Martinez and Casadevall, 2005, Tashiro et al., 2008). The ability of the ECM to provide protection against the host immune system is not limited to the fact that it acts as a physical barrier but also due to the presence of surface proteins.

1.4 Medical importance and impact of infective endocarditis

According to the National Health Service (NHS) UK, IE is characterised as the infection of the endocardium, which comprises the inner lining of the heart chambers and valves (NHS, 2019). IE affects approximately 1 in 30,000 people per year, with increasing incidence and mortality rates as high as 30% during the first year of infection (Liu et al., 2011). Biofilms can render antibiotic treatments ineffective, necessitating surgical interventions to replace the heart valve, prolonging hospitalisation, increasing the risk of recurrent infections, and straining resources (Reddy et al., 2017) (Liu et al., 2011). IE is potentially fatal when left untreated, due to complications including heart murmurs, low red blood cell counts, and valve blockages, which can lead to heart failure or a stroke, due to the disruption of blood flow from the heart (Fernandez Guerrero et al., 2009). IE occurs primarily in patients with damaged or prosthetic heart valves or who have undergone valve replacement surgery and in patients with congenital heart disease or hypertrophic cardiomyopathy (Prendergast, 2004). Paradoxically, endocarditis rates are increasing due to advances in medical care (Prendergast, 2004). According to the NHS, one reason for the increased incidence of IE in the UK is the increased number of patients that undergo valve repair or replacement surgery or surgery to repair congenital heart disease (NHS, 2019). A total of 15%–25% of IE patients are estimated to require surgery to repair or replace a damaged heart valve (NHS, 2019). Even after surgery, the risk of acquiring another infection remains high, subsequently resulting in a 1 in 10 chance of death after the operation (NHS, 2019).

S. aureus is the most commonly identified pathogen associated with IE. *S. aureus* colonises the heart valves after entering the bloodstream via mucosal surfaces, following skin injuries or wounds, which is typical among patients who have undergone surgery (Hall-Stoodley et al., 2012b). According to Murray et al. (2005), between 20% and 65% of IE cases associated with *S. aureus* are fatal, and a large proportion of patients who survive suffer from long-term health conditions, due to damage inflicted upon the cardiac structure, biofilm growth and emboli in the cardiac structure, or secondary

infections (Topan et al., 2015). A previous study recorded that, among 260 patients presenting with *S. aureus*-induced IE, half of these patients had a heart murmur and more than half suffered from congestive heart failure (Hoen et al., 2002, Bor et al., 2013). Critically, the mortality rate was 46% among patients diagnosed with *S. aureus*-induced IE, primarily due to complications related to the central nervous system and late congestive heart failure (Prendergast, 2004). Endocarditis is more common in older people, with half of all cases developing in people over the age of 50 years (NHS, 2019). However, endocarditis cases have been recorded in children, particularly those born with congenital heart defects (NHS, 2019).

1.4.1 Current diagnosis and treatment of infectious endocarditis

As indicated previously, biofilm development can render antibiotic treatments ineffective, resulting in the need for surgical intervention to replace the heart valve, prolonging hospitalisation time, and increasing the risk of recurrent infections (Harro et al., 2020b) (Liu et al., 2011). The development of new diagnostic procedures will greatly decrease the likelihood that a patient will die due to IE, 1 in 5 postop patients die from IE (Fernandez Guerrero et al., 2009, Høiby et al., 2015). The accurate and rapid diagnosis and treatment of IE are critical for reducing the associated mortality rate (Wu et al., 2015). Historically, clinical features, such as fever, cardiac murmur, and peripheral vascular stigmata, were considered classical hallmarks of IE (Prendergast, 2004). However, the majority patients suffering from IE fail to manifest these symptoms at early stages of infection, thereby resulting in a late diagnosis which in turn causes a delay in treatment (Pant et al., 2015). Currently, the modified Duke criteria are used for the clinical diagnosis of IE (Topan et al., 2015), which were established in 1994 specifically for IE diagnosis (Durack et al., 1994, Topan et al., 2015). The diagnostic approach includes evaluating a list of major and minor criteria for positive IE diagnosis, including positive blood cultures from two separate samples, the identification of microbiological agents (e.g. *S. aureus*), the identification of masses on the heart or within the

vascular structure by echocardiography, and several other classic clinical symptoms, such as a fever higher than 38°C (Fernandez Guerrero et al., 2009, Høiby et al., 2015). Since their inception, The Duke criteria have been validated in a wide variety of cases and be both sensitive (> 80%) and highly specific (> 98%) for the diagnosis of IE (Harro et al., 2020a). One drawback of the reliance on microbiological analyses of blood cultures is the phenomenon of culture-negative results, in which blood sample cultures fail to yield positive results, generally due to slow microbial growth in the laboratory following the prior administration of antibiotics (Harro et al., 2020a).

Obtaining a suitable sample from the infection site is crucial for the diagnosis of IE; however, this process is often inconvenient because it involves surgical interventions, such as biopsy, needle aspiration, or the removal of implanted medical devices (Wu et al., 2015). Unfortunately, surgical interventions are often the only option for performing accurate diagnosis of IE patients, due to the many complications associated with *S. aureus,* such as biofilm formation and antibiotic resistance.

Although obtaining a suitable sample from the site of infection can be difficult (Wu et al., 2015), this approach may represent the only option for diagnosing IE, particularly in cases where irregularities have been identified by echocardiography (Hall-Stoodley et al., 2012a). Unfortunately, biofilms associated with infections can often only be confirmed following the removal of implanted devices; therefore, new methods that enable clinicians to identify BAI on medical devices, *in situ,* are necessary (Wu et al., 2015). Moreover, examinations of implanted devices can have ambiguous results. To increase the sensitivity of such assays, extracted devices can be exposed to ultrasonication, to dislodge adherent bacteria (Hall-Stoodley et al., 2012a, Bjerkan et al., 2012). Ultrasonication has been reported to increase the positive culture rate by at least 2-fold (Nelson et al., 2005). As indicated previously, BAI is often mistakenly identified as bacteraemia, producing false-positive bacteraemia results and false-negative BAI results (Hall-Stoodley et al., 2012a). Antibiotic treatments administered for a BAI mistakenly diagnosed

as bacteraemia can make the BAI more difficult to detect, as the antibiotics often reduce the size of the biofilm mass, without eradicating it (Hall-Stoodley et al., 2012a).

Treatments are resource- and time-consuming and can be traumatic for the patient (Pendleton and Kocher, 2015). For example, the treatment of patients with MRSA-native valve endocarditis requires several blood cultures, both before and after treatment, transoesophageal echocardiography, and a daily dose of vancomycin or daptomycin, for six weeks (Harro et al., 2020a). In cases where the patient has a valve surgically removed and replaced, a combination of intravenous vancomycin and rifampicin is administered every eight hours for six weeks, in addition to intravenous gentamicin every eight hours for two weeks (Harro et al., 2020a).

1.5 Overview of non-antibody binding molecules

The use of antibodies as detection tools for diagnostic and research purposes have been successfully applied to this day; however, despite their successes, antibodies have properties than can limit their applications (Bradbury and Pluckthun, 2015), including their large size, reliance on disulphide bonds and glycosylation for stability, and sensitivity to high temperatures. It is also not possible to produce them using bacterial expression systems (Vazquez-Lombardi et al., 2015, Tiede et al., 2014). Moreover, the production of antibodies is expensive, relies on the use of animal models, and then must be re-engineered to be used for humans during clinical applications (Skrlec et al., 2015). These limitations have encouraged the development of protein engineering over the last two decades, resulting in the development of non-antibody binding molecules, which are similar to antibodies in their molecular recognition properties, but with improvements designed to overcome antibody-associated limitations, such as increased thermal stability, smaller sizes, and increased solubility (Skrlec et al., 2015, Vazquez-Lombardi et al., 2015). Most affinity-binding molecules do not contain cysteines, allowing the introduction of cysteine residues for the site-specific coupling of biotin, fluorescent labels, or polyethylene glycol, enhancing utility or stability (Tiede

et al., 2014). These characteristic improvements allow affinity-binding molecules to potentially act as antibodies during research (Wojcik et al., 2010), diagnostics (Theurillat et al., 2010), and drug discovery studies. Affinity-binding molecules could also be used as therapeutic tools by fusing them with albumin or other large proteins to overcome the disadvantage of short circulatory half-lives (Schellenberger et al., 2009). The range of potential uses for non-antibody binding molecules has expanded to include several applications, including treatment and diagnosis, structural studies, and molecular imaging. Since their development, the use of non-antibody binding molecules has been extremely popular in research, diagnostics, and drug delivery, with some having achieved approval to progress to clinical trials, including the scaffolds Avimers (Vazquez-Lombardi et al., 2015), AdNectins™ (Tolcher et al., 2011) DARPin (Binz et al., 2004), Anticalins (Mross et al., 2014), Affibodies (Beuttler et al., 2009), and Affilins (Ebersbach et al., 2007). Although the specificity of non-antibody binding molecules has been investigated extensively, however, they are still considered foreign molecules therefore they can still be recognised by the host immune system which is a potential limitation for their use. Despite, the continuing popularity of using non-antibody binding molecules in research, unfortunately, not much research has been dedicated to investigate their immunogenicity (Vazquez-Lombardi et al., 2015). In this study, a class of non-antibody binding molecule scaffolds, called Affimers, were raised against *S. aureus* biofilm components, with the aim of using the Affimers for the diagnosis of IE, by incorporating a detection system, such as a biosensor.

1.5.1 Affimers

Affimers are a class of affinity-binding molecule scaffold, developed at the University of Leeds by the BioScreening Technology Group (BSTG), for use during molecular recognition and imaging applications (Tiede et al., 2014). The Affimer scaffold was previously referred to as the Adhiron scaffold until they were licenced by Avacta Life Sciences Ltd. Two Affimer scaffolds have been developed that share similar protein conformations. The first Affimer is

based on the sequence of the human protease inhibitor Stefin A, whereas the second scaffold is based on the consensus sequence of the plant cysteine protease inhibitors phytocystatins (Tiede et al., 2014). Consensus protein sequences are often exploited for use as the scaffold for non-antibody binding molecules because the presence of consensus residues at any position enhances the structural and thermal stability of the protein compared with non-conserved residues (Devi et al., 2004). The use of consensus sequences during scaffold design, such as ankyrin repeat proteins (Devi et al., 2004), antibody CH3 domains (Demarest et al., 2004), and Affimers (Tiede et al., 2014), has previously been described and was shown to be successful for increasing protein stability, in several studies.

This study utilised the second Affimer scaffold, which is based on the alignment of 57 phytocystatin sequences, resulting in a stable protein, with enhanced structural and thermal stability and a melting point (T_m) of 101°C (Tiede et al., 2014). Along with their extremely specific target-binding properties, Affimers possess several qualities that make them ideal candidates as a scaffold for the generation of affinity-binding molecules, including small sizes (13 kDa), monomeric structures, a lack of disulphide bonds, and being easily expressed and produced in *E. coli* (Tiede et al., 2014). In addition, Affimers do not contain cysteines within their body, which allows the proteins to be easily modified by the insertion of cysteines at the C-terminus. The Affimer scaffold is diverse, with a library size of 1.3×10^{10} clones. Each clone consists of the phytocystatin backbone, with the incorporation of two randomised amino acid variable loop regions (VRs), which each consist of random, 9-aa-encoding sequences, which exclude cysteine (Tiede et al., 2014). The X-ray crystal structures of the Affimers has been identified and registered with the Protein Data Bank (PDB)(Figure 1.5) (Tiede et al., 2014). Affimers have been identified against several targets, such as Src-Homology 2 (SH2) and vascular endothelial growth factors (VEGF) (Tiede et al., 2017).

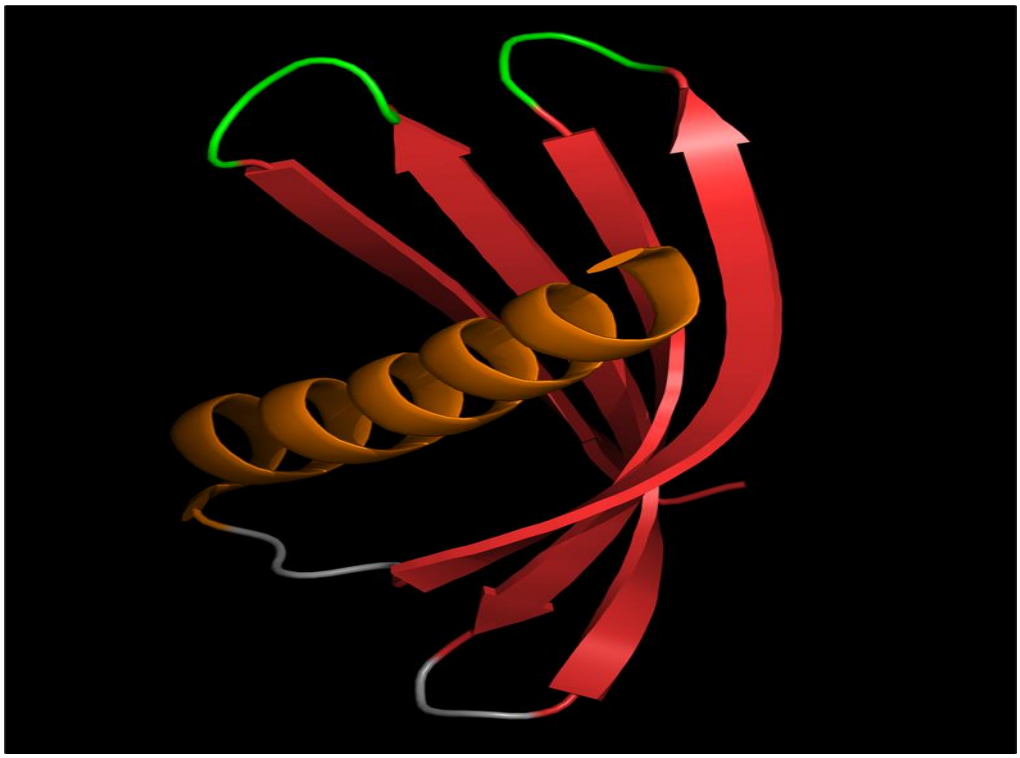

Figure 1.5 Affimer scaffold X-ray crystal structure. (PDB ID number: 4N6T). At a resolution of 1.75 Å, the Affimer core structure consists of one α-helix (depicted in orange) and four anti-parallel β-sheets (depicted in red). The VRs (depicted in green) are located between the first and second β-sheets and between the third and fourth β-sheets.

1.5.2 Generation of Affimers using phage display

In recent years, phage display has been a powerful method that has been used during selection-based systems, for the discovery of new biological targets (Løset et al., 2014). To generate Affimers, the corresponding coding sequence is cloned into a phagemid vector that also contains a truncated version of the gene sequence for the phage minor capsid protein PIII of the M13 filamentous phage. The phagemid is then introduced into *E. coli* by transformation and the transformants infected with a helper phage to allow the complete assembly of the phage (Bernal and Willats, 2004). Through 2-3 cycles of an *in vitro* selection process, called bio-panning, the phage library which consist of the completely assembled phage presenting the Affimer fusion protein on PIII is screened against an immobilised target (Figure 1.6) (Bernal and Willats, 2004). Phage that recognise a ligand from the

immobilised target are then amplified and tested for binding using enzyme linked immunosorbent assay (ELISA) before being sent for sequencing.

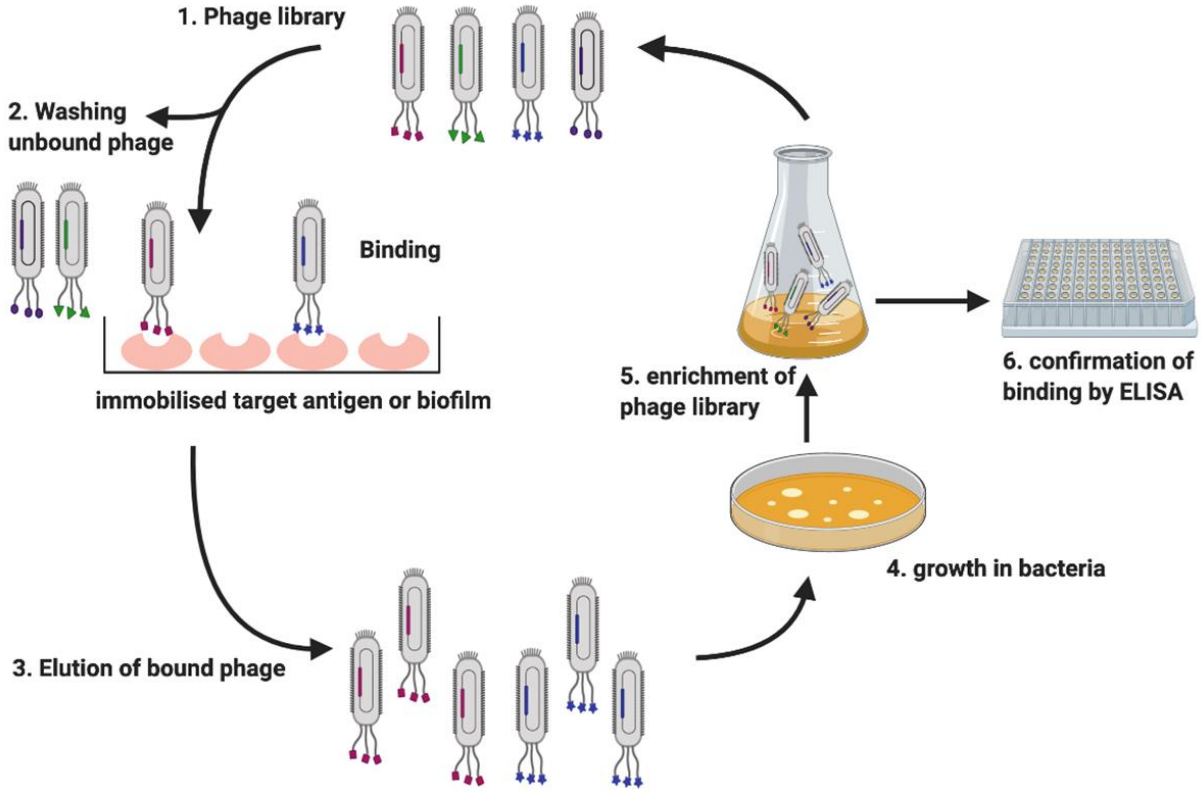

Figure 1.6 Affimer isolation using phage display. The Affimer phage library is incubated with the immobilised target. Unbound phage is washed off and bound phage is eluted. To enrich the phage pool, the eluted phage is then amplified in *E. coli*. This cycle is repeated 2-3 times then isolated phage clones are tested for binding to the target using ELISA. Created with BioRender.com.

1.6 Overview of RNA sequencing

The central dogma of molecular biology was introduced in 1958, by Francis Crick, who described the processing of genetic information encoded by genes. DNA is transcribed into mRNA, which is then translated into proteins (Crick, 1970). The genetic information expressed by an organism influences the organism's phenotype and can change depending on the surrounding

environmental factors (Kukurba and Montgomery, 2015). The transcriptome, which is the resulting transcription product of all mRNAs expressed in the cells, is a useful indicator for interpreting the functional processes of cells under different biological conditions (Kukurba and Montgomery, 2015). Bacterial adaptations to environmental changes are governed by multiple molecules, such as transcription factors, RNA regulators, and sigma factors, which are involved in the regulation of mRNA synthesis and degradation (Mäder et al., 2016). The analysis of the transcriptomes across the bacterial genome can provide quantitative information regarding the transcriptional profiles of different bacteria (Mäder et al., 2016).

1.6.1 RNA sequencing

RNA sequencing (RNA-seq) is a technique that utilises high-throughput, deep sequencing technology to provide quantitative measurements of the transcriptomes expressed during specific conditions, via the sequencing of complementary DNA (cDNA) (Wang et al., 2009). Numerous experimental details, such as RNA quality, the use of technical and biological replicates, the enrichment and depletion of an RNA species. and library design must be considered before performing RNA-seq (Wang et al., 2009) . In general, the first step during RNA-seq is the extraction of total RNA and the performance of an RNA integrity check, which is determined by calculating the RNA integrity number (RIN), based on the intensity of the fluorescence correlation with the size ratio of 16S/23S, which can be obtained from various lab-on-chip devices, such as the Bioanalyzer 2100 (Agilent Technologies, USA) (Kukurba and Montgomery, 2015). Because rRNA comprises 90% of total bacterial RNA, the total RNA is then depleted of rRNA, followed by the selection of mRNA through filtration, which is possible through the addition of a poly-A adapter sequence following RNA fragmentation, which results in the concentration of mRNA. which is amplified by PCR to produce a double-stranded cDNA library. Specific adaptor sequences are then ligated to one or both ends of the cDNA fragment, to enable clustering onto a next-generation sequencing (NGS) platform. The cDNA is then sequenced, and the resulting reads are assembled into a reference genomic sequence, using available bioinformatic tools. RNA-seq offers several advantages over microarray

assays, such as a marked capacity for the detection of low-abundance transcripts. The continuous reductions in sequencing costs, the increasing number of facilities, and accessibility of high-throughput sequencing, in addition to publicly available bioinformatics tools, have made RNA-seq a popular and attractive method for bacterial transcriptome studies (Haas et al., 2012).

1.6.2 Transcriptome analysis techniques

The transcriptome consists of the total transcripts present in an organism at a specific time (Kukurba and Montgomery, 2015). Previously, transcriptome analysis was limited to protein-coding mRNA sequences; however, recently a subset of noncoding RNAs (ncRNA), whose functions were previously unknown, have been identified to be functional (Palazzo and Lee, 2015). ncRNA refers to RNA molecules that do not encode proteins, and the best-characterised and well-known ncRNAs include transfer RNA (tRNA) and ribosomal RNA (rRNA), which are involved in the translation of mRNA (Holley et al., 1965, Urlaub et al., 1995). Recently, other ncRNAs have been identified in eukaryotes, including small nuclear RNA (snRNAs) and small nucleolar RNAs (snoRNAs), which are involved in the splicing and modification of rRNAs, respectively (Mattick and Makunin, 2006). Other recently discovered novel ncRNAs in eukaryotes include micro RNA (miRNA) and piwi-interacting RNA (piRNA), which are involved in the posttranscriptional regulation of gene expression (Stefani and Slack, 2008). Many ncRNAs exist with unknown functions, and as new ncRNAs continue to be discovered and characterised, the scope of transcriptome analyses should expand (Palazzo and Lee, 2015). Previously, studies of gene expression were limited to utilised low-throughput methods, such as quantitative polymerase chain reaction (qPCR) and northern blots. These methods are limited because they are only able to detect and measure the transcript of a single gene (Kukurba and Montgomery, 2015).

1.7 Body-imaging detection of sites of bacterial infection

Microbubbles, which are used in medical diagnostics as a contrast agent for ultrasound imaging (Kujundzic et al., 2007). Microbubbles are small particles ranging from 1-8 µm in size with a gas-filled core and a surrounding shell of proteins, biocompatible polymers and/or lipids (Szabados et al., 2012). When localised ultrasound waves are applied the microbubble oscillates resulting in a detectable backscatter from the reflected sound waves, distinguishing them from surrounding tissue (Sirsi and Borden, 2009). Due to the fact that gas bubbles would dissolve once injected into the bloodstream, the shell surrounding the microbubbles provides stability and containment of the gas, preventing leakage (Sirsi and Borden, 2009). Therapeutic agents can be encapsulated by microbubbles and their release triggered by insonifying *i.e.* targeting a localised area or an object with carefully-controlled sound waves (Szabados et al., 2012).The frequency at which the microbubbles are insonified determines the effective use of the microbubble. The range of effects is dependent on the ultrasound parameters, microbubble size and its physicochemical properties (Sirsi and Borden, 2009). The range of different effects can vary from a mild effect such as acoustic backscatter, which is used for imaging, to a more aggressive effect such as inertial cavitation which is useful for targeted drug delivery (Sirsi and Borden, 2009). Different types of shells can be used to encapsulate the microbubble depending the on the intended application. For example, lipid shells such as Optison microbubbles, which contain perfluoropropane gas, are more responsive to ultrasound due to the thin shell but resulting in rapid shattering of the shell and release of the therapeutic agent, but carry a low payload. Meanwhile protein and polymer shells such as, albumin and TCPG (*tert*-butyloxy-carbonylmethyl polyglutamate) shells, respectively, are more stable increasing the payload that can be carried by the microbubble. Some shells can be charged so that they hold their cargo via electrostatic interactions. Combining different phenomena resulting from insonifying enables the use of microbubble for targeting, imaging and controlled release (Sirsi and Borden, 2009).

1.8 Aims

The impact of biofilm formation on complication of chronic wound infections and the colonisation of medical devices is directly proportional to the increase in the number of patients that need prolonged hospitalisation or replacement or repair of medical devices (Pant et al., 2015). This result in an increase in the economic stress on health care systems and poor quality of life for hospitalised patients. IE often is associated with elderly patients that are already at risk of chronic infection due to weak immunity and patients with congenital heart defects (Pant et al., 2015). Treatment with antimicrobials is not very effective against biofilm on the heart valve and replacement or repair of a heart valve could put the patient's life in greater risk (Bor et al., 2013). To address these issues this study aims to identify and exploit Affimers that would aid in the early diagnosis and potential treatment of IE to prevent any unnecessary surgical intervention. To achieve this, three approaches were pursued in an effort to target proteins associated with *S. aureus* biofilms. Initially, Affimers were raised against SpA and ClfA, two well characterised *S. aureus* surface associated proteins known to be expressed during initiation of biofilm formation. Secondly, another set of Affimers were raised against random *S. aureus* biofilm components from three different strains, the isolated Affimers could most likely recognise the most accessible and prevalent biofilm components. Finally, the third approach taken utilises of RNA seq to obtain transcriptomic date that reflect the gene expression profile associated with *S. aureus* planktonic cells and mature biofilms. Then using statistical analysis to identify the gene products that are highly expressed and most likely to be accessible in biofilm and raise Affimers against them. Ideally finding an Affimer that is able to recognize *S. aureus* biofilm distinguishing them from planktonic cells; this would help identify patients that need repair or replacement of heart valves from those who don't without surgical intervention.

Chapter 2: Materials and Methods

2.1 Strains and plasmids

Laboratory bacterial strains that were used are listed in (Table 2.1).

Table 2.1 Bacterial strains used

Strain	Description	Source
S. aureus **NCTC 83254**	Non-proficient biofilm forming has a 11-bp deletion in *rsbU*, which is a positive regulator of *sigma B* factor.	(Horsburgh et al., 2002)
S. aureus **SH1000**	*S. aureus* 8325-4 with functional *rsbU*	(Horsburgh et al., 2002)
S. aureus **UAMS-1**	Oxacillin susceptible strain isolated from osteomyelitis patient; Proficient biofilm-forming strain	Gillaspy et al. (1995)
S. aureus **USA300 JE2**	A derivative of USA300 LAC strain; cured of plasmids p01 and p03.	(Fey et al., 2013, Voyich et al., 2005)
S. aureus **USA300 FPR *Δspa***	A derivative of *S. aureus* USA300 FPR3757; contains in-frame deletion in the *spa* gene, which encodes protein A; resistant to tetracycline	(Martin et al., 2009)
S. aureus **USA300 FPR3757**	Congenic wild-type for USA300 FPR3757 *Δspa* mutant; community-acquired methicillin-resistant *S. aureus* (MRSA)	Tenover and Goering, (2009)
E. coli **ER2738**	F´proA+B+ *lacIq* Δ(*lacZ*)M15 zzf::Tn10(TetR)/fhuA2 glnV Δ(*lac-proAB*) thi-1 Δ(*hsdS-mcrB*)5	Lucigen UK
E. coli **XL10® Gold**	Used for site-directed mutagenesis *endA1 glnV*44 *recA*1 *thi*-1 *gyrA*96 *relA*1 *lac Hte* Δ(*mcrA*)183 Δ(*mcrCB-hsdSMR-mrr*)173 *tetR* F'[proAB *lacIqZ*Δ*M*15 Tn10(TetR Tn5(KanR)	Agilent UK

***E. coli* BL21 (DE3)**	Strain used for protein expression. *E. coli* str. B F⁻ *ompT gal dcm lon hsdS*$_B$($r_B^-m_B^-$) λ(DE3 [*lacI lacUV5-T7p07 ind1 sam7 nin5*]) [*malB*$^+$]$_{K-12}$(λ^S)	Agilent UK
***E.coli* DH5α**	Used for routine cloning.	Invitrogen UK
	F⁻ *endA1 glnV44 thi-1 recA1 relA1 gyrA96 deoR nupG purB20* φ80d*lacZ*ΔM15 Δ(*lacZYA-argF*)U169, hsdR17($r_K^-m_K^+$), λ⁻	
pET11a	Modified bacterial expression vector encoding *N*-Terminal hexahistidine-encoding sequence and T7 promoter, *Not*I and *Nhe*I restriction sites, ampR	(Tiede et al., 2014)
pBSTG1	Used for expression of Affimer fusion protein in M13 bacteriophage. The phagemid cloning vector derived from pHEN1vector. *Not*I and *Nhe*I restriction sites. KanR	(Stenberg et al., 1991)
pET23a-GFP	A bacterial expression vector with T7 promotor and ampR	

2.2 Bacterial culture growth

E. coli and S. aureus overnight cultures were grown using 10 mL Luria Bertini broth (LB) (Oxoid). *E. coli* cultures were supplemented with 100 mg/mL carbenicillin (Medford Laboratories Ltd) or 50 mg/mL kanamycin and grown until cell culture growth reached mid exponential phase with an absorbance of 0.5-0.6 at 600 nm.

2.3 Growth media

Biofilms were grown on cellulose disk (Millipore) or on black microtiter plates (Greiner) in either brain heart infusion (BHI) agar (Sigma) or BHI medium (Oxoid) respectively or tryptic soya agar (TSA) (tryptic soya broth (TSB)

containing 20 g/l agar (Oxiod)) or TSB (Oxoid) respectively and peptone NaCl glucose **(**PNG) agar (3.3 g/L peptone, 2.6 g/L NaCl, 3.3 g/L glucose, agar 20 g/L) or PNG medium respectively.

2.4 Biofilm growth conditions

Bacterial strains used in this study are listed in Table 2.1. *S. aureus* strains SH1000, USA300 and UAMS-1 were obtained as a gift from the O'Neill laboratory at the University of Leeds. Strains USA300 FPR and USA300 Δ*spa* mutant were a gift from Alice Prince's lab at Columbia University. Strains from glycerol stocks were streaked onto LB agar plates with the appropriate antibiotic selection and were incubated overnight at 37°C to obtain single colonies. 10 mL of LB broth was inoculated with single colony and incubated overnight for 16 h at 37°C with aeration at 230 rpm. Biofilms were then grown on cellulose disks or microtiter plates (Greiner) as described below.

2.5 Biofilm Growth on Cellulose Disk

Cellulose disks were incubated in 10% (w/v) human plasma (Sigma) in 0.05 M carbonate bicarbonate buffer prepared by dissolving the contents of 1 capsule in 100 mL water (Sigma) (Ryder et al., 2012) for 24 h. Disks were then inoculated by submerging in a 5 mL overnight culture and then placed on the surface of a Brain Heart Infusion (BHI) agar plate and incubated at 37°C for 48 h. To remove loosely associated planktonic cells form the surface, biofilms were washed with 1 mL or 10 mL depending on whether they were used for Enzyme Linked Immunosorbent Assay (ELISA) or assessing biofilm adherence respectively. Biofilms were washed with 1 mL 0.01% (v/v) phosphate-buffered saline containing 0.01% (v/v) Tween (PBST) for 1 min with shaking at 150 rpm. For experiments analysing biofilm adherence, biofilms were further treated with 1 mg/ mL cellulase (Sigma) in 50 mM citrate buffer (0.5 M sodium citrate and 0.5 M citric acid, pH 4.6) following the PBST washes.

2.6 Biofilm growth on microtiter plate

Microtiter plates were conditioned for 24 h at 4°C with 20% (v/v) human plasma (Sigma). The wells were then inoculated with 200 µL *S. aureus* overnight culture that had been diluted 1 in 100 in BHI media, and were incubated for 48 h at 37°C with shaking at 350 rpm using a Heidolph incubator 1000 (Heidolph, Germany).

2.7 Molecular biology techniques

2.7.1 Isolation of Affimers using Phage display

Biofilms were grown on cellulose disk on the surface of BHI agar as previously described in Section 2.2.2. Briefly, all biofilms were washed with 1 mL PBST and the remaining material was scraped from the surface of the disk and suspended in 1 mL PBST. All subsequent steps were carried out in Protein LoBind tubes (Eppendorf) by the BioScreening Technology Group (BSTG) at the University of Leeds using a the Affimer phage display library that has been described and widely used (Lopata et al., 2018, Tiede et al., 2014). The target biofilm material was incubated with ~ 1.12 x 10^{12} pfu /mL of pre-panned phage for 2 h at RT and mixed by rotation (20 rpm) using Stuart® SB2 fixed speed rotator (Stuart). The biofilms were centrifuged for 2 min at 12,000 x g and then washed five times with 300 µL of PBS. To elute bound phage, 200 µL of 0.2 M glycine (pH 2.2) was added for 10 min, followed by neutralisation with the addition of 30 µL of 1 M Tris-HCl (pH 9.1) (Sigma). Further elution was performed with 200 µL of 100 mM Triethylamine (Sigma) for 6 min, followed by neutralisation with 100 µL of 1 M Tris-HCl (pH 7). *E. coli* ER2738 cells ~3.8 x 10^{9} cfu/mL were then infected with the eluted phage for 1 h at 37°C, and serially dilution spread on LB agar plates containing 100 µg/mL carbenicillin, which were grown overnight at 37°C. Infected colonies were scraped off of the surface of the plate using 7 mL of 2TY medium (16 g/L Bacto tryptone, 10 g/L Bacto yeast extract, 5 g/L NaCl, pH 7.0) supplemented with 100 µg/mL of carbenicillin and grown at 37°C. The optical density of the culture was measured at 600 nm and the cultures were diluted to an absorbance value of 0.2 at 600 nm of in a total volume of 8 mL of 2TY media. The cultures were

grown for 1 h at 37°C with shaking at 200 rpm and then infected with 0.32 µL of 1 x 10^{14} PFU/ mL M13K07 helper phage. The culture was further incubated for 30 min at 37°C, with shaking 90 rpm, then supplemented with 50 µg/mL kanamycin and incubation overnight at 25°C with shaking (170 rpm). To precipitate the phage, 2 mL of 20% (w/v) polyethylene glycol 8000 in 2.5 M NaCl (PEG-NaCl) was added and then sample incubated overnight at 4°C. Phage was then centrifuged at 4,816 x g for 30 min, the phage pellet was resuspended in 320 µL of TE buffer (1 mM Tris, 1 mM EDTA, pH 8); the phage was transferred to new microcentrifuge tube then centrifuged at 16,000 x g for 10 min. the supernatant containing the phage was diluted with 40% (v/v) glycerol and stored at -80ºC. This bio-panning process was repeated for two more rounds, counter selection steps used to isolation of Affimers specific for each strain will be addressed in more detail in Chapter 4; Section 4.2.1. In the third round of pre-panning, the phage was tested for activity by incubating with the target strain. Positive and negative controls consisting of *S. aureus* planktonic cells and streptavidin magnetic beads (Invitrogen), respectively.

2.7.2 Polymerase chain reaction (PCR)

Primers for amplifying Affimers sequences were designed by the BSTG group and were synthesised using Eurofins Genomics services (Ebersburg, Germany). The sequences of the forward and reverse primers are 5' – ATGGCTAGCGGTAACGAAAACTCCCTG and 5' – TTACTAATGCGGCCGCACAAGCGTCACCAACCGGTTTG, respectively. DNA was amplified using Phusion DNA polymerase (NEB) in 25 µL reactions according to the manufacturer's instructions. Briefly, the reaction consisted of 3% (v/v) DMSO (Sigma), 4.5 mM $MgCl_2$, 0.5 µM forward and reverse primers, 0.8 mM dNTPs (Promega), 100 ng DNA template, and 2 U of Phusion DNA polymerase in 1x Phusion reaction buffer, with a final volume of 25 µL. The PCR product was then digested with *DpnI* (NEB) at 37 °C for 1 h to remove dam-methylated template. PCR products were analysed using agarose gel electrophoresis. DNA concentration was quantified by reading the absorbance at 260 nm using a P300 nanophotometer (Implem, Munich Germany). DNA quality was determined by the ratio of absorbance at 260 nm/280 nm and 260 nm/230 nm (J.F and Russell, 2001). See Table 2.2 for PCR reaction Process.

Table 2.2 PCR settings for thermal cycler

Cycle step	Temperature (°C)	Time (s)	Cycle
Initial Denaturation	98	30	1
Denaturation	98	20	30
Annealing	54	20	
Extension	72	20	
Final Extension	72	600	1
Hold	4	Hold	

2.7.3 Colony PCR (cPCR)

A single transformed colony was picked from an agar plate then suspended in 20 µL of PBS, 2 µL of the suspension was used as template DNA for the PCR reaction. PCR conditions are the same as described above.

2.7.4 Agarose gel electrophoresis

DNA was visualised by running on a 0.8-1.2 % (w/v) agarose. Briefly, an appropriate amount of agarose powder was mixed with 100 mL of TBE buffer (Severn Biotech). Agarose was dissolved by microwaving suspension until solution was clear then cooled to ~50°C and allowed to set on a Wide Mini-Sub Cell GT Cell electrophoresis system (Bio-Rad). PCR samples were mixed with 6x DNA loading dye (NEB) to a final ratio of 1 x before loading onto gel. The gel was run for 45 min at 12 V/cm.

2.7.5 Preparation of pET11a

2.7.6 Restriction digests

Restriction enzymes were purchased from NEB. Briefly, 50 µL of the PCR product and 20 µg of pET11a were double digested using *NotI*-HF™ and *NheI*-HF™ overnight at 37°C. Restriction digest of the plasmid was performed in a reaction volume of 500 µL. The reaction included 50 µL 10 x CutSmart™ buffer and 200 U of

each enzyme. Following restriction digest, 125 µL of digested pET11 was incubated with 14 µL of Antarctic phosphatase reaction buffer and 5 U of Antarctic phosphatase (NEB) for 15 min at 37 °C to remove the phosphorylated 5'and 3' ends. The Antarctic phosphatase was heat inactivated by incubation for 5 min at 65 °C.

2.7.7 Gel purification of pET11a

The reaction mix was loaded onto a 0.7% (w/v) agarose gel and run at 100 V for 20 min. The DNA band was visualised using a UV box and band was excised using a clean scalpel. DNA was purified using Qiagen gel extraction kit (Qiagen) and the concentration was measured. The digested plasmid was stored at -20 °C.

2.7.8 DNA Ligation

The ligation of PCR-amplified Affimer sequence into pET11a was performed by incubating 75 ng pET11a and 25 ng Affimer sequence PCR product with 1 µL T4 DNA ligase (NEB), then mixed with DNase free water (Sigma) to reach a final volume of 20 µL then incubated overnight at room temperature.

2.7.9 Affimer sequence subcloning

Ligation products were transformed into *E. coli* XL10-Gold competent cells (Agilent Technologies) by incubating 1 µL ligation product with the 50 µL competent cells on ice for 30 min. Cells were then incubated at 42°C for 45 s and immediately incubated on ice for 2 min. Cells were diluted serially (10^{-2}, 10^{-4}) then 100 µL of each were spread on to LB agar supplemented with carbenicillin at a final concentration of 0.01 µg /mL and incubated overnight at 37°C. Colonies were screened for the presence of plasmid with the correct Affimer sequence using colony PCR described in Section 2.3.2.1. Plasmids was purified using Qiagen mini prep kit according to manufacturer's instructions. The Affimer sequence was confirmed by Sanger sequencing (Sanger et al., 1977), 20 µL of each plasmid (100 ng/µL) were sequenced using universal forward and reverse T7 primers (25 pmol) using the services of GENEWIZ. Selected plasmids were introduced by transformation into chemically competent *E. coli* BL21 Star™ (DE3) cells as described by the supplier (Life Technologies).

2.7.10 Protein expression and purification

2.7.11 Expression and purification of Affimers

Overnight cultures of a transformed BL21 (DE3) colony were grown at 37°C, 230 rpm in LB media supplemented with 100 µg/ mL carbenicillin (LB-carbenicillin) supplemented with 1% (w/v) glucose. 625 µL of overnight culture were added to 50 mL of fresh LB-carbenicillin medium and incubated at 37°C with shaking at 230 rpm. Once culture reached an absorbance at 600 nm of 0.8, protein expression was induced by addition of IPTG (Melford Laboratories Ltd) to a final concentration of 0.5 mM and cultures were grown for 6 h at 30°C, 150 rpm. Cells were harvested by centrifugation at 4,816 x g for 15 min and stored at -20°C. Thawed cell pellets were resuspended in 1 mL lysis buffer (PBS, 0.001 M Imidazole; pH 7.4) supplemented with 0.1 mg/ mL lysozyme (Sigma), 0.01% (v/v) Tween-20 (Sigma), (10 U/mL) DNase I (NEB), 1x cOmplete™, EDTA-free Protease Inhibitor Cocktail (Sigma) and incubated on a rotator for 20 min at room temp. Lysates were heat denatured by incubation for 20 min at 50°C, and insoluble proteins and cell debris were pelleted by centrifugation at 16,000 x g for 20 min. 300 µL of HisPur™ Ni-NTA resin (Thermo Scientific) was washed in 1 mL Lysis buffer and centrifuged at 1,000 x g for 1 min. Cleared lysate was incubated with the equilibrated resin for 1 h on a rotator at room temperature, then centrifuged for 1 min at 1,000 x g. Supernatant was stored at -20°C and resin was washed with 1 mL of Wash Buffer (PBS, 0.02 M Imidazole; pH 7.4) until the absorbance of the wash solution at 280 nm was less than 0.09. Resin was resuspended in 5 mL of Wash Buffer and collected into a Pierce Centrifuge Column (Thermo Scientific). Affimer was eluted with 500 µL elution buffer (PBS; 0.3 M imidazole; 10% (v/v) glycerol; pH 7.4) and then centrifuged at 1,000 x g for 1 min and the eluate was collected. The elution step was repeated twice and Affimers were then dialyzed in dialysis buffer (PBST) overnight at 4°C.

Affimers were analysed by SDS-PAGE and concentration was measured by the BCA assay by comparing absorbance to known concentrations of BSA

standard. The heat denaturation step of the protein purification protocol was excluded when Affimers were required for SPR experiments.

2.7.12 SDS-PAGE

SDS polyacrylamide gels consisted of a 15% (v/v) resolving gel (3.475 µL H_2O (Sigma), 30% (v/v) arylamide (29:1 Acrylamide: bis-Acrylamide), 1 mM Tris-HCl pH 8.8 (Sigma), 0.1% (v/v) SDS, overlaid with a 5% (v/v) stacking gel (3.425 mL H_2O, 30% (w/v) or (v/v) [Delete as appropriate] Acrylamide (29:1 Acrylamide:bis-Acrylamide), solution 2 mM Tris-HCl pH 6.8 (Sigma), 0.1% (v/v) SDS. Briefly, 0.1% (v/v) TEMED and 0.01% (v/v) APS was added and mixed by inversion and the gel was allowed to polymerise. Before samples were loaded, the gel was preheated by running in SDS electrophoresis buffer (Biorad) for 20 min at 25 mA.

Protein samples were mixed with equal volume of 2 x SDS sample buffer (1 M Tris-HCl pH 6.8, 4% (v/v) SDS, 20% (v/v) glycerol, 10% (v/v) β-mercaptoethanol, 1% (v/v) Bromophenol blue, dH_2O) then denatured at 95°C for 10 min, cooled and loaded onto the SDS-PAGE gel; gel was run using Mini-PROTEAN® Tetra Vertical Electrophoresis Cell (Bio-Rad) at 12 V/cm for 1 h. Proteins were visualised by staining the gel with Instant Blue (Expedeon) according to the manufacturer's instruction.

2.7.13 Accurate mass determination

The molecular weight of purified Affimers was confirmed using MALDI-TOF mass-spectrometry using an M-class ACQUITY UPLC (Waters UK, Manchester, UK) interfaced to a Xevo G2-XS Q-TOF mass spectrometer (Waters UK, Manchester, UK). Processing was carried out by Dr Rachel George at the Mass Spectrometry Facility at the University of Leeds. Affimer proteins samples (5 µM) were desalted by loading 1 µL into MassPREP protein desalting column (Waters UK, Manchester, UK); then washed with a 10% solution of solvent B in solvent A (solvent B consisted of 0.1% formic acid in acetonitrile, solvent A consisted of 0.1% formic acid in water) for 5 min using an injection rate of 25 µL/ min. The bound protein was eluted by using a gradient of 2-40% solvent B in A over 1 min using an injection rate of 25 µL/ min. The column was subsequently washed with 95 % solvent B in A for 6 min

before re-equilibration at 5% solvent B in A. The eluted Affimer from the column were directed in to the mass spectrometer (MS) via a Z-spray™ electrospray source (Waters UK, Manchester, UK). The MS was operated in positive TOF mode using a capillary voltage of 3.0 kV, sample cone of 20 V and source offset of 80 V. The source temperature was set to 100°C and de-solvation was achieved at 250 °C. Affimer mass calibration was performed by a separate injection of [Glu]-fibrinopeptide b at a concentration of 250 fmol/ µl in MS/MS mode using a CID voltage of 28 V. Data was processed using MassLynx v4.1 software supplied with the mass spectrometer. Resulting mass was calculated by comparison with calculated mass of biotinylated Affimer obtained using (ProtPram). Resulting mass showed an increase of (149.2 amu) which were indicative of the mass of a methionine, this was subtracted from the LC-MS obtained mass to match that of the calculated mass of the Affimer.

2.7.14 Affimer biotinylation

150 µL of 0.5 mg/mL of purified Affimer were mixed with an equal volume of tris (2-carboxyethy l) phosphine (TCEP) Disulphide-reducing gel (Thermo Scientific) and incubated for 1 h on a rotator at room temperature. The reaction was centrifuged at 1,000 x g for 1 min and 130 µL of reduced Affimer were mixed with 6 µL of 2 mM biotin-maleimide solution (Sigma) and incubated at room temperature for 2 h. Unincorporated biotin was removed by passing through a Zeba spin desalting columns (Thermo Scientific) according to the manufacturer's instructions. Affimer concentration was measured by BCA assay (Thermo Fisher) using a FLUOstar Omega plate reader (BMG LABTECH).

Biotinylation was confirmed via enzyme-linked immunosorbent assay (ELISA). Briefly, 50 µL of PBS were added to Nunc-Immuno™ MaxiSorp™ strips (Thermo Scientific); 1 µL of biotinylated Affimers were added to each well and incubated overnight at 4°C. Wells were washed with 200 µL PBS and then blocked with 250 µL of 10 x Casein blocking buffer (BB) (Sigma) and

incubated at 37°C for 3 h. Following this, wells were washed with 200 µL of PBST then 0.5 mg/mL, high Sensitivity Streptavidin Horseradish Peroxidase (HRP) (Thermo Scientific) was diluted 1000-fold in 2 x BB and 50 µL was incubated with biotinylated Affimers for 1 h at room temperature with shaking at 160 rpm. Wells were then washed six times with 200 µL of PBST, and then 50 µL of 3,3',5,5'-tetramethylbenzidine (TMB) (Seramun) was added and allowed to develop for 3 min. Absorbance was measured at 620 nm, values that were higher than that of the negative control (non-biotinylated Affimer) were considered positive.

For SPR experiments biotinylated proteins were dialysed in PBST using a dialysis membrane with a Molecular weight cut-off (MWCO) 6300 (spectra/Por®).

2.8 Enzyme Linked Immunosorbent Assay (ELISA)

2.8.1 Affimer screening using ELISA

Biofilms were grown on cellulose disks conditioned with 10% (w/v) plasma for 48 h. To remove loosely associated cells, biofilms were washed with 1 mL PBST with shaking at 150 rpm. The biofilms were then scraped from the cellulose disk and suspended in 2 mL PBST to achieve a semi homogeneous mix. To decrease the level of nonspecific binding, the 50 µL of biofilm mix was then aliquoted into Eppendorf tubes that were pre-incubated overnight in 2 x (BB (which is commonly used to decrease nonspecific binding (Jenkins and Bogema, 2016). Biotinylated Affimers were diluted in 2x BB to a final concentration of 10 µg/mL and 50 µL of each Affimer were mixed with each biofilm sample for 1 h at room temperature on a rotator (Progen Scientific) Biofilms were then washed twice with 200 µL PBST and 50 µL of 10 µg/mL of HRP (Thermo Scientific) were added to each tube and incubated for 1 h at room temperature on a vibrating platform (Heidolph VIBRAMAX 100) with shaking at 300 rpm. Biofilms were then washed seven times with 200 µL PBST. 50 µL of TMB were added to each well for 15 s, then 50 µL of 0.16 M sulphuric acid were added to each well and transferred to a new 96-well plate (Greiner Bio-One). Absorbance was measured at 450 nm using a FLUOstar Omega plate reader (BMG LABTECH). Biofilms were then washed twice with 200 µL PBST and 50 µL of 10 µg/mL of HRP (Thermo Scientific) were added

to each tube and incubated for 1 h at room temperature on a vibrating platform (Heidolph VIBRAMAX 100) with shaking at 300 rpm. Biofilms were then washed seven times with 200 µL PBST. 50 µL of TMB were added to each well for 15 s, then 50 µL of 0.16 M sulphuric acid were added to each well and transferred to a new 96-well plate (Greiner Bio-One). Absorbance was measured at 450 nm using a FLUOstar Omega plate reader (BMG LABTECH).

For ELISAs used to measure Affimer binding to planktonic cells, 50 µL of overnight culture (1 x 10^9 cells) was incubated with the Affimers and was analysed as described above.

2.8.2 Phage ELISA for prokaryotic biofilms

Phage ELISA was carried out by Dr. Christian Tiede from the BioScreening Technology Group (BSTG) at the University of Leeds. Individual *E. coli* ER2738 colonies that were infected with the phage that contained the Affimer sequence were picked and grown in 100 µL of 2TY media containing 100 µg/ mL of carbenicillin in a 96-deep well plate at 37 °C, shaking at 1050 rpm overnight. A 25 µL aliquot of the overnight culture was added to 200 µL of 2TY media containing 100 µg/mL carbenicillin and incubated for 1 h at 37 °C with shaking at 1050 rpm. M13K07 helper phage (10 µL of 1x10^{11} PFU/ mL) was added to the culture and samples were incubated for 30 min at room temperature with shaking at 450 rpm. Kanamycin was added to a final concentration of 25 µg/ mL and cultures were incubated overnight at 25 °C with shaking at 750 rpm.

The *S. aureus* strains SH1000, USA300 and UAMS-1 were grown in BHI media on 96-well plates conditioned with 20% (v/v) human plasma (Sigma) to promote biofilm formation. Human plasma was used as a negative control. 200 µL of 2x BB (Sigma) were incubated in each well for 1 h at room temperature. The wells were then washed with 300 µL of PBST for 5 min with shaking 3 times. Plates were then blocked for 1 h with 200 µL of 2 x BB. Wells were then washed with 300 µL of PBST. 40 µL of phage-containing medium and 10 µL of 10x BB were added to the biofilm-coated plates so that each Affimer was tested against the biofilms and negative control wells containing plasma. The plates were incubated for 1 h at room temperature with shaking

at 230 rpm. Wells were washed with 300 µL of PBST. Anti-fd-Bacteriophage-HRP antibody (Seramun) was diluted 1:1000 in 2 x BB and 50 µL was added to each well. The wells were then washed ten times with 300 µL of PBST. 50 µL of TMB substrate solution SeramunBlau® fast (Seramun) was added to each well and left to develop for 3 min (Seramun, Heidesee, Germany) then the absorbance at 620 nm was measured.

2.9 Confirm Affimer binding using pulldown

2.9.1 Protein A pulldown using Nickel-affinity chromatography

HisPur™ Ni-NTA resin (Thermo Scientific) was first equilibrated with PBS containing 0.01 M imidazole (pH 7.4). Affimers (287.6 pmol) were mixed with 2.5 µL of Ni-NTA resin and incubated for 1 h at room temperature, transferred to Pierce™ centrifuge column (Thermo Scientific) and centrifuged for 1 min at 1,000 x g to remove unbound Affimers. The pellet was resuspended in PBST and Protein A (287.7 pmol) was added to the mix and incubated at room temperature for 1 h, the unbound Protein A was removed by centrifugation for 1 min at 1000 x g. The resin was then washed twice with 20 µL of wash buffer (PBS containing 0.02 M imidazole, pH 7.4). Bound proteins were eluted by incubating with 20 µL of elution buffer (PBS containing 0.25 M imidazole, pH 7.4) for 10 min at room temperature. Following this, the collection column was centrifuged for 1 min at 1,000 x g and the eluate was collected. Samples from each of the steps described above analysed using SDS-PAGE.

2.9.2 Pulldown of ClfA using streptavidin magnetic beads.

Affimers and protein A controls were added in two-fold excess over the binding capacity of Dynabeads™ magnetic streptavidin beads (400 pmol of biotinylated protein per mg of magnetic beads) (Invitrogen) following the manufacturer's recommendations. 0.5 mg (50 µL) of magnetic beads were first washed three times with 1 mL wash buffer (PBST) according to manufacturer's instructions. The magnetic beads were mixed with 400 pmol of biotinylated Affimers for 30 min by rotation at room temperature. The bound Affimers were separated from the unbound using a magnetic stand for 2 min, then ClfA 10.6 µg (200 pmol) was mixed with the magnetic bead-bound Affimers for 30 min at room temperature with rotation. Magnetic beads were

washed five times with 1 mL of 1 x PBST, and then bound Affimers were eluted by boiling the magnetic beads in 20 µL of 0.1% (w/v) SDS for 5 min. Eluted proteins were analysed using SDS-PAGE.

2.10 Measuring Affimer binding Affinity using SPR

2.10.1 SPR using commercial protein A sensor chip

To measure the binding affinity of anti-PA Affimer to Protein A, purified Affimers were injected onto a commercial chip to which modified Protein A had been immobilised (GE Life Sciences). This was done using a Biacore3000 (GE Healthcare) with the assistance of Dr. Iain Manfield at the Centre for Biomolecular Interactions technology facility at the University of Leeds. Affimers were dialysed overnight in PBST in 4℃, then the Affimers were diluted in PBST to a concentration of 1 µM. The same batch of PBST used to dilute the Affimers was first injected on to the surface of the chip and between each Affimer injection, 200 µl of Affimers or PBST were injected with the flow rate was set to 50 µL/ min.

2.10.2 Immobilisation of Affimers on Streptavidin-coated sensor chip

To remove stabilizers from the surface of the chip, 20 µL of NaCl/NaOH solution was passed over the surface of the streptavidin sensor chip for 1 min. This was done three times. Biotinylated Affimers were diluted to a range of dilutions to (1 nM-1000 nM) then injected over the surface of the chip with a flow rate set to 5 µL/min.

2.10.3 Immobilisation of PA on the surface of Ni-NTA sensor chip

A Carboxymethyl dextran 5 (CM5) (GE Life Sciences) chip was inserted into a Biacore3000 and washed with 0.1 M sodium acetate buffer (pH 5.0) at a flow rate of 20 µl/ min. The dextran groups on the surface of chip were activated by injection of 35 ul of NHS/EDC (Biacore). Protein A at concentration of 5 mg/ mL or 20 mg/ mL in sodium acetate buffer was then injected until desired amount of protein was immobilised, in which the immobilised protein that produces a signal high enough to detect and does not saturate the surface of the chip. Unreactive material was removed by

washing the surface of the chip with 20 µl of high-salt buffer (75 mM sodium acetate containing 1 M NaCl pH 5.6). The above steps were done using PA diluted in a range of concentrations of sodium acetate buffer (0.1 to 10 mM, pH 4.5 to 5.5) as pH can affect the efficiency of immobilisation.

2.10.4 SPR to measure binding affinity of anti-PA Affimer

Affimer was diluted in PBST to 1 µM and 200 µL was injected on the surface of Ni-NTA chip. The injection flow rate was set to 50 µL/min and changes in refractive index were recorded. Data was analysed using BIAevaluation Software (GE Life Sciences)

2.11 Biofilm RNA sequencing and analysis

2.11.1 RNA isolation

Overnight 5 ml planktonic cultures and biofilms and were grown as previously described in Sections 2.4 and 2.4.1, respectively. To preserve cellular RNA prior to RNA isolation, planktonic cultures were treated with 1/8th the sample volume of Stop solution (5% (v/v) saturated phenol in absolute ethanol. Immediately after removing planktonic cultures from the incubator, 125 µL Stop solution (5% (v/v) phenol in absolute ethanol) was added for every 1 mL of culture and the suspension mixed by inversion. Biofilms were also treated by adding 125 µL of Stop solution in 1 mL of PBST to the surface of the biofilm and incubation for. The biofilm was then removed by scraping as described in Section 2.4.1. In addition, a batch of biofilms was processed with Stop solution being added only after the cells have been removed from the cellulose disk and washed four times in PBST to remove loosely associated cells. 125 µL of stop solution was present in the 1 mL of PBST used to resuspended cells from the biofilm.

Following treatment with the stop solution mix, the cells were pelleted using a microcentrifuge at 13,000 x g for 10 min. The supernatant was removed and the pellet was resuspended in 385 µL Kirby lysis buffer (2% w/v SDS, 12 % w/v sodium 4-aminosalicilate, 12 % (v/v) phenol mixture, 0.05 M Tris-HCl pH 8) (Sigma) (Kieser et al., 2000) and mixed by vortexing for 1 min. Samples

were transferred to lysing matrix B tubes (MP BIOMEDICALS) and lysed using FastPrep®-24™ homogenizer (MP BIOMEDICALS) for 3 cycles of 50 s at 6.5 M/s, with incubation on ice for 1 min between each cycle. Samples were centrifuged at 13,000 x g for 1 min, mixed with an equal volume of acid phenol: chloroform: isoamyl alcohol pH 4.5 (25:24:1) and centrifuged at 13,000 x g for 10 min at 4 °C. The aqueous phase was collected and nucleic acid was precipitated by the addition of NaCl to a final concentration of 0.15 M, transferred to a new tube, mixed with 2.5 x volumes of absolute ethanol and incubated for 30 min at -80°C. After incubation, the sample was then centrifuged at 13,000 x g for 10 min at 4°C, the supernatant was removed and the pellet allowed to dry in air for 2 to 3 min. The pellet was dissolved in 700 µL of RNase-free water and further extracted with an equal volume of acidic phenol (pH 4.5). The sample was centrifuged at 13,000 x g for 10 min at room temperature. The aqueous layer was collected and an equal volume of chloroform was added, samples were centrifuged for 10 min at 13,000 x g at room temperature. The aqueous layer was collected and NaCl was added at a final concentration of 150 mM, then 500 µL of absolute ethanol were added and mixed and incubated at -80°C for 30 min. After incubation samples were centrifuged at 13,000 x g for 30 min at 4 °C. The pellet was washed twice with 200 µL of 70% (v/v) ice-cold ethanol, then air dried and resuspended in 40 µL of RNase-free water and then stored at -80°C. Nucleic acid was visualised by running on a 1.2% (w/v) agarose gel and total nucleic acid concentration was measured using a UV nanophotometer set at A260.

2.11.2 DNase I treatment

To remove contaminating DNA, samples were digested with 2 µL DNase I (4 U) for 1 h at 37 °C. Samples were then transferred to 1.5 mL Eppendorf tubes and RNase-free water was added to a final volume of 500 µL. The sample was then mixed with 500 µL acidic phenol: chloroform (Ambion). Samples were then centrifuged at 13,000 x g for 10 min at room temperature. The aqueous phase was collected and an equal volume of chloroform: isoamyl alcohol (24:1) (VWR Life Science) was added then mixed and centrifuged at 13,000 x g for 10 min at. The aqueous layer was collected and an equal volume of NaCl 0.15 M was added followed by addition of 500 µL of absolute

ethanol and incubation at -80°C for 30 min. After incubation, samples were centrifuged at 13,000 x g for 30 min at 4°C. The pellet was then washed twice with 200 µL of ice cold 70% (w/v) or (v/v) ethanol, the pellet was allowed to air dry then resuspended in 20-30 µL of RNase-free water. RNA concentrations were measured spectrophotometrically. Samples were stored at -80°C.

2.11.3 RNA sequencing

RNA sequencing was performed by Novogen using Illumina HiSeq-PE150 sequencing. Fragments were selected and sequenced on an Illumine HiSeq-PE150 platform (paired ends, read length 150 bp). RNA samples were prepared and shipped according to their specification.

2.11.4 RNA sequencing data analysis

RNA sequencing was performed by Novogene. Data was received in a zip file format which was uncompressed to a fastqsanger.gz format, data analysis was done using Galaxy software version 0.36.5. Trimming of the poly A tail adaptor sequence was done using the Trimmomatic tool, input reads for forward and revers strands were in (fastqsanger.gz) format set to paired-end reads, trimmomatic operation was set to sliding window trimming, number of bases to average across: 4, average quality required above 20. Sequence alignment was performed using Bowtie 2.0 software with input data was from forward and reverse paired files output from trimmomatic, analysis was set to galaxy default settings. The reference genomes for the alignment was S. aureus NCTC 8325 (NC_007795.1) downloaded as a GFF3 file from the NCBI data-base. This produced (BAM) file consisting of aligned reads. The reads associated with each gene position was determined using Stringtie, the input data was the output of Bowtie BAM file format, read information was set for reverse strand, reference genome was used to guide assembly, and average read length was set to 75 reads setting. This produced a (.gtf) file consisting of assembled transcripts counts and two tabular files one consisting of gene counts and the other with transcript counts. Genes that were deferential expression were identified using DEseq2 software with input data was from Stringtie output transcript counts file, settings. The DEseq2 output from galaxy

is two files, files consisting of plots are in pdf format and the result files are in tabular format.

Chapter 3: Determining the potential of Anti-Protein A (PA) and Anti-Clumping factor A (ClfA) Affimers as targets for detection of Staphylococcus aureus biofilm infection

3.1 Introduction

Staphylococcus aureus (*S. aureus*) planktonic cells can adhere to biotic and abiotic surfaces through attachment via cell wall anchored proteins which leads to colonisation of these surfaces and ultimately to biofilm formation (Foster and Hook, 1998). The colonisation of surfaces by *S. aureus* is influenced by several factors, including pH, surface tension and host plasma components. Several cell wall anchored proteins contribute to attachment to surfaces, which predominantly include the microbial surface components recognizing adhesive matrix molecules (MSCRAMMs) (Mazmanian et al., 2001). The MSCRAMMs are a family of proteins that are covalently anchored on the peptidoglycans of *S. aureus* cell wall (Mazmanian et al., 2001). Several MSCRAMMs share binding specificity against the same host components such as Clumping factor A (ClfA) and fibrinogen binding proteins (FnbA, FnbB) which all bind fibrinogen and platelets. Others can bind several host proteins such as Protein A (PA) and ClfA (Foster et al., 2013). PA and ClfA are two of the most important MSCRAMMs as they play multiple roles in *S. aureus* virulence such as involvement in biofilm formation and evasion of the immune system (Kwiecinski et al., 2014). Once a *S. aureus* cell encounters a surface, adherence is initiated by the expressed MSCRAMMs such as PA and ClfA and secreted adhesins such as delta-haemolysin (Kostakioti et al., 2013). *S. aureus* planktonic cells attach to a surface by utilizing cell wall anchored proteins whereby each is specialised in binding different host components (Moormeier, 2017). However, at this stage attachment is not finalised, that is to say that the cells can return to a planktonic cell state when faced with conditions which favour growth in the planktonic state, such as nutrient availability (Wu and Outten, 2009) or hydrodynamic force (Dunne, 2002, Goller and Seed, 2010). Irreversible attachment to a surface relies on the ability of the bacteria to withstand shear forces to remain attached to the surface (Kostakioti et al.). Contact with a surface results in changes in gene

expression and down regulation of factors favouring the planktonic state, such as initiation of transcription of the *ica* operon resulting in the production of polysaccharide intercellular adhesin (PIA) (Arciola et al., 2015).

Developing tools for detection of *S. aureus* biofilm formation to aid in diagnosis and potential treatment of IE requires the ability to detect the presence of proteins that are produced during different stages of biofilm formation. In this chapter, the raising of Affimers against the known protein targets PA and ClfA that are present on the cell wall and contribute to *S. aureus* biofilm formation will be described. Furthermore, production and purification of anti-PA, anti-ClfA and anti-biofilm Affimer will be described; further characterisation of the anti-PA and anti-clfA well be achieved by confirming specificity to their respective targets and identification of the binding kinetics. These proteins are produced and anchored onto the cell wall of *S. aureus* bacterial cell during the attachment stage of biofilm formation (Beenken et al., 2004). The multiple important roles that PA and ClfA play in *S. aureus* virulence during infection and their contribution to biofilm formation and stability makes them ideal targets for diagnosis and treatment of biofilm infections. Detection of these proteins can give an indication that the biofilm is still not fully mature, what could lead to easier treatment. Since they are expressed on the cell wall, both PA and ClfA are easily accessible as targets for Affimers *in vivo* and *in situ*. Also, the fact that both proteins are expressed in most *S. aureus* strains suggest that they would be good targets to raise Affimers against. Both proteins are also commercially available and well-studied

3.2. Results

3.2.1. Characterisation of Affimers

Affimers were raised against *S. aureus* PA and ClfA using phage display, by utilising the Affimer phage library which consisted of approximately 1.3×10^3 phage clones presenting Affimers (Tiede et al., 2017). Full-length recombinant PA (supplied as full-length biotinylated protein) (ThermoFisher) and partial length ClfA (supplied as truncated partial recombinant protein) (MyBioSource)

were used as target ligands for the phage library (Section 2.5.1). In preparation for screening with the phage library both, PA and ClfA, were biotinylated using EZ-Link NHS-SS-biotin (Thermo Fisher Scientific) by Dr. Christian Tiede and then immobilised on the surface of Streptavidin-coated microtiter plates. The phage display enrichment process yielded 26 phage clones expressing Affimers raised against PA and 48 phage clones expressing Affimers specific for ClfA. To identify the nucleotide sequences of anti-PA and anti-ClfA Affimers, Phagemid sequences were amplified by PCR and the products sequenced using the Sanger method (Sanger and Coulson, 1975) by the services of GENEWIZ Genomics, UK. The nucleotide sequences were translated into amino acid sequence using the translation tool ExPASy (https://web.expasy.org/translate/), the phagemid amino acid sequence consisting of the anti-PA Affimer is shown as a representative (Figure 3.1 A). Sequencing of the anti-PA and anti-ClfA Affimer phage clones resulted in the identification of a single unique amino acid sequence for the anti-PA Affimer and 16 unique sequences for the anti-ClfA Affimers.

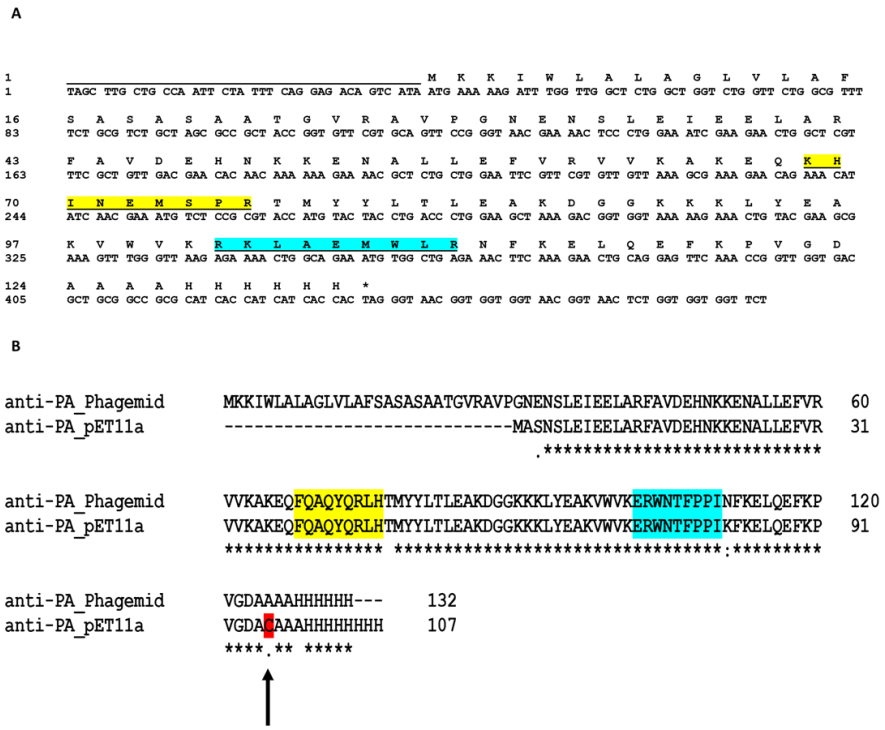

Figure 3.1 Sequence of anti-PA Affimer. A. Translation of Phagemid anti-PA Affimer nucleotide sequence to amino acid sequence identifying the position of the two variable regions of the Affimer. **B.** Anti-PA Affimer amino acid sequence alignment of phagemid and pET11a vectors (clustalo-I20191121-141439-0035-27778694-p1m); arrow indicates the location of the modification of the Affimer sequence by insertion of cysteine. Variable peptide regions are highlighted in yellow (variable peptide region 1) and blue (variable peptide region 2).

3.2.2. Affimer subcloning

One of the advantages of using Affimers is their ability to be expressed in prokaryotic host cells such as *E. coli* (Tiede et al., 2017). To achieve this the Affimer coding sequence was amplified by PCR from the phagemid vector and subcloned into pET11a plasmid containing the pBR322 origin of replication which is suitable for replication in *E. coli*. (Section 2.5.4) (Lorence, 2012, Tiede et al., 2017). The pET11a plasmid also consisted of an ampicillin resistance gene which was used as a selection marker to confirm transformation into *E. coli* competent cells when grown on LB medium supplemented with Carbenicillin (J.F and Russell, 2001). The pET11a plasmid consisting of the Affimer coding sequence was transformed into *E. coli* BL21(DE3) competent cells which utilise a T7 promoter-driven expression system. To allow site specific chemical modification of the Affimers a cysteine residue was

introduced into the Affimer coding sequence at the C-terminus using PCR (Section 2.5). Subcloning of the Affimers coding sequence and expression in *E. coli* was performed with the assistance of the BioScreening Technology Group (BSTG) group at the University of Leeds (Section 2.5).

To confirm that the correct sequence and addition of a cysteine residue have been inserted, the Affimers were sequenced using the services of GENEWIZ Genomics, UK (Sanger and Coulson, 1975). The resulting amino acid sequence of each Affimer was compared to the original phagemid amino acid sequence by alignment using the Clustal Omega alignment program available on EMBL-EBI (Figure 3.1 B). The amino acid sequences between the phagemid and pET11a expression vector were similar as indicated with the presence of the correct unique anti-PA variable loop sequence which encode the specific interaction sight to PA apart from the desired presence of an inserted cystine (Figure 3.1 B) to allow modification of the protein by biotinylation (Tiede et al., 2017). Here the anti-PA Affimer is shown as a representative example to a typical confirmation of subcloning and confirmation of insertion of the correct Affimers sequences that was performed for all Affimers generated in this thesis. Phylogenetic analysis of the 16 unique anti-ClfA Affimers sequences indicated the presence of four groups of Affimers with recognisable sequence similarities (Figure 3.2).

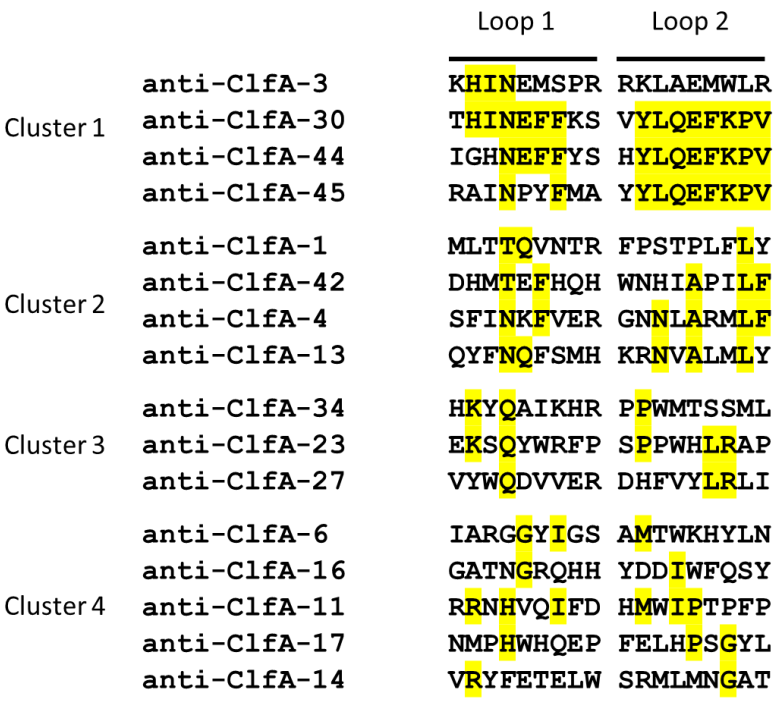

Figure 3.2 Alignment of anti-ClfA Affimer amino acid sequences of the two variable loops. Phylogenetic analysis alignment indicates similarities between the anti-ClfA Affimers amino acid sequence using Clustal Omega. Similarities between Affimer amino acids within each variable loop sequences are highlighted.

3.2.3 Affimer purification and accurate mass detection

For further investigation of the ability to bind to their target *i.e.* PA or ClfA, the PA-specific Affimer and selected representatives of ClfA specific Affimers (Table 3.1) along with selected biofilm specific Affimers (Section 4.4.2) from each cluster were purified using immobilised metal affinity chromatography (Figure 3.3.) and their identity confirmed using Liquid Chromatography-Mass spectrometry (LC-MS) (Figure 3.4). LC-MS was performed by Dr. Rachel George as part of a service provided by Biomolecular Mass Spectrometry facility at the University of Leeds. The main peaks represent dimeric and monomeric anti-PA Affimer Two forms of anti-PA Affimer (Figure 3.4). Multiple small peaks are present that correspond to residual matrix components; the peak peaks present of a few peak (14840.70 Da) corresponds to the size of lysozyme which is used in the during Affimer purification process (Section 2.7.10).

Table 3.1. Selected Anti-PA and anti-ClfA Affimer

Affimer	VR Loop 1	VR Loop 2	No. of Repeat
anti-PA	FQAQYQRLH	ERWNTFPPI	26
anti-ClfA-3	KHINEMSPR	RKLAEMWLR	5
anti-ClfA-30	THINEFFKS	VYLQEFKPV	2
anti-ClfA-1	MLTTQVNTR	FPSTPLFLY	4
anti-ClfA-4	SFINKFVER	GNNLARMLF	1
anti-ClfA-27	VYWQDVVER	DHFVYLRLI	2
anti-ClfA-6	IARGGYIGS	AMTWKHYLN	12
anti-ClfA-16	GATNGRQHH	YDDIWFQSY	8
anti-ClfA-17	NMPHWHQEP	FELHPSGYL	2

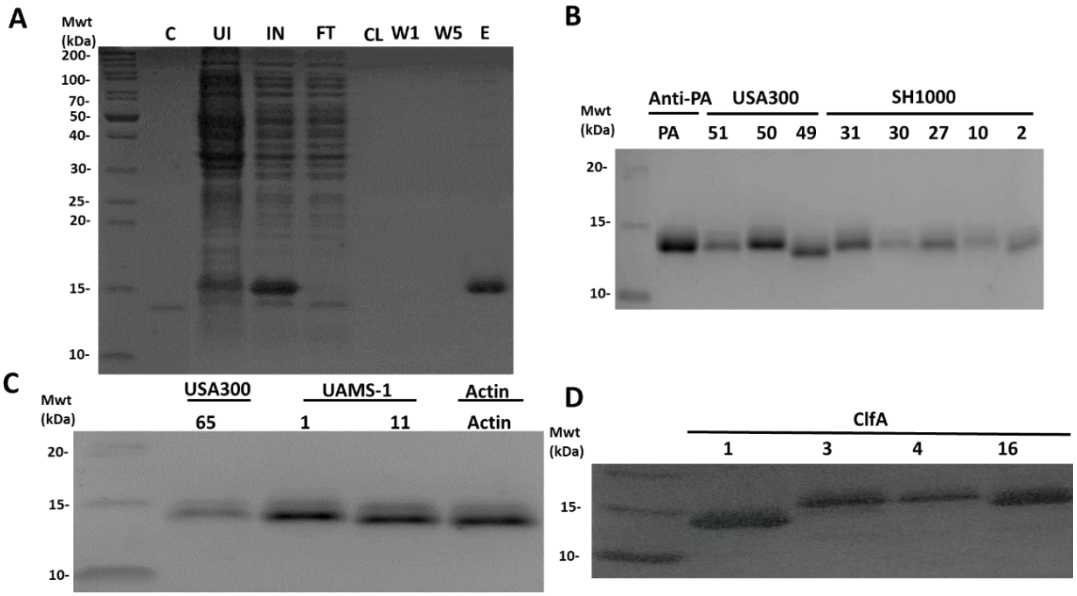

Figure 3.3 Purification of Affimers. A. SDS-PAGE gel showing steps of Affimer purification using His-tagged anti-PA Affimer as a representative example for immobilised metal-affinity chromatography; Samples were separated on a 15% (v/v) polyacrylamide gel with SDS and stained with Coomassie Blue. Gel annotation: anti-Actin Affimer control (C), uninduced sample (UI), induced sample (IN), cleared lysate (CL), flow through (FT), Wash (W), elution (E). **B.** Anti-PA and anti-Biofilm Affimers described in (Chapter 4); on gel from left to right: Anti-Protein A, anti-USA300 (51, 50, 49), anti-SH1000-(31, 30, 27, 10, 2) respectively. **C.** Bands from left to right anti-USA300 (65), anti-UAMS-1 (1, 11), anti Actin Affimer **D.** Anti-ClfA Affimers (1, 3, 4, 16).

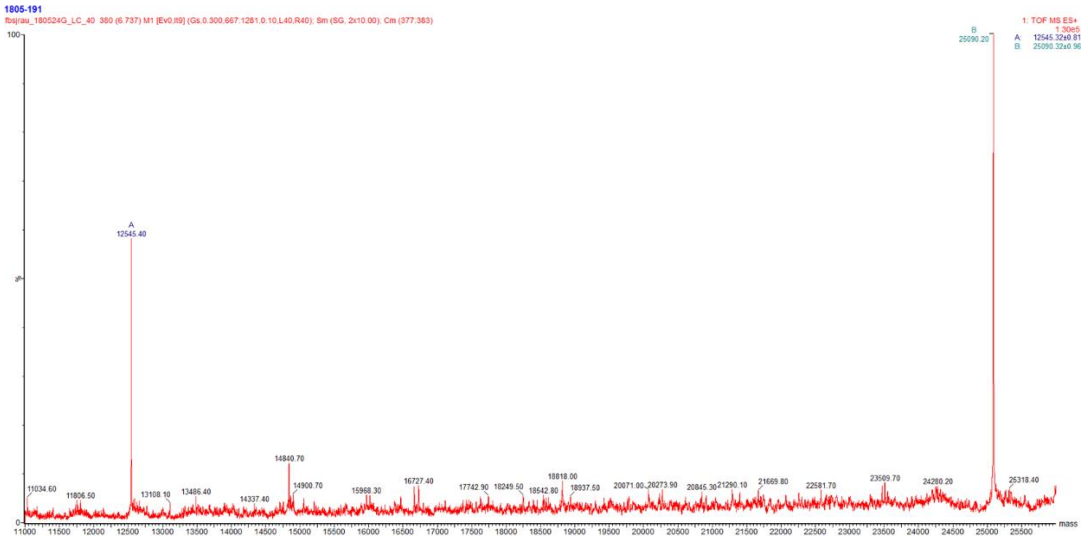

Figure 3.4 TOF-MS spectrum of anti-PA Affimer. Peak A represents the monomeric anti-PA Affimer monomer 12545.40 Da and peak B represents anti-PA Affimer dimer (25090.20 Da). Figure represents a typical spectrum of Affimers using PA as an example. The expected mass was calculated by subtraction the mass of a methionine residue from the observed mass. MS was performed by Dr. Rachel George at the Mass Spectrometry Research Facility at the University of Leeds (Section 2.7.13).

3.2.4. Confirmation of anti-ClfA Affimers binding to ClfA

Initially, the ability of all of the 48 Phage clones expressing anti-ClfA Affimers were screened for binding to ClfA using phage ELISA by Dr. Christian Tiede from the BSTG group at the University of Leeds (Figure 3.5). ClfA was biotinylated to allow immobilisation on the surface of a streptavidin-coated 96-well microtiter plate, and the 48 phage clones expressing anti-ClfA Affimers were incubated within the wells. Unbound phage clones were removed by washing with PBST, and then wells were incubated with an anti-fd-Bacteriophage-HRP antibody conjugate (Seramun). Binding of the antibody was detected by addition of TMB and measuring the absorbance at 620 nm, resulting from the oxidation of TMB by HRP. An anti-yeast Sumo Affimer (anti-ySumo) phage clone (supplied by the BSTG group at the University of Leeds), which was produced from a completely different and independent enrichment process, was used as a negative control in the experiment (Hughes et al.,

2017). Phage clones that showed an absorbance value higher than the control were considered as positive binders for ClfA (Figure 3.5).

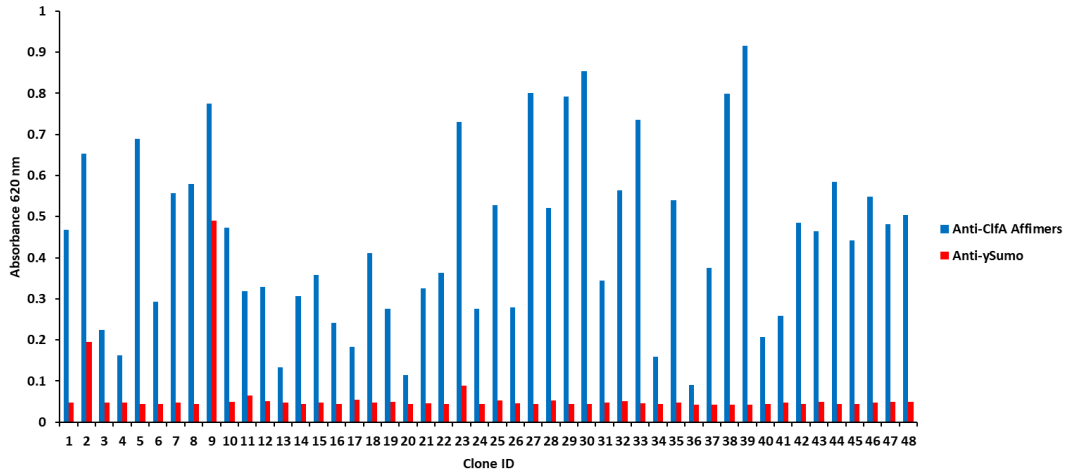

Figure 3.5 Screening of anti-ClfA Affimer clones using phage enzyme-linked immunosorbent assay (ELISA). Analysis of binding of 48 phage clones expressing anti-ClfA Affimers to immobilised ClfA. Phage clone expressing anti-ySumo Affimer was used as a negative control. For more details refer to (Section 2.5.2) Binding was detected using a secondary antibody anti-fd-bacteriophage-HRP conjugate. After addition of TMB absorbance was measured at 620 nm.

Although phage ELISA indicated successful binding of the anti-ClfA Affimers expressed on the phage to biotinylated ClfA (Figure 3.5), it was necessary to confirm that the Affimers would retain the ability to bind ClfA while not being expressed on the phage. Therefore, immunoprecipitation was employed to investigate binding of purified anti-ClfA Affimers to ClfA. First, selected anti-ClfA Affimers were expressed in *E. coli,* then purified via immobilised metal-affinity chromatography using Dynabeads™ magnetic streptavidin beads (Invitrogen) and used as bait for ClfA in a pulldown assay. The purified anti-ClfA Affimers (1, 3, 4 and 16) were biotinylated using maleimide chemistry and bound to streptavidin magnetic beads (Section 2.7.5.1). Unbound Affimers were removed by washing with PBST. ClfA was incubated with the beads and unbound ClfA was removed in the flow through. The remaining bound ClfA was eluted by boiling in 20 µl of 0.1% (v/v) SDS. (Figure 3.6 A. Lane 8, 11, 14; B. Lane 8). The presence of a band of 52-kDa corresponding to ClfA in the elutes of anti-ClfA-1,3, 4 and 16) (Figure 3.6. Panel A. Lane 8, 11, 14) but not in elutes of the Streptavidin magnetic beads or anti-Actin Affimer (Figure 3.6 B. Lane 8) is indicative of anti-ClfA Affimers binding to ClfA and the anti-Actin

Affimer not binding to ClfA. Streptavidin magnetic beads were used as a control to show that ClfA does not bind non-specifically to the beads (Figure 3.6 A. Lane 5). Results from the pulldown suggest that anti-ClfA-1, 3 and 4, bind ClfA, which matches with the results from the phage ELISA. However, for anti-ClfA-16 the results were not unambiguous as the band representing the Affimer was less intense than that of anti-ClfA-1,3 and 4; this could indicate that anti-ClfA-16 does not bind to ClfA with the same affinity as the other Affimers therefore the majority of the Affimers was not retained in the elute.

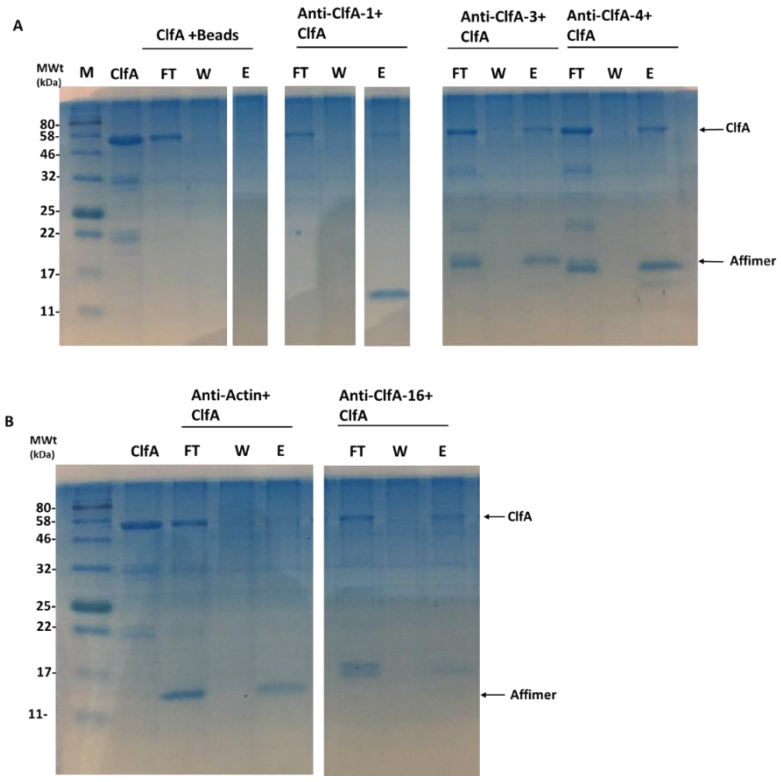

Figure 3.6 Confirmation of binding of anti-ClfA Affimer to ClfA. 20% SDS-PAGE gel showing biotinylated Anti-ClfA Affimers (1, 3, 4, 16) immobilisation onto streptavidin magnetic beads and used to pulldown ClfA. Negative control (anti-actin Affimer), annotation on gel: Flow through (FT), PBST wash (W) and pulldown elution fraction (E).

3.2.5 Confirmation of anti-PA binding to PA

Phage ELISA was not suitable for PA screening because of cross reactivity observed between PA and the anti-fd-Bacteriophage-HRP secondary

antibody (Section 4.3.3.1). Therefore, confirming binding of the anti-PA Affimer to PA was possible only after expression in *E. coli* and purification.

To investigate the ability of the anti-PA Affimer to bind PA, the purified hexa-histidine-tagged recombinant anti-PA Affimer was rebound to Ni-NTA resin and used to pulldown PA. Anti-ClfA-3 Affimer was used as a negative control as it should not bind protein A. Unbound protein A, anti-PA or ClfA were removed in the flow through and the bound proteins were eluted using elution buffer (PBS containing imidazole, pH 7.4) (Figure 3.7 Lane 4 and 5). Regarding the negative control with anti-ClfA-3, PA was found in the flow through and only the anti-ClfA-3 Affimer was retained in the elution fraction (Figure 3.7 Lane 6, 7), indicating that it does not bind PA. As a control to confirm that PA does not cross-react with the nickel resin, only protein A was incubated with the resin, all PA was removed in the flow through and no PA was retained in the elution (Figure 3.7 Lane 9, 10). PA was retained in the elution fraction when incubated with anti-PA Affimer bound resin (Figure 3.7 Lane 6) indicating that anti-PA binds specifically to PA.

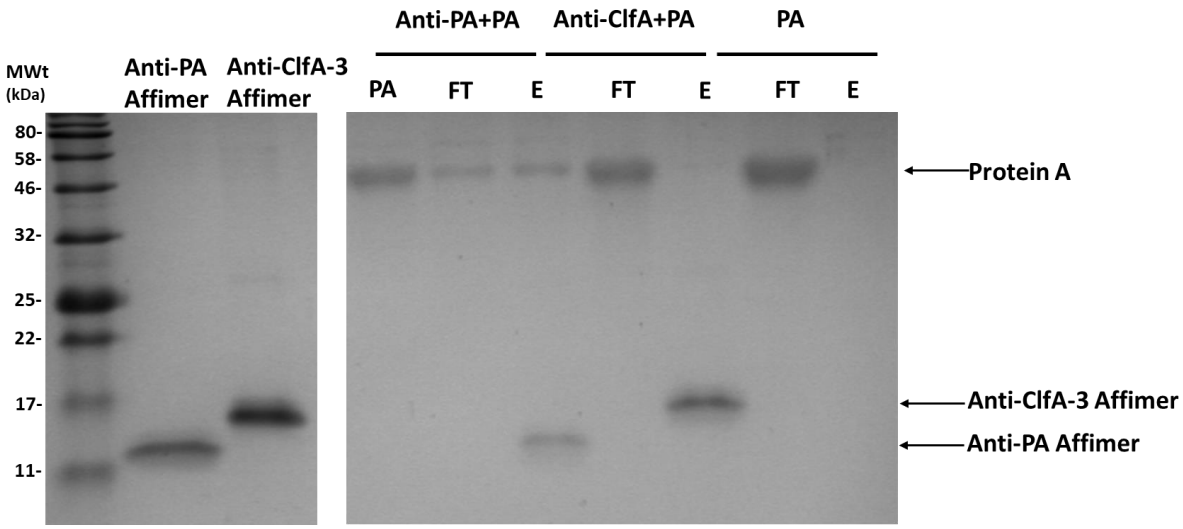

Figure 3.7 Confirmation of anti-PA Affimer binding to PA. A 15% (v/v) polyacrylamide gel with SDS showing the ability of the anti-PA Affimer to pulldown PA using Ni-NTA resin. Anti-PA was incubated with the Ni-NTA resin, and unbound anti-PA was removed by washing with wash buffer. PA was added to the anti-PA and Ni-NTA resin mix, and excess PA was removed. Bound anti-PA and PA were eluted using 20 µL of elution buffer (PBS containing 0.25 M imidazole, pH 7.4). Equal volumes of the remaining proteins bound to the resin were loaded on to SDS-PAGE gel. Lane (1) shows Protein molecular weight marker; Lane (2) shows anti-PA Affimer; Lane (3) shows anti-ClfA-3 Affimer; Lane (4) PA; Lane (5, 6) Anti-PA shows pulldown PA FT and E; Lane (7, 8) anti-ClfA pulldown PA, Lane (9, 10) Protein A only. Annotation of the SDS gel are as follows: Flow through (FT), Elution (E).

3.2.6 Investigation of binding kinetics of anti-PA using Surface Plasmon Resonance (SPR)

Since the anti-PA Affimer was confirmed to bind PA via pulldown assays, the next step was to further characterise binding of the anti-PA Affimer to PA to establish the affinity of the interaction and kinetics using Surface Plasmon Resonance (SPR). SPR measurements were carried out using a BIAcore 3000 instrument (GE LifeSciences). SPR is a technique where binding kinetics are measured via an optical biosensor based on changes in the binding signal resulting from the interaction between two molecules (Michel et al., 2017). The interaction between the two molecules is presented in the form of a sensorgram which can be used to extract the binding kinetics information. SPR was employed in order to measure the binding kinetics, which provide valuable information on whether the anti-PA Affimer is suited to be used as a potential diagnostic or therapeutic tool and can be incorporated into a

biosensor for detection of *S. aureus* biofilm formation. With SPR it is possible to monitor interactions between proteins and obtain binding kinetics in real time. Upon injection a change in the binding signal is seen. The amount of protein binding to the surface is indicated by the increase in the number of response units (RU). The rate of change in binding signal will be used to calculate binding kinetics such as association and dissociation rates. To obtain binding kinetics, the SPR sensorgrams are processed using the BIA evaluation software™. To normalise the generated sensorgrams, data for all FCs were overlaid over each other using the plot overlay function. Then the injection start times for all FCs were aligned and set to the same point and that point was set to zero. Subsequently, the reference FC binding curve resulting from PBST injection was subtracted from the other binding curves. To obtain binding kinetics (K_{on}, K_{off}, KD), binding curves and fitted curves were generated using BIA evaluation software™ and then replotted using Microsoft Excel.

To measure the binding affinity of the anti-PA Affimer to PA, a commercially available PA sensor chip was used (GE Healthcare life Sciences), which is commonly used to immobilise antibodies via PA binding (Chu et al., 2014). The sensor chip consists of four flow cells (FC). Each FC surface is coated with a layer of carboxymethylated dextran matrix with immobilised recombinant PA. IgG was used as a positive control for PA binding and to provide a reference point to compare binding kinetics. Anti-Actin Affimer was used as negative control to identify the level of non-specific binding to the PA sensor chip. Affimers and IgG were injected onto the surface of the commercial PA chip at a concentration of 1 µM. Both the anti-PA Affimer and IgG showed binding to PA (Figure 3.8 A, B), with IgG showing a change in binding signal (1200) which is about 2.9-fold higher than that of the anti-PA Affimer (410 RU). The anti-Actin Affimer did not show any binding to PA (Figure 3.8 C) as the change in signal resulting from injection of the anti-Actin Affimer over the PA surface is not indicative of binding but is similar to that of a buffer injection. This signal was about 6.6-fold lower than that of anti-PA Affimer (410 RU) and about 20-fold lower than that of IgG (1200 RU). The PA chip was also used to test binding of Affimers raised against *S. aureus* biofilm

(Chapter 4) to PA. The anti-biofilm Affimers injected over the PA surface showed change in binding signal similar to that of the anti-Actin Affimer, suggesting that they do not bind PA.

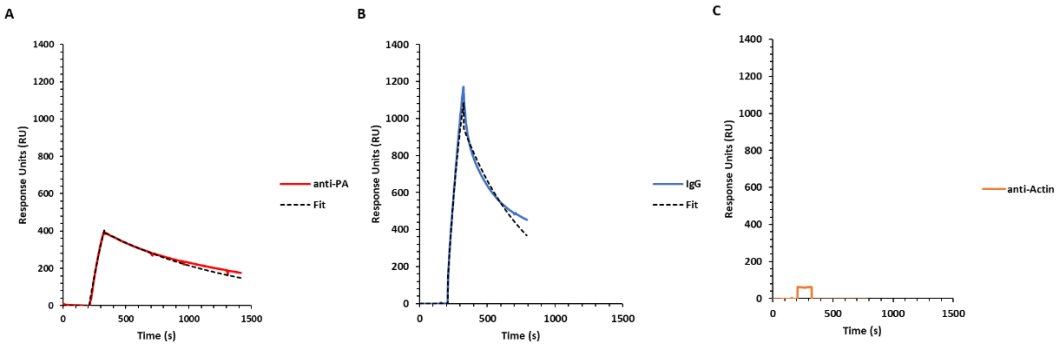

Figure 3.8 Measuring affinity of anti-PA Affimer for Protein A on a commercial PA chip using Surface Plasmon Resonance (SPR). Sensorgrams showing binding to commercial PA sensor chip, with actual data represented by coloured curve and fitted data represented by black curve. A. Anti-PA Affimer (1 µM) binding to commercial PA chip B. IgG (1 µM) binding to commercial PA chip. C. Anti Actin (1 µM) (negative control). Data shown is one dataset. Fitted curves were generated by Biacore analysis software.

The PA chip was utilised to investigate if anti-PA Affimer can block IgG binding to PA. This will provide useful information such as if the anti-PA Affimer has the same binding sites as the IgG or if the binding sits are adjacent to each other interfering with binding of the other molecule. This approach was achieved by performing two injections. First, anti-PA Affimer was injected over the chip followed by a second injection consisting of an injection of IgG. As control, anti-PA Affimer and IgG were injected alone on to the surface of the chip (Figure 3.9 A, B). To account for slow dissociation of anti-PA Affimer or IgG from the chip buffer was injected after each injection. Then anti-PA Affimer (1 µM) was injected and IgG (1 µM) was injected immediately after (Figure 3.9 C). The resulting change in binding signal resulting from the IgG injection was 378 RU which is 2.8-fold lower than 1050 RU when IgG was injected alone (Figure 3.9 B, C). This suggests that partial blocking of the IgG binding position was achieved.

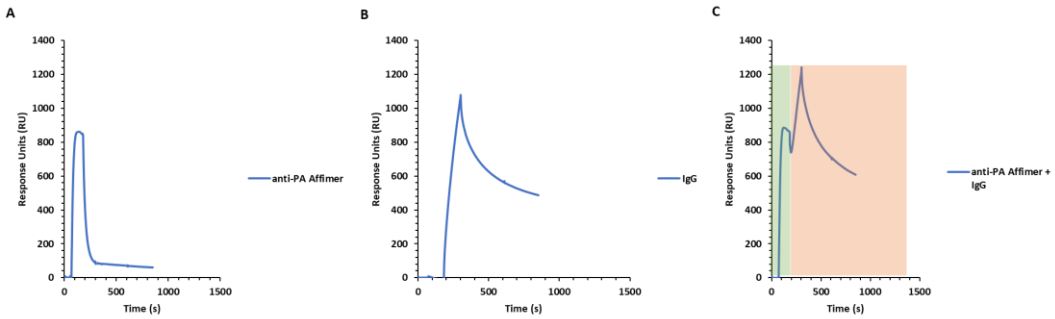

Figure 3.9 Blocking IgG binding to PA using anti-PA Affimer. Sensorgram showing injection of anti-PA Affimer to block IgG binding to PA sensor chip. **A.** anti-PA Affimer (1 µM). **B.** IgG (1 µM). **C.** Anti-PA Affimer (1µM) (green shaded area), followed by IgG 1µM (orange shaded area). Shaded area border indicates injection start.

The PA chip surface is saturated with PA, which presents limitations such as introducing the possibility of rebinding of anti-PA Affimer or IgG to immobilised PA, as the surface saturation could interfere with obtaining accurate binding kinetics. Also, the inability to obtain complete blocking of IgG binding to PA by the anti-PA Affimer might be because the concentration of anti-PA used was not enough to completely block all IgG binding sites since the surface of the chip is saturated with PA.

3.2.7 Immobilisation of proteins on SPR sensor chip

In order to avoid the limitations associated with the commercial PA chip, such as absence of a reference FC and the saturated chip surface, Carboxymethyl dextran 5 (CM5) and Streptavidin (SA) (GE Healthcare life Sciences) chips were prepared in house. Thereby different amounts of PA or anti-PA Affimer were immobilised on the surface of a CM5 or SA sensor chip, to obtain surfaces with high and low density of immobilised PA or Affimer. To quantify the amount of protein immobilised, the changes in response units before and after each injection was recorded. In each chip FC1 was left empty to act as a reference surface, to account for chip-chip variation, anti-actin Affimer controls were included.

Before immobilisation of proteins on the surface of the CM5 chip, a pH scouting step was included to determine the most optimal buffering condition to allow coupling whilst maintaining an appropriate pH for the protein to remain stable (Drescher et

al., 2009). Proteins were diluted in NaAc buffer with different ionic strength and a range of pH (4.5-5.6). Each mix of protein and buffer were injected separately on to the surface of the chip and RUs were recorded before and after injection to investigate which buffer will result in immobilisation of PA (Figure 3.10). The buffer which resulted in immobilisation of PA was a 0.01 % PBST with 10 mM NaAc pH 5.0, the surface of the chip was conditioned using the buffer, then PA was injected onto the CM5 chip surface. Response units accompanying the change of binding signal were recorded 2 min after the stop of the injection to monitor and confirm immobilisation by maintaining the same RUs. Proteins were immobilised on the surface of SPR CM5 sensor chip via amine coupling whereby RU values were 99 and 1964 for low- and high-density surfaces of PA respectively (Figure 3.10 Panel A and B respectively). The concentration of PA to be immobilised on each injection is reflected in the amount of increase in change in RUs, as duration of each injection and quantity of the analyte being immobilised affect the increase in RUs.

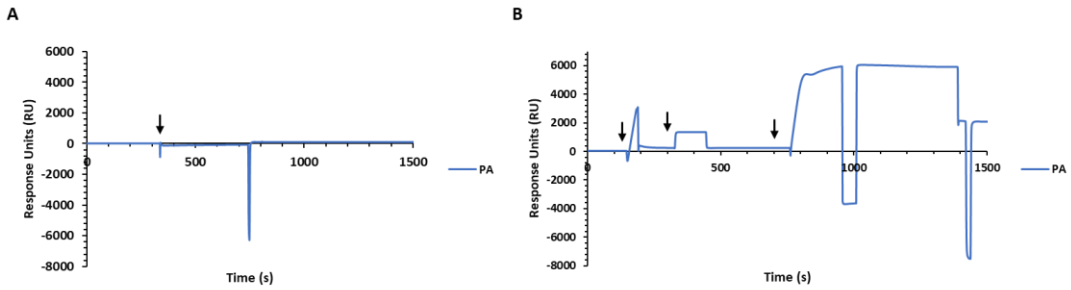

Figure 3.10 Immobilisation of PA on CM5 sensor chip. Protein A was injected over an activated CM5 chip surface using a flow rate of 5 µL/ min. A. Injection of Protein A (5 µg/ ml) to immobilise protein with response signal equivalent to 99 RU B. Injection of Protein A (20 µg/ ml) to immobilise protein with response signal equivalent to 1964 RU. Injections times indicated by arrows.1 RU ~1 pM/ mm^2.

3.2.8 Measuring binding affinity of anti-PA using CM5 chip

To identify the limit of detection of the high-density PA surface, anti-PA Affimer was titrated over the chip using a range of concentrations. anti-PA Affimer was injected on to the surface of CM5 chip in concentrations ranging from (0.125-1 µM) (Figure 3.11).

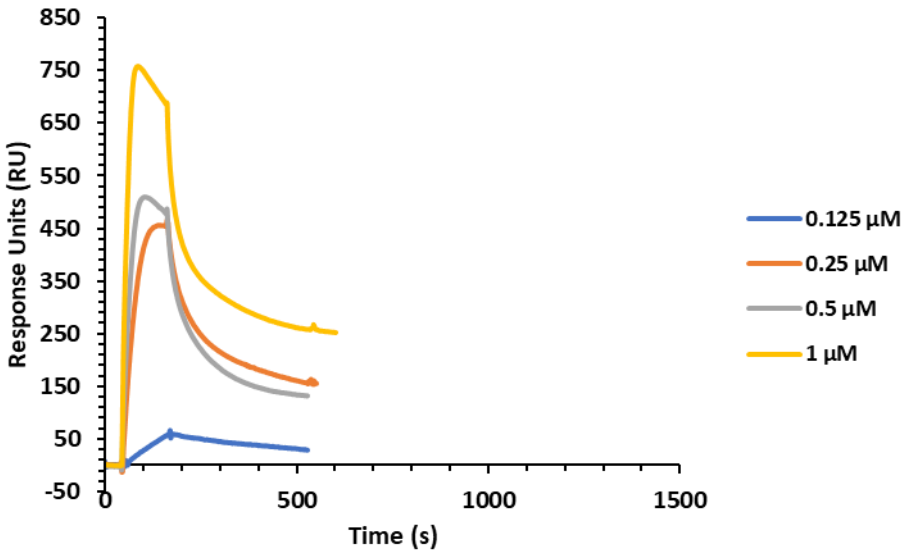

Figure 3.11 Sensorgram showing a concentration dependent change in binding signal using SPR. Injection of anti-PA Affimer onto surface with immobilised PA (1964 RU) using a range of concentrations (0.125- 1µM).

The highest concentration (1 µM) caused the greatest change in binding signal therefore, it will be used for comparison with kinetic values of IgG binding to protein A (Figure 3.12). The anti-PA Affimer and IgG binding curves were fitted as mentioned in (Section 3.3.4). The average of the constants for binding kinetics of anti-PA Affimer and IgG to PA are summarised in (Table 3.2). Average K_D of anti-PA Affimer recorded on the CM5 chip is (118 nM) which is 2.8-fold lower than the K_D recorded on the PA chip which is (333 nM). This confirms that the PA chip has limitations when trying to measure binding kinetics confirming that the choice to use the CM5 chip was the right one. Although the affinity of the anti-PA Affimer to PA was lower by about 20-50-fold (K_D 118 nM and 333 nM) than that of other previously characterised Affimers to their targets such as, Affimer against diclofenac (K_D 73 nM) and anti-Tenascin C (TNC) Affimer with K_D of 5.7 nM and (Koutsoumpeli et al., 2017, Tiede et al., 2017). However, it is within the parameters of an expected Affimer K_D as they vary with a wide range of K_D ranging from nM to µM (Koutsoumpeli et al., 2017). The Affinity of the anti-PA Affimer to PA for the CM5 and PA chips is about 59 and 160-fold lower respectively than that of reported IgG affinity to PA with a K_D ranging from 2 to 10 nM (Choe et al.,

2016, Rispens and Vidarsson, 2014). This however does not exclude the use of the anti-PA Affimer as it possesses many attributes such as its small size and ease of production that make it a suitable alternative to antibodies (Tiede et al., 2017).

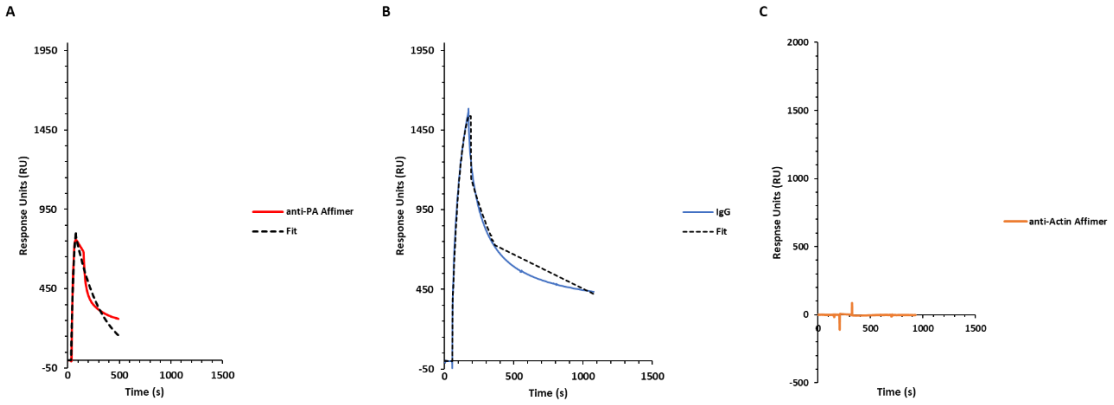

Figure 3.12 Measuring affinity of anti-PA Affimer for Protein A using SPR. Sensorgram showing: A. Anti-PA binding to PA (760 RU). **B.** IgG binding to PA (1540 RU) Actual data represented by coloured curve, fitted data represented by black curve. **C.** Anti-Actin Affimer binding to PA. Data are from at least three independent replicates.

Table 3.2 Binding kinetics for anti-PA Affimer and IgG

	PA chip	CM5 chip	PA chip	CM5 chip
	Anti-PA Affimer		**IgG**	
k_{on} ±SD (M^{-1} s^{-1})	1.33E+04 SD± 1.68E+04	1.32E+04 SD± 5.73E+03	4.27E+03 SD ±1.31E+03	1.65E+04 SD± 9.93E+02
K_{off} ±SD (s^{-1})	6.77E-03 SD± 9.60E-03	1.51E-03 SD± 1.26E-03	1.41E-03 SD ±4.67E-04	2.31E-03 SD± 4.98E-04
K_D±SD (nM)	332 SD± 157	118 SD± 7.33E-08	362 ± SD 141	140 SD± 312
Standard deviation (SD)				

3.2.9 Investigation if the anti-PA Affimer can compete with Mouse monoclonal antibodies (mAB) for PA binding

To further investigate if the anti-PA Affimer can compete for binding to PA, a modified approach was used. The intent was to investigate the ability of mAB to block binding of PA to the anti-PA Affimer. This approach was achieved by immobilisation of PA and anti-PA onto the surface of an SA chip. The SA chip surface is made up of dextran with immobilised streptavidin. For immobilisation onto the SA chip anti-PA Affimer and PA were biotinylated using EZ-Link NHS-SS-biotin (Thermo Fisher Scientific) (Section 2.7.5.1). The total increase in change in binding signal resulting from immobilisation of PA was equal to 515 RU (Figure 3.13 A) and that of anti-PA Affimer was equal to 474 RU (Figure 3.13 B).

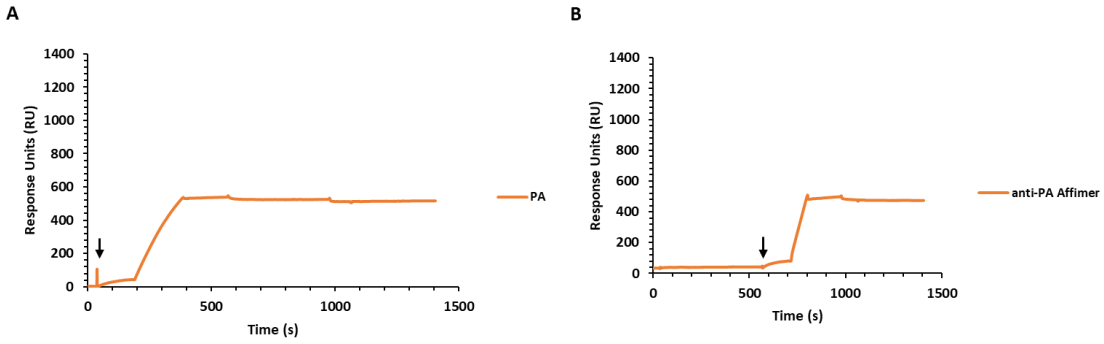

Figure 3.13 Immobilisation of proteins on streptavidin sensor chip. A. Immobilisation of PA (515 RU). **B.** Immobilisation of Anti-PA Affimer (474 RU). Biotinylated PA or anti-PA Affimer were injected onto the activated surface of the chip using a flow rate of 5µl/ min, injection times indicated by arrows.

The ability of the anti-PA Affimer to compete with mAB for binding to PA was investigated in an attempt to characterise the binding site of the Affimer and whether the binding position is shared between the Affimer and mAB. The possibility that the anti-PA binds to PA in a way that would prevent binding of mAB would indicate that the Affimer could be utilised as a therapeutic tool to prevent opsonisation. This was achieved by performing a co-injection, in which first PA is injected over the surface with immobilised anti-PA Affimer then immediately after a second injection consisting of a mix of PA and mAB

at 1:1 or 1:5 molar ratio. Single injections of PA and mAB were used as controls to indicate the expected range of binding signal. Single PA (0.01 µM) or mAB (0.05 µM) injection resulted in a change in binding signal equivalent to 71 and 179 RU respectively (Figure 3.14 A, B). Next, PA and mAB were co-injected onto the SA chip in which PA 0.05 µM was injected first, followed by a second injection consisting of 0.05 µM PA and 0.05 µM mAB (Figure 3.14 C). Sensorgram for the co-injection on surface with immobilised PA resulted in no change in binding signal when PA was injected and a change in binding signal equal to 120 RU after the second injection consisting of PA and mAB (Figure 3.14 C). Furthermore, sensorgram for the co-injection on surface with immobilised anti-PA Affimer when protein A is injected, a change in binding signal equal to 44 RU occurs which confirms the result of the control (Figure 3.14 D). During the second injection a total change in binding signal equal to 215 RU is seen (Figure 3.14 D). This 4.8-fold increase in binding signal could be due to the fact that mAB is already bound to PA in solution forming a larger molecule which results in a larger change in binding signal when binding on the surface. This suggests that PA can bind both anti-PA Affimer and mAB simultaneously and that mAB does not block anti-PA Affimer binding to PA when competing at a 1:1 ratio.

When the injection of PA and mAB onto the SA chip surface with immobilised anti-PA Affimer is performed using a 1:5 ratio of PA: mAB and where PA (0.01 µM) is injected first a change in binding signal equal to 75 RU occurs. The second injection consisting of PA (0.01 µM) and mAB (0.05 µM) only resulted in change in binding signal equal to 85 RU. This 10 RU increase does not indicate PA is binding to immobilised anti-PA Affimer, indicating that using 5-fold the concentration of mAB is sufficient enough to prevent PA from further binding to anti-PA these are data from singe replicates, the results are not confirmed. This suggests that the anti-PA Affimer cannot compete with immunoglobulins for PA binding, therefore using the anti-PA Affimer in a therapeutic application to prevent opsonisation is most likely not achievable.

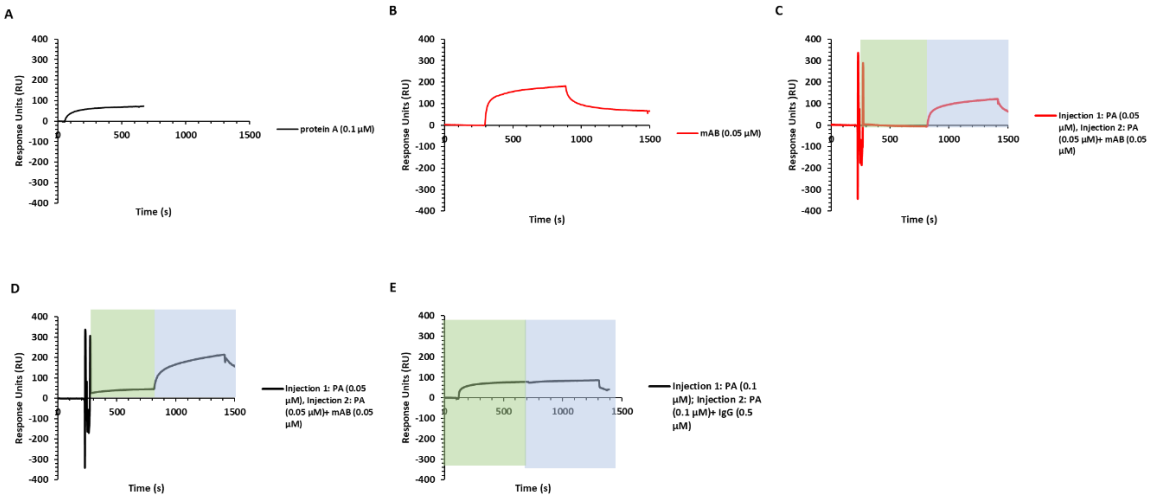

Figure 3.14 Blocking PA binding to anti-PA Affimer using mAB. Sensorgram showing attempted blocking of PA binding to immobilised anti-PA Affimer using mAB. A. Injection of Protein A (0.01 µM) onto surface with immobilised anti-PA Affimer (71 RU); **B.** Injection of mAB (0.05 µM) onto surface with immobilised PA (179 RU); **C.** Co-injection of PA and mAB onto surface with immobilised PA; **D.** Co-injection of PA and mAB onto surface with immobilised anti-PA Affimer. **E.** Co-injection of PA and mAB onto surface with immobilised anti-PA. Green shaded area represents of first injection, blue shaded area represents of second injection. Data from single replicate.

3.3 Discussion

PA and ClfA are both promising candidates to target using Affimers for detection applications in diagnosis or therapeutics for endocarditis and possibly other *S. aureus* related infections. The focus of this chapter is to investigate the interaction of Affimers raised against the *S. aureus* proteins PA and ClfA against their prospective targets. The selection and production of the Affimers is described in detail throughout this chapter. The ability of the Affimers to interact with their targets is investigated using a combination of techniques such as phage ELISA (ClfA only), pull-down assays and SPR.

Raising Affimers against PA using phage display was successful in which 26 phage clones with the anti-PA Affimer sequence were isolated. However, upon identification of the sequence of the anti-PA Affimer phage clones, it was found that all the clones share the same sequence. Although, it was hoped that multiple Affimers with different sequences would be isolated thereby providing multiple potential PA binders. The fact that 26 phage clones were isolated and only one sequence was identified indicates that they recognised

the most accessible binding ligand on PA. Therefore, when measuring the binding kinetics of the interaction of the anti-PA Affimer with PA it was hoped that anti-PA would have a high affinity for PA which would indicate that the anti-PA Affimers would be able to compete with host components for PA binding during in vivo detection of *S. aureus* biofilm. SPR measurements of the binding kinetics between anti-PA binding to PA indicated that anti-PA bind to PA with an average K_D of 118 nM (Table 3.2). This K_D is 1.8-fold lower than the average K_D that was recorded for mAB (K_D of 140 ±312 nM) (Table 3.2), Furthermore, the K_D that was recorded for mAB is not within what is expected from a typical IgG binding to PA reaction which is reported as ranging from K_D 2 to 10 nM (Choe et al., 2016, Rispens and Vidarsson, 2014). Similarly, the K_D values for IgG did were much lower than the reported K_D values. This is probably due to the fact that the fitted curves used to calculate the binding kinetics which are generated by the BiaCore™ software did not fit the binding curve in a way that would allow accurate calculation of the binding kinetics. On the other hand, the K_D of the anti-PA Affimer (118 nM) is within an acceptable range of recorded Affimer typical Affimer K_D, such as, Affimer against diclofenac (K_D 73 nM) and anti-Tenascin C (TNC) Affimer (K_D of 5.7 nM) (Koutsoumpeli et al., 2017, Tiede et al., 2017).

The fact that anti-PA is able to recognise immobilised PA provides proof of principle for use anti-PA as a tool for detection of *S. aureus* biofilm, further confirmation that anti-PA is a viable candidate to consider of imaging and diagnostic application of *S. aureus* biofilm is indicated by anti-PA binding to *S. aureu*s biofilms which will be discussed in Chapter 4. Part of the importance of PA in *S. aureus* virulence is its ability to bind various classes of antibodies mostly IgG and IgM (Foster et al., 2014, Yang et al., 2003). Therefore, the potential for the use of anti-PA for therapeutic applications such as preventing PA binding to immunoglobulins thereby preventing opsonisation was investigated (Foster et al., 2014, Yang et al., 2003). It is a possibility that the Anti-PA Affimer might occupy the same binding sites as IgG, therefore it was thought that it could compete with IgG over these sites. Another possibility is that the binding sites are different but close enough that Affimer binding can block interaction of IgG with its binding site. Unfortunately, no blocking was

achieved in attempts at blocking PA binding to IgG via anti-PA (Figure 3.10). This was understandable since IgG has a higher affinity to PA than the anti-PA Affimer, furthermore, protein A has 4-5 IgG binding sights (Foster et al., 2014, Yang et al., 2003). In this experiment an equimolar ratio of anti-PA and IgG were allowed to compete for PA binding, which is not sufficient amount of anti-PA to compete since as mentioned above PA has 4-5 IgG binding sights (Foster et al., 2014, Yang et al., 2003). Therefore, a higher molar ratio (5 to 10-fold higher) between anti-PA and IgG should be used in order to allow completion between anti-PA and IgG. The potential of anti-PA to be used to prevent opsonisation in *S. aureus* biofilm colonisation depends on the amount of anti-PA needed to compete with IgG in the host body.

Both Affimers were confirmed to bind their prospective targets, however further investigation into their ability to be used as a diagnostic tool to detect *S.* aureus biofilm in IE still needs to be explored. Initial investigation on that front have already been attempted for one of the anti-ClfA Affimers. The characterised anti-ClfA Affimers which were confirmed to bind ClfA via pulldown (Figure 3.8) were passed on to PhD student Jack Caudwell who is working with Professor Bruce Turnbull and Professor Stephen Evans at the University of Leeds and are part of the collaboration team with Dr. Jon Sandoe at Leeds General Infirmary. The collaboration team have been successful in attempting to characterise the interaction between anti-ClfA-1 Affimer and ClfA and found that anti-ClfA-1 is able to bind ClfA with a K_D of 64 nM using Isothermal titration calorimetry. Furthermore, they were able to successfully conjugate anti-ClfA-1 Affimer to a dipalmitoylphosphatidylcholine (DPPC) lipid microbubble. The targeted the anti-ClfA-1 Affimer coated microbubble demonstrated that they are able to bind to recognise *S. aureus* UAMS-1 biofilms grown in microfluid devices. With their success, the possibility of using anti-PA Affimer and the other anti-ClfA Affimers in conjugation with microbubbles for *S. aureus* biofilm imaging is now more feasible.

Although the anti-ClfA-1 Affimer has been successfully characterised as mentioned above, there are still 15 more anti-ClfA Affimers that could be further characterised by determining their affinity for ClfA. Since the sequence

of these Affimers are different this suggests that they might recognise different binding sights on ClfA. Furthermore, the ability of the anti-ClfA Affimers to block ClfA binding to fibrinogen could be investigated. Initially this was intended as part of characterisation of the selected anti-ClfA Affimers (Table 3.1). This will allow selection of the Affimer. However, further characterisation of anti-ClfA Affimers by measuring binding kinetics for binding to ClfA using SPR was not achieved; this was because immobilisation of ClfA was not successful which was due to the fact that ClfA was solubilized in Tris-HCl buffer which interferes with the immobilisation. Several dialysis steps were carried out in PBST to Tris-HCL but there were still traces of Tris-HCL even after dialysis which prevented ClfA from attaching to the sensor chip surface. Due to time limitation and other factors such as the quantity of ClfA protein that was left over from previous experiments was not sufficient to attempt other methods to immobilise ClfA. If sufficient time and amount of ClfA was available, biotinylation of ClfA and immobilisation onto the surface of a streptavidin chip would have been a reasonable approach to then obtain binding kinetics for anti-ClfA Affimers.

Understanding where the anti-PA and anti-ClfA Affimers bind to their perspective targets is an important aspect of their characterisation. For the Affimer to be clinically useful in detection of *S. aureus* biofilm, they need to be able to recognise regions involved in the function of their targets (i.e. PA and ClfA) in order to inactivate them or interfere with their function if used for therapeutic applications. Furthermore, the binding sight would need be exposed in its natural environment which would most likely be the same as ones involved in the protein function. Identify the interaction between anti-PA and anti-ClfA Affimers to their prospective targets is possible using X-Ray co-crystallisation. The ability to identify Affimer-target complex was successfully demonstrated in previous studies (Robinson et al., 2018). Therefore, examining the ability of the anti-PA and anti-ClfA Affimers to occupy PA and ClfA binding sights Identification of the Affimer binding sight would be valuable information to investigate the ability of Affimers to be used to inhibit biofilm formation by interfering with the IgG or fibrinogen binding sights using structural studies. The crystal structure of Protein A IgG binding sight and ClfA

fibrinogen binding sight are both available in Protein Data Bank (PDB); the crystal structures of ClfA Fibrinogen gamma receptor (PDB ID: 2VR3) and IgG FC gamma receptor (PDB ID:3AY4).

The results obtained in this chapter demonstrate that it is feasible to obtain Affimers specific for *S. aureus* ClfA and PA proteins. This provides proof of concept of the specificity of the Affimers as well as providing several possibilities for the exploration of different applications of the Affimers as diagnostic or therapeutic tools. Recently, Affimers raised against fibrinogen were developed to be used as therapeutic tools to minimize bleeding and stabilize blood clots in patients (Kearney et al., 2019). The Affimers showed promising binding data to immobilised fibrinogen with a K_D of 52 and 38 nM that resulted in delayed fibrinolysis of clots formed from purified fibrinogen (Kearney et al., 2019). The incorporation of Affimers in biosensors is another potential non-invasive method that can be used for detection of biofilm components in patient samples. Several approaches for incorporation of Affimers with biosensors can be used such as covalent binding via cross-linkers, adsorption or entrapment (Liébana Girona and Drago, 2016). Incorporation of Affimers in biosensors has been demonstrated previously when Affimers raised against dichlorodiphenyltrichloroethane (DDT) and fibroblast growth factor receptor 3 (FGFR3) were immobilised onto impedimetric biosensors (Thangsunan, 2018). As part of the biofilm life cycle where an increase in cell density is observed in mature biofilm, parts of mature biofilm are dislodged from the biofilm and circulate in the body to colonise different surfaces (Novick and Geisinger, 2008). This is under the regulation of quorum sensing which is under the control of accessory gene regulator (*agr*) operon which plays an important role in *S. aureus* biofilm dispersal (Novick and Geisinger, 2008). Therefore, as a proof of principle Affimers can be incorporated in a biosensor device and purified S. aureus biofilm matrix components such as, extracellular DNA (eDNA) or polysaccharide can be injected onto the biosensor surface with immobilised Affimers to investigate if the Affimers are able to detect these components in vitro. Upon successful detection of the purified biofilm components, further investigation can be conducted using blood samples from and IE animal model or IE patients

where the presence of *S. aureus* biofilm formation has been confirmed. The ability of Affimers within biosensors to specifically detect biofilm components in blood samples in spite the presence of several plasma proteins such as fibrinogen and components of the immune system such as immunoglobulins, would provide a powerful bedside diagnostic tool that would enable monitoring biofilm growth and effectiveness of treatments which could potentially shorten hospitalisation time as a result of early diagnosis.

Chapter 4: Investigation of the potential of anti-*S. aureus* biofilm Affimers

4.1 Introduction

S. aureus can form a biofilm by colonisation of native or prosthetic heart valves causing infective endocarditis (IE). IE is associated with a 30% mortality rate in the first year in hospitalised patients as reported by the National Health Service UK (NHS, 2019). This leads to prolonged treatment with a combination of anti-microbial therapy resulting in prolonged hospitalisation. According to the NHS, 15-25% of IE patients will need replacement surgery at some point during the infection, which if left untreated can lead to heart failure or stroke (Gould et al., 2012). To minimise further complications associated with hospitalised patients with IE, early diagnosis and treatment are the major challenges (Liesman et al., 2017) . Even though anti-microbial therapy is the primary choice of treatment of *S. aureus* biofilm infection, they often prove ineffective due to the biofilms recalcitrance to antibiotics due to the presence of persister cells as well as the ability of the matrix to limit diffusion (Otto, 2008). The effectiveness of antibiotics in the treatment of biofilms could be improved by the early detection of *S. aureus* biofilm formation, before the establishment of a mature biofilm which is more resistant to antibiotic treatment (Section 1.4.1) (Hall-Stoodley et al., 2012). In order for the successful diagnosis of biofilm formation, a suitably-sized sample from the site of infection is essential along with several blood cultures that are needed to continuously monitor progression of treatment (Gould et al., 2012). However, obtaining a sufficient sample may be inconvenient, due to the requirement of a biopsy or removal of an implant (Wu et al., 2015). Echocardiography, which is widely used for the diagnosis of endocarditis, cannot confirm the presence of a biofilm (Hall-Stoodley et al., 2012). Therefore, most biofilm-associated infections on medical implants are only confirmed after the removal of the implanted devices, a procedure that may be life threatening (Gould et al., 2012). However, early detection might not be

possible in cases such as IE where diagnosis takes a long time because they rely on blood cultures (Wu et al., 2015). New methods that enable clinicians to identify biofilms on medical devices *in situ* are needed to reduce complications and mortality for IE patients, which will reduce the cost of hospitalisation (DeSimone and Sohail, 2018).

In order to advance biofilm detection methods in the hospital setting, first understanding the development of biofilm growth in a laboratory setting in a way that accurately reflect conditions of biofilm formation in the body is essential (Moormeier and Bayles, 2017). The majority of biofilm growth models are low throughput and require multiple components such as tubing and flow cells and a pump all of which could all become contaminated easily (Ryder et al., 2012). A simple and well-defined method capable of high-throughput biofilm growth has been established (Ryder et al., 2012). The cellulose disk model enables the assessment of biofilm formation by assessment of the adherence of cells to the cellulose disk. This technique incorporates human plasma which consist of proteins such as fibrinogen and fibronectin that facilitate attachment via interaction with *S. aureus* adhesins such as ClfA and FnbA respectively to facilitate attachment thereby mimicking physiological conditions (Keane et al., 2007). Adherence to a surface is initiated by interaction of *S. aureus* surface proteins such as ClfA (clumping factors A) and fnbpA and fnbpB (fibronectin binding proteins A and B) to plasma components such as fibrinogen and fibronectin (Keane et al., 2007, O'Brien et al., 2002). Given the recent success and reproducibility of biofilm growth using the cellulose disk model in previous work(Ryder et al., 2012), the cellulose disk model has been adopted in this work.

Much work involved in the diagnostics and clinical detection has relied on the use of artificial proteins that bind to a target such as Affimers (Tiede et al., 2017). Affimers, which were developed by the BSTG group at the University of Leeds, have been proven to be successful in detection of their intended targets. Examples of success include Affimers against Growth factor receptor-bound protein (SH2) domain and Vascular Endothelial Growth Factors receptor 2 (VEGFR2) (Johnson et al., 2012, Pershad et al., 2010, Sharma et

al., 2016, Tiede et al., 2017). As described previously in (Section 3.1). Affimers are small proteins that are thermo-stable and can recognize a protein and bind to it with affinities similar to antibodies (Tiede et al., 2017). Affimers have potential for being a used as diagnostic tools for detection of *S. aureus* biofilms associated with IE. The successful recognition of purified *S. aureus* PA and ClfA by the anti-PA and anti-ClfA Affimers was demonstrated in the previous chapter (Section 3.3). This provided a great incentive to raise Affimers against *S. aureus* biofilm components, to identify targets that could be strictly presented in biofilm and not planktonic cells. Affimers were raised against biofilms of one laboratory strain and two community acquired *S. aureus* strains. *S. aureus* strain SH1000 is a laboratory strain which became proficient in biofilm formation as a result in reinstatement of an intact *rsbU* gene present in the parent strain *S. aureus* 8325-4 (Horsburgh et al., 2002). The *rsbU* gene functions to encodes the alternative sigma factor SigB which is a regulator of stress response that leads to expression of *S. aureus* adhesins necessary for biofilm formation (Nicholas et al., 1999). *S. aureus* USA300 and UAMS-1 are community acquired isolates from patients with chronic infection (Sassi et al., 2015, Tenover and Goering, 2009). UAMS-1 is a Oxacillin-susceptible strain (SSA) from an osteomyelitis patient (Sassi et al., 2015), whilst USA300 is an Methicillin resistant strain (MRSA) strain that was associated with several chronic skin, cardiovascular and pulmonary infection (Tenover and Goering, 2009). Strains were selected based on biofilm forming capabilities (O'Neill, 2010, Planet et al., 2013, Grande et al., 2014).

4.1.1 Aims

Work in this chapter involved: 1) Optimisation of the cellulose disk biofilm model, including the effect of human plasma and growth media on *S. aureus* biofilm adherence; 2) The generation of Affimers raised against biofilms using three modification of the phage ELISA method which typically involves the use of anti-M13 bacteriophage antibody for detection of Affimer binding to its targets, by removal of the Affimers from the context of the phage and using a reporter which does not bind components of *S. aureus* biofilms such as streptavidin-HRP conjugate instead of using anti-M13 antibody-HRP

conjugate which binds Protein A. Optimisation of the ELISA method used for detection of Affimer binding to biofilms by identification of suitable reporters to uses and confirmation of Affimers binding to *S. aureus* biofilm.

4.2 Results

4.2.1 Optimisation of biofilm adherence to cellulose disk

The cellulose disk model was originally developed to study *S. aureus* SH1000 biofilm growth with the incorporation of 4% human plasma (Ryder et al., 2012). The cellulose disk model was adapted and optimised to include a total of four (PBST) washes along with the cellulase treatment. Here the cellulose disk model was used to assess adherence of *S. aureus* SH1000, USA300 and UAMS-1 biofilms to cellulose disks preconditioned with human plasma. Biofilms were grown on Brain heart Infusion agar (BHA) for 48 hr on a cellulose disk conditioned with various concentrations of human plasma. Conditioning the cellulose disks with 4% human plasma had been reported for strain SH1000 to greatly improve adherence of cells to the disk, in which a greater proportion of cells remained adherent to the disk after a series of PBS washes and cellulase treatment compared to non-conditioned disks (Ryder et al., 2012). To determine/confirm the optimal concentration of human plasma to use for sufficient *S. aureus* biofilms adherence, *S. aureus* strains SH1000, USA300 and UAMS-1 were grown on cellulose disks conditioned with 4% and 10% (v/v) human plasma and disks without conditioning with human plasma. Biofilms were subjected to a series of four washes with phosphate-buffered saline with Tween 0.01% (PBST), and then treated with cellulase. Cellulase has been previously reported to induce detachment of biofilm by degrading polysaccharide matrix resulting in dissociation of cell from the biofilm (Cescutti et al., 1998, Loiselle and Anderson, 2003). The purpose of the washes along with the cellulase treatment was to assess the level of adherence of the cells to the cellulose disk as a result of conditioning with each concentration of human plasma. In order to assess the adherence of the cells to the cellulose disks, the optical density of each wash and the cellulose treatment were measured at 600 nm and expressed as a percentage of the total biofilm

biomass (Figure 4.1). The total amount of biofilm biomass was divided into two groups: non-adherent and adherent cells, the non-adherent cells refers to the loosely associated cell presumed to be planktonic cell population removed by the first wash while the adherent cells refers to the total cells removed by the remaining washes and cellulase treatment. SH1000 biofilm growth after conditioning the cellulose disk with 4% or 10% human plasma resulted in an 1.2 and 1.23-fold increase respectively in the number of adherent cells after washing with PBST compared to non-conditioning. A 1.3 and 1.5-fold increase respectively in the percentage of adherent cells was observed for USA300 when conditioned with 4% or 10% human plasma compared with non-conditioning. Conditioning with 4% or 10% human plasma only yielded about 1.47 and 1.42-fold increase respectively in the percentage of adherent cells compared with non-conditioning for UAMS-1. When assessing the adherence level of each strain, it was noticed that there is a difference in the adherence of the three strains to the cellulose disk. Compared to USA300 and UAMS-1, SH1000 appears to adhere more tightly to conditioned and non-conditioned cellulose disks which is evident by the number of adherent cells remaining after the PBST washes and cellulase treatment in all conditions (Figure 4.1). Furthermore, it was noticed that the percentage of non-adherent cells decreased after conditioning the disk with human plasma increased which was expected. This was also noticed in a previous study, in which a clear difference in the level of adherence was observed in the percentage of adherent cells for SH1000 biofilm when conditioning with 4% human plasma which resulted in a 9.3-fold increase in the number of adherent cells compared biofilm grown on non-conditioned disks (Ryder et al., 2012). However, here only a 1.2-fold increase in the number of adherent cells was observed for SH1000 biofilm between conditioning with 4% human plasma and non-conditioning (Figure 4.1).

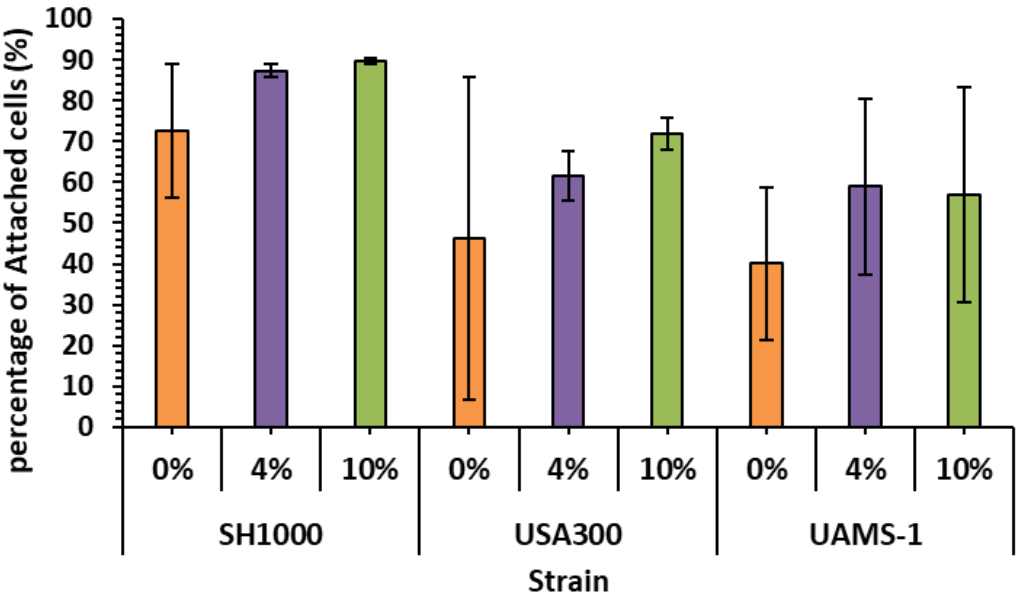

Figure 4.1 Optimisation of S. aureus biofilm growth using the cellulose disk model. Biofilms for the *S. aureus* strains SH1000, UAMS-1 and USA300 were grown on non-conditioned cellulose disks and cellulose disks conditioned with 4%, and 10% human plasma diluted with 0.05 M carbonate bicarbonate buffer on BHI for 48 hr. Data represents percentage of adherent population for each biofilm. Data values represent the mean of two biological replicates.

Biofilm growth is influenced by different factors one of which was the presence of host proteins that facilitate adherence which was discussed above, another is growth medium which provide the necessary nutrients that allow maturation and the formation of a more stable biofilm (Nyenje et al., 2013). In order to obtain sufficient amounts of biomass for the Affimer selection process the effect of growth media known to effect biofilm growth is investigated

Growth of biofilms was tested on cellulose disks preconditioned with 10% human plasma then grown on BHA, Tryptic soy agar (TSA) and Peptone-NaCl-glucose agar (PNG), based on previous work that suggests that growth conditions can alter biofilm matrix composition (Schwartz et al., 2012). As mentioned earlier the cellulose disk model was optimised for biofilm growth on BHA, also, both BHA and TSA are commonly used media to promote biofilm formation in *S. aureus* (Lade et al., 2019, Wijesinghe et al., 2019). Furthermore, BHA has been previously confirmed to greatly increase the

production of extracellular polysaccharide and promote maximal adhesion in *S. aureus* biofilm (Wijesinghe et al., 2019). PNG has been previously documented to promote production of phenol soluble modulins (PSMs), resulting in an increase in biofilm resistance to dispersal and matrix degradation by enzymatic treatment (Schwartz et al., 2012). Out of all three medias, SH1000 biofilms showed the highest percentage of adherent cells on BHA after four PBST washes compared to biofilms of USA300 or UAMS-1, indicating the reproducibility of the results in (Figure 4.1). SH1000 growth on BHA showed a 1.1 and 1.6-fold increase in the percentage of adherent cells on TSA and PNG respectively (Figure 4.2 A). USA300 biofilm growth on TSA resulted in a 1.6 and 2.8-fold increase in the percentage of adherent cells when compared to biofilms grown on BHI and PNG respectively. Also, UAMS-1 biofilm growth on TSA showed similar results to USA300 in which a 1.7 and 1.9-fold increase in the percentage of adherent cells was recorded compared to BHA and PNG respectively (Figure 4.2 A). Despite the fact that TSA supported a higher percentage of adherent cells for USA300 and UAMS-1 than BHA, the total of the average of the optical density recorded for USA300 and UAMS-1 biofilm were similar for TSA and BHA as that on TSA, while the total average optical density recorded for SH1000 biofilm growth on BHI was 2-fold higher than that on TSA. This is also supported by the visual assessment of representative photographs of the biomass formed by SH1000, USA300 and UAMS-1 biofilms grown on BHA and TSA and PNG, in which visual inspection of the colour, texture and morphology for each biofilm were considered (Figure 4.2 B). Along with the recorded percentage of adherent cells optical density measurements and the photographic representation of biofilm growth suggest that BHA supports greater biofilm growth than TSA and PNG. Therefore, BHA was selected to use to grow biofilms for all experiments throughout this study, this was particularly important for Affimer production since the increase in biomass generated for SH1000 biofilm would result in the presentation of more target to be recognised by phage expression Affimers during the phage display screening in the next section.

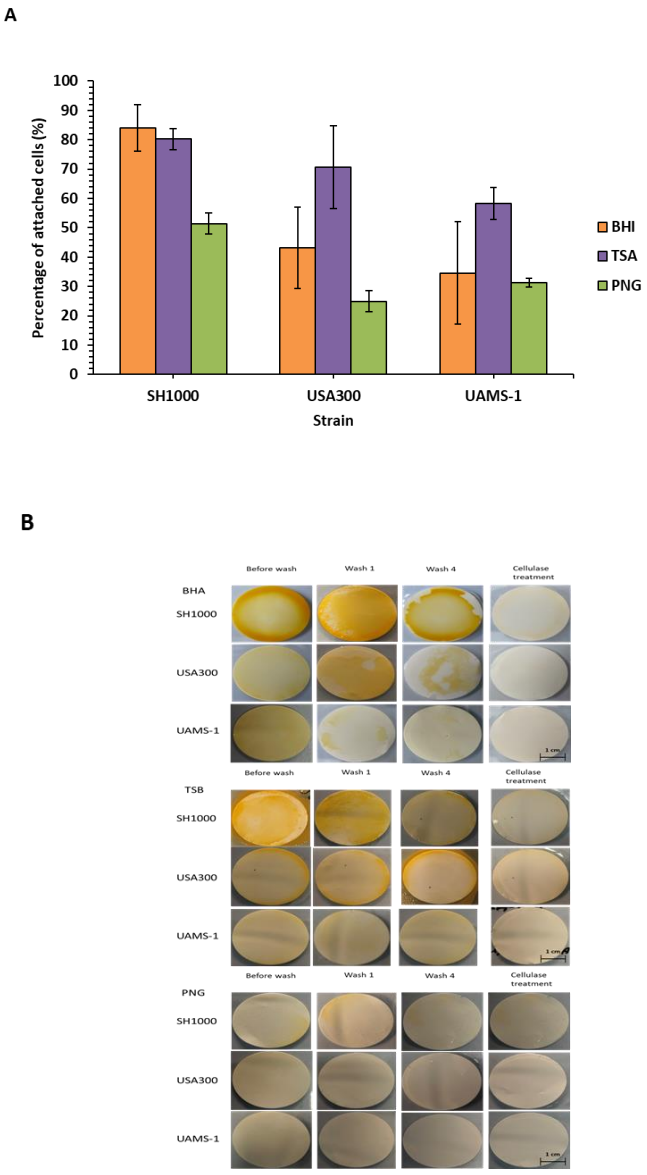

Figure 4.2 Effects of growth media on adherence of biofilms to cellulose disks. A. Graph represent percentage of total adherent of *S. aureus* biofilms grown on cellulose disks conditioned with 10% human plasma on BHA, TSA and PNG agar for 48 h. Biofilms were washed four times with PBST then treated with cellulase, optical density was measured at 600 nm. Data are mean of three biological replicates. **B.** Photographs of SH1000, USA300 and UAMS-1 biofilms grown on BHA, TSA and PNG agar.

To ensure that sufficient amount of biomass is available to perform the selection of Affimers against *S. aureus* biofilm using phage display, therefore, performing multiple washes during biofilm processing as was done previously was counterproductive. Also, as previously described above the adherence of each strain to the cellulose disk was different, therefore the number of washes

needed to obtain enough biomass for each strain should be taken into consideration. To determine the number of washes that would result in obtaining a sufficient amount of biomass to use for the selection of Affimers, SH1000, USA300 and UAMS-1 biofilms were grown as described previously then washed with PBST four times and treated with cellulase. The optical densities of each wash and cellulase treatment were recorded and expressed as a percentage of the total biomass removed by each wash (Figure 4.3). After the first wash with PBST, 10%, 28% and 43% of the cells were removed from the total biomass for SH1000, USA300 and UAMS-1 respectively (Figure 4.3). The second wash resulted in the removal of 4% 37% and 17% of adherent cells from the disks for SH1000, USA300 and UAMS-1 respectively, the third wash removed 7%, 18% and 7% of adherent cells from the disks for SH1000, USA300 and UAMS-1 respectively (Figure 4.3). While the fourth wash only removed 5%, 5% and 7% of adherent cell from the disks for SH1000, USA300 and UAMS-1 respectively (Figure 4.3). To determine the total biomass of each biofilm, the biofilms were treated with cellulase to remove the remaining adherent cells from the disk. Cellulase treatment resulted in the removal of the remaining adherent cells from the disks, cell removed from the disk constituted 72%, 11% and 25% of the total cells for SH1000, USA300 and UAMS-1 (Figure 4.3). Moreover, since the goal is to obtains Affimers that recognise biofilm components, treatment with cellulase would result in the degradation of the biofilm matrix which would work against that goal so the cellulase treatment was excluded from preparatory steps leading to Affimer selection (Loiselle and Anderson, 2003). If the cellulase treatment was excluded, the first and second wash removed a greater percentage of cells from USA300 and UAMS-1 biofilms than the other washes, while the first and third washes removed a greater percentage of cells from SH1000 biofilm (Figure 4.3). The difference between the percentage of cells removed by each wash between each strain could be due to strain differences or batch variation and handling, particularly in the case of the second and third washes for SH1000. This led to the conclusion that perfuming several washes would not be sensible as most of the biomass is removed and instead one wash is sufficient to remove

non-adherent cells and enough biomass would remain to use for the selection of Affimers.

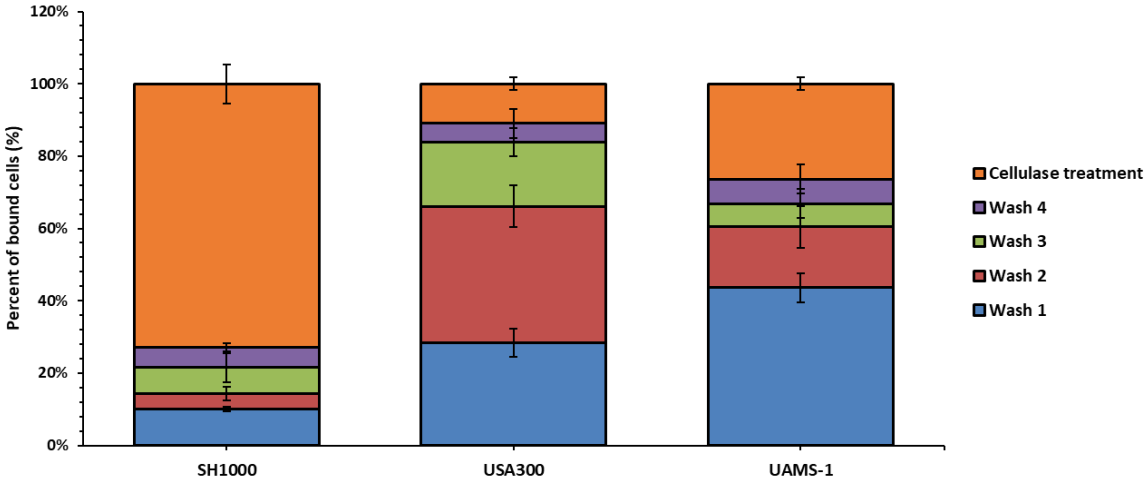

Figure 4.3 Assessment of the effectiveness of PBST washes and cellulase treatment in removing loosely associated cells and adherent cells from *S. aureus* biofilms. *S. aureus* biofilm were grown on cellulose disks conditioned with 10% human plasma on BHI agar for 48 h, then washed 4 times with PBST then treated with cellulase. The optical density values were measured at 600 nm then expressed as percentage are based on the mean of two biological replicates.

4.2.2 Generation of Affimers against *S. aureus* biofilm

In preparation for generation of Affimers against *S. aureus* biofilms, SH1000, USA300 and UAMS-1 biofilms were grown for 48 h on cellulose disks pre-conditioned with 10% human plasma on the surface of BHA. Biofilms obtained from a single cellulose disk were first washed once with PBST to remove the non-adhered cell population from the surface of the biofilm, and the remaining biomass was removed from the disk by physical scraping and suspended in PBST to a achieve a semi-homogenous mix. Biofilms were then provided to the BSTG group at the University of Leeds to be used for generation of Affimers. Affimers specific for *S. aureus* biofilms were generated using phage display, this was done by incubation of the naïve phage library with SH1000 or USA300 or UMAS-1 biofilms. In order to isolate Affimers which were both biofilm and strain specific, two counter selection steps were performed. The

purpose of the counter selection was to deplete the phage library from phage specific against biofilms and PC of the other two stains. The first counter selection step entailed pre-panning the phage library against biofilm from the other two strains, the second counters selection step entailed panning of the pre-panned phage library against PC from the target strain as described in (Section 2.5.1). The counter selection to isolate Affimers that are specific for the target strain biofilm (e.g. SH1000) was performed by incubation of the library with mixed biofilm from the other two strains (i.e. USA300 and UAMS-1) for four rounds of pre-panning, after the fourth pre-panning round the pre-panned phage was split and panned against biofilm from the target strain, biofilm from the other two strains separately and a negative control (magnetic beads). Phage that bound the target strain biofilm was eluted and enriched by infection of *E. coli* cells; the enriched phage library was then used for the second counter selection against PC of the target strain. The enriched phage library underwent four pre-panning rounds against the target strain PC, unbound phage was then panned against the target strains biofilm for two panning rounds, magnetic beads and biofilm from the other two strains were used as controls. Bound phage was eluted and the phage pool was now further depleted of phage that recognises PC of the target strain. The phage pool was then enriched by infection of *E. coli* cells then grown in 2TY media and plated on LB agar plates supplemented with carbenicillin.

The selection process against all *S. aureus* biofilms yielded a total of 133 phage clones presenting Affimers, to identify the sequence of the Affimers, the phage-mid DNA was extracted and isolated then amplified by PCR and the product was sent for DNA sequencing using the services of GeneWiz. Sequencing revealed 38 unique Affimer sequences, 26 were isolated from the selection against SH1000 biofilm while only 8 and 4 were isolated from the selection against USA300 and UAMS-1 biofilms respectively. From the unique Affimer sequences identified, 11 Affimer sequences were repeated multiple times, suggesting that the target of these Affimers could be present at a higher frequency in the biofilm that other targets or that they are more accessible to the Affimers. Therefore, they were selected to be screened for binding against *S. aureus* biofilm (Table 4.1).

Table 4.1 Variable region sequences for selected Affimers raised against *S. aureus* biofilm

Affimer	Loop1	Loop2	No. of Repeats
SH1000-2	PLYQHIRES	YANYNRAKP	4
SH1000-10	TQMLSPSQH	WIKFWPEYG	11
SH1000-27	RVIKHYRYS	NLPDELSTD	2
SH1000-30	YSYGMIKES	APSVWPFLA	2
SH1000-31	LEMLMPSSH	LTKFFNTFS	2
USA300-49	GATNGRQHH	YDDIWFQSY	4
USA300-50	PNFKSRWGP	NEPWQTNYS	26
USA300-51	TQPHRQYYP	EPWLWSYEV	3
USA300-65	EKSQYWRFP	SPPWHLRAP	2
UAMS-1-1	NPETKEHHV	GYWFQAHRM	17
UAMS-1-11	PQDSSEYHT	RFGYPYDGH	22

4.2.3 Screening of biofilms

4.2.3.1 Biofilm screening using phage ELISA

In preparation to for screening of Affimer binding to *S. aureus* biofilm using ELISA, a method that would allow multiple samples to be tested at the same time was needed. Although the cellulose disk method provides a high-throughput method for biofilm production, it could present some limitations such as, difficulty of handling when attempting to screen Affimer binding to multiple biofilms at the same time. Therefore, screening of Affimers binding to multiple *S. aureus* biofilms at the same time could be performed by growing

biofilm on microtiter plates conditioned with human plasma. To choose the most suitable concentration of human plasma to use to condition microtiter plates that would yield maximum adherence and biomass production, SH1000 biofilms were grown for 48 h in brain heart infusion (BHI) media on the surface of microtiter plates conditioned with 4% and 10% (v/v) human plasma. The media was removed and biofilms were washed four times with PBST then treated with cellulase to remove the remaining biofilm, the optical density of each wash and cellulase treatment was recorded and expressed as a percentage of the total biofilm biomass. Similar to previous results when testing adherence of cells to the cellulose disk (Figure 4.1), adherence to the microtiter plate suggests that 10 % human plasma would yield better adherence than 4% (Figure 4.4). Also, similar to the previous result as (Figure 4.3) were observed, in which the proportion of cells removed decreased with each wash prior to cellulase treatment (Figure 4.4). However, the total percentage of adherent cells remaining after each wash was higher for biofilms grown on the cellulose disk. Furthermore, the biomass produced by growth on the microtiter plates was much less than that produced by the cellulose disk and the amount of biofilm lost during washing with PBST was much greater. Therefore, using the microtiter plate was only be used to identify a suitable reporter and investigate the ability of unlabelled IgG to block anti-M13 antibody binding to PA.

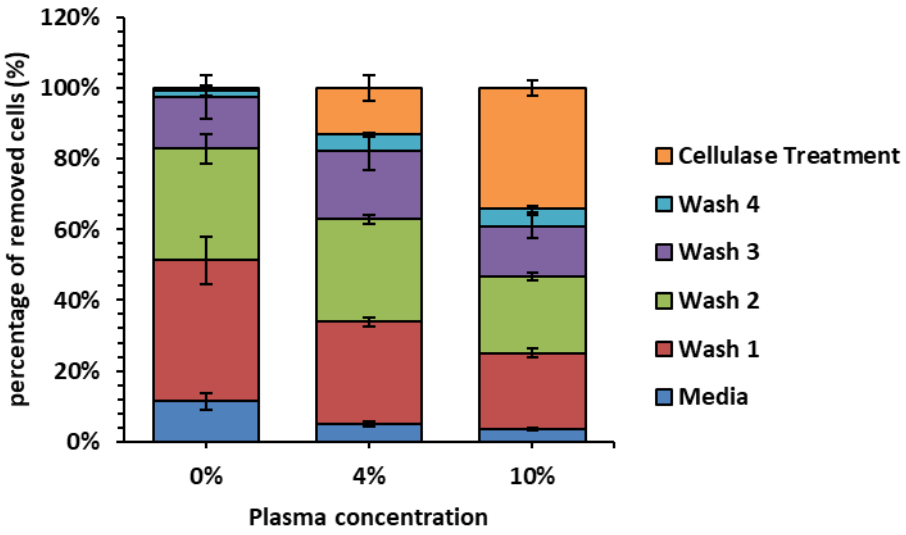

Figure 4.4 Assessing the adherence of biofilm to microtiter plates. Graph showing adherence of SH1000 biofilms grown in BHI media on microtiter plates non-conditioned (0%) and conditioned with 4, 10 human plasma. Biofilms were washed 4 times with PBST and treated with cellulase (1 mg/ ml). Absorbance of each wash and cellulase treatment was measured at 600 nm. Controls include non-conditioned wells (0%). Data presented are the mean of three biological replicates.

Initially detection of Affimer binding to *S. aureus* biofilm was to be investigated using phage ELISA, in which phage presenting Affimers were incubated with *S. aureus* biofilms grown on microtiter plates conditioned with 10% human plasma. However, the ability of PA on the surface of *S. aureus* to bind IgG was expected to cause a problem since an anti-M13-HRP conjugate is used as a secondary antibody for detection of phage binding. It was later confirmed that indeed anti-M13-HRP antibody binds PA therefore using phage ELISA would not be a suitable method of detection of Affimer binding.

4.2.3.2 Biofilm screening using purified biofilm specific Affimers against *S. aureus* biofilm

The 11 selected Affimer sequences were subcloned into an expression vector pET11a with the assistance of the BSTG group and introduced by transformation into *E. coli* BL21 (DE3) cells for protein production (Section 3.3.2). Affimers were then purified using immobilised metal affinity chromatography via an oligohistidine tag that was present at C-terminus. The Affimers were biotinylated using maleimide chemistry via reduction of

disulphide bonds from free cysteines incorporated into Affimers C-terminus via the subcloning strategy (Section 3.3.2). To confirm binding to *S. aureus* biofilm, Affimers were screened against SH1000, USA300 and UAMS-1 biofilms; with the assistance of Dr. Christian Tiede from the BSTG group the screening was done double-blind in triplicates using the same batch of biotinylated Affimers in which the identity of the Affimers were hidden until completion of the screening. Biofilms in this experiment were grown for 48 h on cellulose disks conditioned with 10% human plasma on the surface of BHA, biofilms were washed as indicated previously (Section 2.8.1), the remaining biomass was scraped of cellulose disk and suspended in PBST then transferred to a microfuge tube pre-incubated in blocking buffer (BB) as described in (Section 2.8.1). To decrease non-specific binding Affimers were diluted in BB, the same blocking buffer used to dilute the Affimers was used as a negative control along with an Affimer specific for Actin which was provided by the BSTG group as described in (Section 2.8.1). Detection of binding was achieved by probing with streptavidin-HRP conjugate and assaying the associated enzymatic activity. Assessment of Affimer binding was done by comparing the binding signal of each Affimer to that of blocking buffer, significance of binding was determined for each individual experiment by calculation of p-values using a student t-sets (Table 4.2).

Despite the depletion of Affimers that were specific for the other strains during the Affimer selection process, their appears to be no strains specificity in Affimers binding to *S. aureus* biofilm. It was expected that the Affimers would bind components of each biofilm with different specificity, since the previous results indicate a difference in the adherence level of each biofilm which could be an indicator of different biofilm composition (Figure 4.1). However, this was not what was observed, as the majority of Affimers recognised components of USA300 and UAMS-1 biofilm with statistical significance in more experiments than SH1000 (Table 4.2).

One Affimer (SH1000-27) did not show significant binding to any of the biofilm tested, suggesting that the target of this Affimer is probably expressed at a low level that would not produce a high enough binding signal that is detectable above the signal of the anti-Actin Affimer. Other Affimers (SH1000-

30, USA300-51) recognised targets on only one biofilm, SH1000-30 showed significant binding to SH1000 biofilm and USA300-51 showed significant binding to USA300 biofilm, suggesting that they might be specific for these biofilms (Table 4.2). However, both SH1000-30 and USA300-51 only showed significant binding to SH1000 and UAS300 biofilms in only two experiments respectively (Table 4.2). Some Affimers (SH1000-2, USA300-50, UAMS-1-1, UAMS-1-11) recognized targets presented on two biofilms (Table 4.2). SH1000-2 Affimer appears to recognise a common target present on SH1000 and UAMS-1 biofilms, however, it only showed significant binding to SH1000 and UAMS-1 biofilm in one experiment, suggesting that the target was not easily accessible to the Affimer or is not produced at high quantities. One the other hand, USA300-50, UAMS-1-1 and UAMS-1-11 seem to all recognise targets significantly on USA300 and UAMS-1 biofilm except for UAMS-1-11 which only showed significant binding to USA300 in one experiment (Table 4.2). The fact that several Affimers recognise targets on both UAMS-1 and USA300 suggest that the biofilm composition is similar. Moreover, four Affimers (SH1000-10, SH1000-31, USA300-49, USA300-65) showed significant binding to all three *S. aureus* biofilms. However, of these significant binding was not detected in all three experiments instead, SH1000-10, SH1000-31 and USA300-65 only showed significant binding in one or two experiments, for example, significant binding of SH1000-10, SH1000-31 and USA300-65 Affimers to SH1000 biofilm was observed in one experiment (Table 4.2). Similarly, significant binding to USA300 biofilm was observed for SH1000-10, SH1000-31 Affimers in one experiment, however, USA300-65 showed significant binding in all three experiments (Table 4.2). This suggests that the targets for SH1000-10 and SH1000-31 Affimers are expressed at a higher rate or are more accessible in UAMS-1 biofilm than SH1000 and USA300 biofilm.

Although SH1000 produces a greater amount of biomass than USA300 and UAMS-1 which could indicate the presence of multiple targets that could be recognized by the Affimers. However, none of the Affimers seem to bind SH1000 biofilms in more than one experiment with statistical significance except for SH1000-30 and USA300-49 which bound SH1000 biofilm with

statistical significance in only two of the experiments (Table 4.2). It is unclear why most of the Affimers did not recognise any targets on SH1000 biofilm but recognised targets on USA300 and UAMS-1, particularly the five Affimers (SH1000-2, SH1000-10, SH1000-27, SH1000-30, SH1000-31) isolated from the selection against SH1000 biofilm. The reason why some Affimers only showed significant binding to a particular strain in one experiment is unknown, however this does not completely exclude the ability of the Affimers to bind these target, a possible explanation could be that the accessibility or expression level of that target could be due to strain differences influenced by biofilm batch variation or other factors. As noticed previously in (Figure 4.1) a clear variation between the biofilm was evident, this was thought to influence the chances of Affimer binding. The composition of SH1000 biofilm matrix differ greatly from that of USA300 and UAMS-1. However, it seems that the difference in the level of adherence observed previously in (Figure 4.1) does not significantly affect the expression of the targets that the Affimers bind to, particularly for USA300 and UAMS-1.

Initially it was hypothesised that since SH1000 and USA300 produced more biomass than UAMS-1, the majority of Affimers would recognise target on SH1000 or USA300 however it is found that that was not the case (Table 4.2). Six Affimer (SH1000-10, SH1000-31, USA300-49, USA300-65, UAMS-1-1, UAMS-1-11) showed significant binding to UAMS-1 biofilm in all three experiments and one Affimer (USA300-50) showed significant binding in two experiments. Out of these Affimers, three Affimers (USA300-49, USA300-50, USA300-65) also showed significant binding to USA300 biofilm in all three experiments; one Affimer (UAMS-1-1) bound significantly to USA300 biofilm in two experiments and two Affimers (SH1000-31, UAMS-1-11) bound significantly to USA300 biofilm in only one experiment (Table 4.2). Indicating that some targets presented on UAMS-1 are also presented on USA300 biofilm. Affimers that showed binding to all three biofilm tested suggesting that they might be universal binders of *S. aureus* biofilm (USA300-49 and SH1000-10). USA300-50 and SH1000-30 Affimers showed significant binding only to USA300 and SH1000 biofilm respectively. This suggests that they recognize

components present on UAMS-1 and USA300 biofilm in different quantities but not present on SH1000 biofilm. In addition to USA300-50, UAMS-1-1 and UAMS-1-11, the fact that SH1000-10, SH1000-31, USA300-49 and USA300-65 showed significant binding to USA300 and UAMS-1 biofilm further confirms the similarity between USA300 and UAMS-1 biofilms. Also, USA300 is a MRSA strain and UAMS-1 is a MSSA strain, this could be an indicator that these Affimers recognise a target that is expressed at a higher level in antibiotic tolerant strains. Based on the ELISA results, the more likely Affimer candidate to be universal *S. aureus* biofilm binders to take forward for further analysis are USA300-49 and USA300-65. This suggests that the composition of SH1000 biofilm is significantly different than that of USA300 and UAMS-1 biofilm in terms of the proteins present and the quantity at which they are present. However, two particular Affimers (USA300-49 and USA300-65) stood out as they also showed significant binding to SH1000 biofilm, even though they only showed significant binding to SH1000 biofilm in two and one experiment respectively, they are the most likely candidates to consider for further investigation. Furthermore, the fact that Affimer screening against *S. aureus* biofilms was done double-blind, gives confidence to the results obtained and that there was no bias with selection of Affimers USA300-49 and USA300-65 as potential candidates to take forth for further characterisation. On another note, although some Affimers showed significant binding to *S. aureus* biofilms it is a possibility that they recognise intracellular components that are also present in biofilm do to cell lysis (Montanaro et al., 2011). Intracellular proteins and DNA are often present in the biofilm matrix, however the quantity in which they are present can be different do to batch variations (Montanaro et al., 2011).

Further characterisation of Affimers included Screening of Affimers against PA which indicated that none of the Affimers bind PA, this could be a result of depletion of Affimers that recognise PA during the counter selection step against PC.

Table 4.2 Screening of Affimers against *S. aureus* biofilm

Affimer	SH1000			UAMS-1			USA300		
UAMS-1_1	NS	NS	NS	++++	+++	++	NS	++++	+++
SH1000_10	NS	NS	+++	++++	+++	++++	NS	NS	++
UAMS-1_11	NS	NS	NS	++++	+++	+++	NS	NS	++++
SH1000_2	NS	NS	+++	NS	++++	NS	NS	NS	NS
SH1000_27	NS	NS	NS	NS	NS	NS	NS	NS	NS
SH1000_30	NS	+++	++	NS	NS	NS	NS	NS	NS
SH1000_31	NS	NS	+++	++	++++	+++	NS	NS	+++
USA300_49	NS	++	+++	++++	+++	+++	++++	+++	+++
USA300_50	NS	NS	NS	NS	++++	+++	++++	+++	++++
USA300_51	NS	NS	NS	NS	NS	NS	NS	++++	++++
USA300_65	++++	NS	NS	++++	++++	++++	++++	+++	++++
Anti-Actin	NS	NS	NS	NS	NS	NS	NS	NS	NS
Blocking buffer	NS	NS	NS	NS	NS	NS	NS	NS	NS

Note: P-values for each replicate were calculated using student's t. test using Microsoft Excel (+ = P< 0.01, ++= P<0.001, +++= P<0.0001, ++++= P<0.00001, NS = non-significant).

4.2.4 Investigation of Affimers ability to bind Protein A

The involvement of PA in *S. aureus* biofilm formation is well documented, so it was reasonable to assume that one or more of the Affimers raised against *S. aurus* biofilms might bind PA (O'Gara, 2007). In order to investigate the possibility that the 11 Affimers raised against biofilm bind PA, biotinylated Affimers were immobilised on the surface of a streptavidin coated 96-well microtiter plate. PA (ThermoFisher) was added to each well consisting of biotinylated Affimers or empty well with no Affimer, unbound PA was removed by washing with PBST. Detection of Affimers binding to PA was achieved by probing with IgG-HRP conjugate and assaying the associated enzymatic activity. The anti-Actin Affimer was used as a negative control and the anti-PA Affimer raised in Chapter 3 was used as a positive control. Affimers that showed binding at a level compared to anti-PA Affimer were considered positive for binding to PA. Assessment of binding significance was determined by comparing the level of Affimer binding to that of anti-Actin and calculating p-values using student t-test. None of the Affimers raised against *S. aureus* biofilm were confirmed positive for binding PA when compared with the anti-PA Affimer (positive control) (Figure 4.8). this suggests that in the biofilms used for selection of Affimers PA was not accessible or a more likely possibility is that during the counter selection against PC the pool of phage expressing Affimers that recognise PA was severely depleted thereby no Affimers that bind PA were isolated.

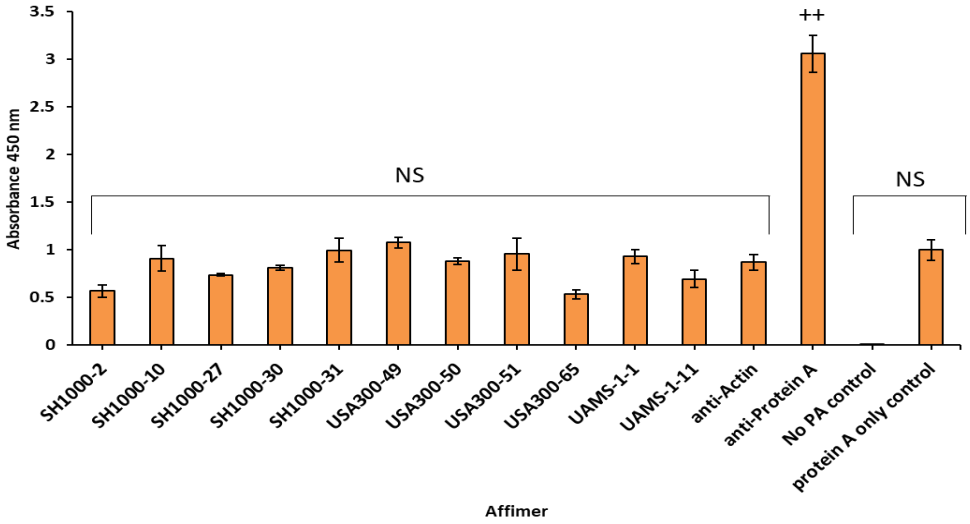

Figure 4.5 Analysis of the ability of anti-biofilm Affimers to bind purified Protein A. Biotinylated biofilm specific Affimers binding was detected using IgG-HRP conjugate. Oxidation of TMB was stopped using sulfuric acid. The absorbance was then measured at 450 nm. Controls include anti-Actin Affimer, No PA (Affimer only), Protein A only (no Affimer). Absorbance values are the mean of three technical replicates, with error bars indicating the standard deviation. P-value for each replicate was calculated for the average mean of Affimer against anti-Actin Affimer using student t. test using Microsoft Excel (+ = P< 0.01, ++= P<0.001, +++= P<0.0001, ++++= P<0.00001, NS = non-significant).

4.3 Discussion

The need for development of a reliable method that would allow early diagnosis of IE is dependent on the production of Affimers specific for *S. aureus* biofilms that show a high level of specificity and affinity against *S. aureus* biofilm. The isolation of Affimers that showed specific binding to *S. aureus* biofilms is the first step to achieve that goal. Therefore, the work presented in Chapter 4 explored the possibility of raising Affimers against *S. aureus* strain SH1000, USA300 and UAMS-1 biofilm components and testing their ability to recognise these biofilms. To raise Affimers against *S. aureus* biofilms initially, the level of adherence of cells and effect of growth media on biofilm formation were assessed using the cellulose disk model. Affimers were then raised against biofilm components using phage display; identification of

the sequences of the Affimers indicated that eleven Affimers presented unique sequences. Therefore, these Affimers were selected to be screened against *S. aureus* biofilm. This approach proved successful in which some of the Affimers (USA300-49, USA300-65) raised randomly against *S. aureus* biofilm components were indeed able to recognise biofilm components with statistical significance. The fact that none of the Affimers tested showed significant binding to SH1000 in all three experiments suggest that its quite difficult to raise Affimers against SH1000 biofilm using the approach used in this study (Figure 4.4). However, the fact that some Affimers significantly recognised targets on SH1000 in one or two experiments could just mean that the targets are less accessible to the Affimer or produced at a lower rate than in USA300 and UAMS-1. Affimer screening against *S. aureus* biofilm indicated that the majority of Affimers recognise a common target between USA300 and UAMS-1 biofilm. This, also indicates that there is still room for modification in the Affimer selection process. Although, the selection of Affimers against *S. aureus* biofilm was successful in yielding Affimers that recognise *S. aureus* biofilm, however, there are several limitations noticed with the phage display counter selection steps during the pre-panning. This most possibly resulted in the depletion of the library of Affimers that had the potential to be universal *S. aureus* biofilm binders. Modification of the phage display strategy used by elimination of the counter selection step against biofilm from the non-target strains and only performing a counter selection against PC would allow isolation of a larger selection of Affimers. Furthermore, removing the counter selection step against biofilms would allow isolation of Affimers the recognise common biofilm components between the three strains. On a different note, growth conditions and media composition greatly influenced the quality of biofilms formed by any organism (Nyenje et al., 2013). *S. aureus* biofilms growth on different media showed that there is variation between the strains in biofilm mass and integrity. The difference in growth could be due to the effect of the media this was apparent for SH1000 and USA300 biofilm growth on BHA and TSA which produced more biomass than UAMS-1 on both BHA and TSA. Different component involved in biofilm formation could be expressed at higher or lower amount due to different nutrients present in the

growth media. The effect of growth media on biofilm growth has been previously explored, several studies have indicated significant differences in biofilm structure and resistance to degradation between biofilms grown on different growth media. For example, growth media that contain a high salt concentration such as PNG has been reported to induce production of PSM in *S. aureus* biofilms, which resulted in the formed biofilms to be more resistant to degradation by enzymatic treatment (Schwartz et al., 2012). Also BHA and TSA have been extensively used to promote adherence and biofilm formation in *S. aureus* as they induce the production of PIA (Wijesinghe et al., 2019). Therefore, another approach to consider for generating a wider selection of Affimers is raising Affimers against *S. aureus* biofilms grown on TSA and PNG mediums. Growth on different media would result in isolation of Affimers against biofilm components that might not be present or less expressed on biofilms grown on BHA.

Another modification in the selection of Affimers is the adaptation of a different biofilm growth model. The cellulose disk model has been proven to be useful in assessment of cellular adherence (Ryder et al., 2012, Tran et al., 2009). The cellulose disk model was modified by the incorporation of three extra washes to provide a more accurate assessment of adherence. Although other biofilm models were available such as the drip flow reactor and Lubbock chronic wound biofilm models, the cellulose disk model along with being high throughput, consisted of less components and was much more easily manageable. The Lubbock chronic wound biofilm model for example is more adapted in the investigation of the effect of antibiofilm agents on multiple species biofilm (Brackman et al., 2013, Sun et al., 2008). The drip flow reactor biofilm model is low throughput and more laborious in handling (Manner et al., 2017). All biofilm growth models have advantages and disadvantages but will be considered for future investigation as when utilised properly they can prove useful depending on the intended application. Furthermore, biofilms grown using these methods might consist of different components to those grown using the cellulose disk model or the same components might be present but in different quantities. This could be exploited in which Affimers can be raised against biofilms grown using the microfluid chambers in order to isolate

different Affimers that recognise different targets that might be expressed do to the continues flow in the microfluid chamber that more accurately represents biofilms grown on heart valves of IE patients.

4.3.1 Identification of Affimer targets

The next step in characterisation of Affimer would include identification of the target that the Affimers bind to. This will enable identification of potential limitations associated with binding that target such as accessibility in vivo and the presence of host components that could interfere with binding of the Affimers such as, IgG binding to PA. To follow up further characterisation of the Affimer targets, preliminary experiments were performed to extract biofilm matrix components from the cells using high salt washes and different enzymatic treatments. Enzymes known to degrade these components such as proteinase K (proteins) DNaseI (DNA) and dispersin B (polysaccharide) have been used previously and proven successful in isolation of biofilm matrix components from UAMS-1 biofilm (Schwartz et al., 2012). However, initial attempts towards replicating this work did not show that the method is as effective as reported, the lack of extracted materials from biofilms grown on the cellulose disk made further investigation was not possible. This could be because the method used to generate the biofilms in the study were grown using the drip flow reactor biofilm model which often greater biomass than the cellulose disk model due to the small size of the disk. Further work is needed in optimisation of the extraction method and quantity of biofilm to use to achieve a quantifiable amount of materials is needed.

Chapter 5: Investigation of transcriptional changes associated with *S. aureus* biofilm formation using RNA sequencing

5.1 Introduction

The association of *S. aureus* biofilms with chronic infections has been a topic of interest in the past two decades, *S. aureus* is a commensal organism that inhabits the human skin and nasal flora; therefore, it is able to easily get access to wounds and reach and colonise native or implanted medical devices and catheters (Bjarnsholt, 2013, Del Pozo and Patel, 2007). The ability of *S. aureus* to form biofilm along with the vast array of virulence factors greatly complicates treatment and diagnosis *S. aureus* biofilm associated infections (Hall-Stoodley et al., 2012). Furthermore, biofilm cells are phenotypically different that planktonic cells; therefore, treatment and diagnosis typically used for *S. aureus* infections might not be as effective when dealing with biofilm associated infections (Hall-Stoodley et al., 2012). Moreover, antibiotic treatment can be limited due to the emergence of antibiotic resistant strains is a factor that can add complication when treating biofilm infections, as well as the presence of cells in a dormant state with in the biofilm such as small colony variants and persister cells that are not affected by antibiotic treatment causes further difficulties in treatment (Balaban et al., 2004, Lewis, 2007). Furthermore, the protection provided by the biofilm matrix in limiting the diffusion of antibiotics through the biofilm renders the antibiotic less effective which can be the causes of mutations that convey resistance in some cases (Mah and O'Toole, 2001, Mok and Brynildsen, 2018). The presence of virulence factors that work to evade the host immune system by masking *S. aureus* antigens or IgG binding such as capsular polysaccharide (*cap*) and protein A (*spa*) renders the immune system less effective and treatment or diagnosis using monoclonal antibodies ineffective (Visansirikul et al., 2020).

Understanding the differences between the gene expression pattern of planktonic cells and biofilm cells would provide a better understanding of how

to target components that are specifically involved in biofilm formation. One approach to understanding these differences is to identify genes that are differentially expressed between biofilm cells and planktonic cells. Identification of patterns associated with gene expression can provide insight on the importance of certain metabolic and physiological pathways and changes that can trigger phenotypic changes between planktonic cells and biofilm cells. Employing technologies such as RNA sequencing (RNA-seq) is a useful approach to use to determine changes in the transcriptional profile of bacteria and other organisms to gains philological in site between planktonic cells and biofilm cells (Kukurba and Montgomery, 2015).

The genetic information expressed by an organism influences the organism's displayed phenotype and can change depending the surrounding environmental factors (Kukurba and Montgomery, 2015). The transcriptome which is the resulting transcription product of all mRNA expressed in the cells is a useful indicator to interpret the functional processes of the cells under different biological conditions (Kukurba and Montgomery, 2015). Bacterial adaptation to changes in the environment is governed by multiple molecules such as transcription factors, RNA regulators and sigma factors that are involved in the regulation of mRNA synthesis and degradation (Mäder et al., 2016). Analysis of the transcriptomes across the bacterial genome provides quantitative information pertaining to the transcriptional profile the bacteria (Mäder et al., 2016).

5.1.1 Aims

In this chapter the main objective was to identify *S. aureus* genes encoding components that are primarily involved in biofilm formation and not planktonic. growth. Such component may provide better targets for identifying sites of infection associated with endocarditis. Affimers against such components could be raised as described in Chapter 3 for Protein A or Clumping Factor A, or may already have been the targets of Affimers selected as part of Chapter 4 (although not yet associated with a specific target). In addition, characterisation of the expression of genes within biofilms produced *in vitro* should provide insight into the underlying physiological state and provide a

benchmark for comparison against *in vivo* material isolated from patients. Whilst work already described in this thesis has shown a wide range of Affimer sequences can be readily selected using biofilms prepared in the lab, it remains to be shown that these biofilms mirror *S. aureus* associated with endocarditis. There was also interest in determining whether the physiology of cells removed during washing of biofilms differed significantly from those that were used to select Affimers.

5.2 Results

In order to gain physiological insight on the differences between planktonic cells and biofilm cells, RNA was extracted from planktonic cells and biofilm cells. The transcriptomic profile of planktonic cells and biofilm cells was analysed using differential expression analysis. Furthermore, cell wall associated proteins were analysed based on their gene expression to identify suitable candidates to raise Affimers against.

5.2.1 Purification of total RNA from Staphylococcus aureus planktonic culture and biofilm

To prepare *S. aureus* samples for RNA extraction, planktonic cells were grown in LB medium and biofilms were grown on cellulose disks on Brain heart infusion Agar (BHI) as described in (Section 2.2.2). RNA was purified from *S. aureus* strain SH1000 planktonic cells cultures (planktonic cells) and biofilms using acid phenol extraction method (Kieser et al., 2000) (for more details refer to Section 2.4 and 2.4.1 respectively). To preserve cellular RNA prior to RNA purification and halt cellular metabolism, planktonic cultures and biofilms were treated with a Stop solution consisting of 5% (v/v) saturated phenol in ethanol (Section 2.11.1). As observed previously in (Section 4.3), treatment of *S. aureus* biofilm with four PBST washes results in the removal of cells that are loosely attached cells leaving attached cells that were used to select Affimers. Since bacterial cells are distributed at different densities within the biofilm, the transcriptional profile of these cell might differ depending on their proximity to the surface of the biofilm (Kostakioti et al., 2013). This was taken into account when preparing biofilm samples for RNA extraction. To assess

the effectivity of the stop solution on halting cellular metabolism RNA from biofilm was collected at different stages of harvesting, in which biofilms were treated with stop solution before or after washing (Figure 5.1 B and C). Unlike planktonic cells, which were directly treated with the stop solution (Figure 5.1 A), cells within of the biofilm might not get equal exposure to the stop solution due to the ability of the biofilm to limit diffusion of the stop solution to reach cells in deeper layers of the biofilm (Kostakioti et al., 2013). It was a concern that adding the stop solution to the biofilms at different stages during RNA extraction would have significant changes in differential gene expression. To account for the variation in gene expression resulting from quenching metabolism, biofilm samples were treated with the stop solution in a matter that would include the stop solution with the PBST washes for the attached biofilm cells (Figure 5.1 B); as for the loosely attached cells which well be referred to as detached cells from now on, the stop solution was included after the PBST treatment (figure 5.1 C). Detached cells removed from the biofilm by the PBST treatment were insufficient to obtain enough RNA concentration for sequencing individually, so the washes containing the detached biofilm cells were pooled together.

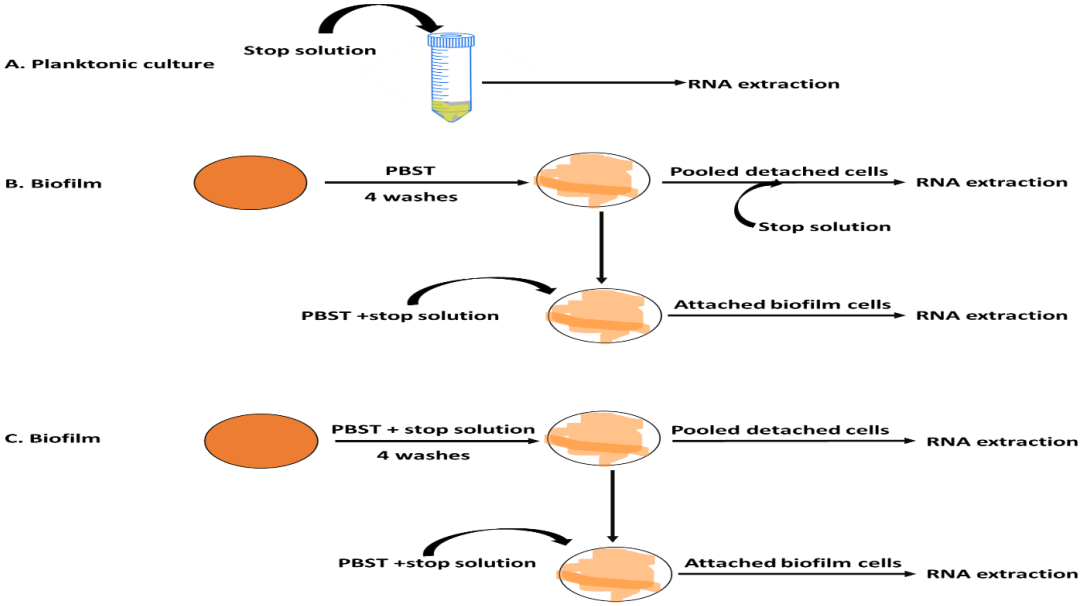

Figure 5.1 Schematic representation of preparation nucleic acid extraction from *S. aureus* planktonic culture and biofilm by quenching metabolism with stop solution. A. Planktonic cell culture treated with stop solution. **B.** biofilms which detached cells were treated with stop solution after washing with PBST washes only. **C.** biofilms treated with 4 PBST washes supplemented with stop solution at the start of RNA harvesting. For each biofilm sample detached biofilm cells were pooled, attached biofilm cells remaining after PBST treatment were removed from the disk

The purpose of extraction of the nucleic acid is to obtain samples that consisted only of RNA and not DNA. This was achieved by treatment of the total nucleic acid extracted from all samples with *DNase*I, which will digest the DNA leaving only RNA (Section 2.11.2). RNA sample concentration was determined by measuring the absorption at 260 nm using a UV nanophotometer. Sample purity was confirmed using agarose gel electrophoresis (Figure 5.2). After confirming the absence of a band corresponding to genomic DNA (gDNA), RNA samples were sent for sequencing. The quality of data generated from sequencing is dependent on the sample quality and library preparation, to ensure reliable data quality control was performed at each step leading to the data analysis (Kukurba and Montgomery, 2015). RNA sequencing was carried out using the services of Novogene using the Illumine HiSeq PE150 sequencing platform which generates 150-bp paired ends fragment size; the fragment size was selected

to ensures better quality data and more accurate sequence assembly fragmentation (Kukurba and Montgomery, 2015). To generate the library for sequencing, first rRNA was depleted using Ribo-zero kits (Zhao et al., 2014). Then enrichment of the population of mRNA was performed by first fragmentation of the mRNA using fragmentation buffer (NEB), followed by reverse transcription of mRNA in to single stranded cDNA using random hexamers as primers. The synthesised strand was used as a template to synthesise the complementary using DNA polymerase I (NEB) and RNase H (NEB) and addition of dNTPs (NEB) where the dTTP were replaced with dUTP). The now synthesised double stranded cDNA were purified using AMPure XP beads (Beckman Coulter™). The double stranded cDNAs were end-repaired and polyadenylated to allow for ligation of the poly-A adapter sequence, then selected based on size using AMPure XP beads. The strands containing uracil were then degraded using USER (Uracil-Specific Excision Reagent) (NEB). The remaining strands were amplified by PCR the purified using AMPure XP beads.

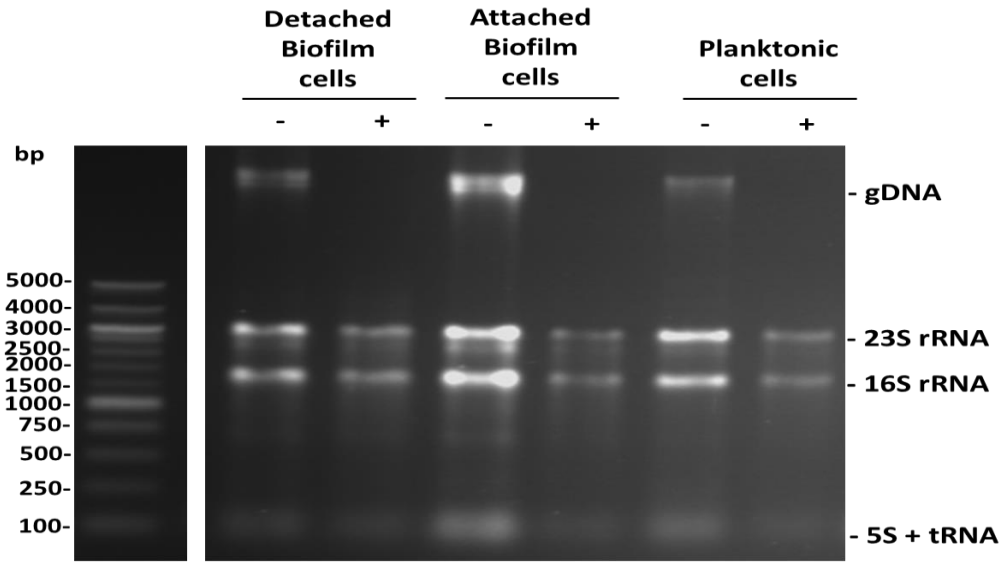

Figure 5.2 Analysis of total nucleic acid and rRNA isolated from *S. aureus* SH1000 grown as planktonic culture and biofilm. Samples were analysed by gel electrophoresis using a 1.2% (w/v) agarose gel. Lanes contain *S. aureus* strain SH1000 planktonic cells, biofilm first wash and biofilm, total nucleic acid for each sample was treated with (+) or without (-) *DNase* I.

5.2.2 RNA sequencing data processing

To properly analyse RNA-seq data, the results from sequencing must be assessed and processed using a bioinformatics approach in which a pipeline of programs are used to convert the sequencing results to data that can be analysed using a statistical approach (Kukurba and Montgomery, 2015). Sequencing raw data was obtained in a FASTQ file format which consist of information detailing the sequences and quality score for each sample. The low-quality reads and adaptor sequence were removed from all data using Trimmomatic® software (Galaxy Version 0.38.0). The quality of reads was judged based on their Phred score which is commonly used to assess the quality of sequencing reads (Bolger et al., 2014). The Phred score for the reads was 33 across all samples which indicates that base calling error rate of 1:1000 indicating good quality sequences (Bolger et al., 2014). The remaining sequences with good quality reads were then aligned against the reference genome sequence of *S. aureus* NCTC 8325 which is the congenic wild type for SH1000; reference sequence was obtained from National Centre for Biotechnology Information (NCBI) (Accession number: CP000253); mapping of reads was done using Bowtie2 Galaxy Version 2.3.4.3 (Langmead and Salzberg, 2012). Aligned reads were then assembled into transcripts and counted using StringTie software (Galaxy Version 1.3.6) (Pertea et al., 2015). Calculation of differential expression (DE) of genes was performed using DESeq2 (Galaxy Version 2.11.40.6). DESeq2 was chosen because it was asserted by Love et al. (2014), that its sensitivity is relatively higher compared to the other platforms because it can distinguish between fluctuation in the ratio of fold change by decreasing the estimated log2 fold changes for genes with low mean counts closer to zero, thus decreasing basis resulting from excessive estimation of fold changes for genes with low mean counts and obtaining more realistic quantitative results (Love et al., 2014). Deseq2 utilises an algorithm that fits a generalized linear model (GLM) for each gene by simulating the read counts based on a negative binomial distribution and generates outputs consisting of constants showing the strength of gene expression and the log2 fold change between different samples (Love et al., 2014).

5.2.3 Identification of Deferentially expressed gene between *Staphylococcus aureus* samples

Differences between the gene expression of planktonic cells and biofilm cells was expected as it is well documented in the literature that cells within a biofilm are phenotypically different than planktonic cells (Resch et al., 2005) . Furthermore, variation in different phenotypes within the biofilm cells population also exist such as small colony variants and persister cells (Lewis, 2007, Loss et al., 2019, Singh et al., 2009). Therefore, it was reasonable to hypothesise that cell that are removed from the surface of the biofilm by washing (i.e., detached biofilm cells) would have a different gene expression profile because they could express a different phenotype then attached cells that remained adherent after washing. To investigate the validity of this hypothesis, biofilm samples were collected at different stages of harvesting and the metabolism of both attached and detached biofilm cells samples was quenched with the stop solution at different stages of RNA harvesting as indicated earlier (Figure 5.1 B and C). It was also taken into account, that if there were differences in gene expression between attached and detached biofilm cells, it could be due to a change brought on by difference in sample preparation or variation between replicates which can also affect gene expression and thereby influencing DE analysis (Kukurba and Montgomery, 2015). Therefore, to identify the differences in the transcriptional profile between planktonic cells and biofilm cells, first variation in the transcriptional profile between attached and detached biofilm cells and the result from quenching cellular metabolism at different stages of harvesting needed to be explored. To account for false discovery rate due to multiple samples, the Dixon's Q test (Q-test) were set using the Benjamini–Hochberg procedure (Benjamini and Hochberg, 1995). Genes that met the cut-off threshold level of $Q \leq 0.01$ also referred to as the adjusted p-value were designated to be differentially expressed (Lai, 2017). Pairwise comparisons of the transcriptional profile of attached and detached biofilm cells revealed only one differentially expressed gene when comparing attached and detached cells which were treated with the stop mix at the beginning of RNA harvesting, no

differentially expressed genes were identified for attached and detached biofilm cells were identified for samples which were not treated with the stop mix at the beginning of RNA harvesting. This suggests that attached and detached biofilm cells share the same transcription profile and that any differences between biofilm samples could be negligible. Despite there being no significant differences in the number of differentially expressed genes indicated by the DE analysis between attached and detached biofilm cell population in both conditions, it was noticed that a significant number of cells were removed by washing. A possible explanation is that the removed cells are not embedded firmly within the matrix and are present on the outer surface of the biofilm making them more susceptible to being removed by mechanical force exerted by the washing. Furthermore, when investigating the effect of quenching metabolism at different stages of RNA harvesting by comparing the gene expression of attached biofilm cells or detached biofilm cells for samples treated to quench metabolism during or at later stages of RNA harvesting; only 3 genes were differentially expressed when comparing the gene expression of the two attached biofilm cells samples and one gene was differentially expressed when comparing the two detached biofilm cells samples. This suggests that similarly to the pairwise comparison of attached and detached biofilm cells, the point in which metabolism was quenched does not affect the transcriptional profile of biofilm cells and the differences in gene expression between the differently prepared biofilm cells samples is not detrimental to the differential gene expression analysis and could be neglected. Therefore, the gene expression data for the attached biofilm cells for samples treated to quench metabolism at the beginning or at later stages of RNA harvesting were pooled together. Other pairwise comparisons were also conducted between attached and detached cells against pooled attached and detached biofilm cells which indicate presence of only one differentially expressed gene in both comparisons; these comparisons further strengthen the argument that there is no significant difference between attached and detached cells or between samples treated with the stop mix at the beginning or at later stages of RNA harvesting. Using differential expression analysis, the gene expression of planktonic cells was compared with gene expression of pooled attached

biofilm cells which indicated the presence of 144 differentially expressed genes, the distribution of differentially expressed genes which are deemed up-regulated in or down-regulated in planktonic cells based on a log2 fold change≥±1 is displayed in a volcano plot (Figure 5.3).

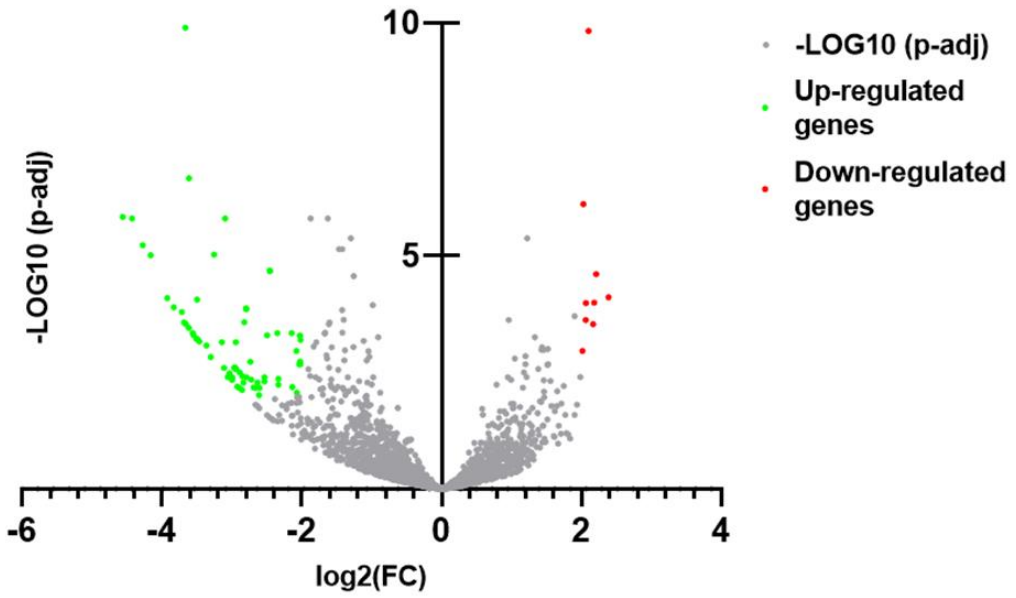

Figure 5.3 Volcano plot representing distribution of differential gene expression of *S. aureus* planktonic cells compared to biofilm cells. Differentially expressed genes based on adjusted p-value (p-adj)≤ 0.01. Green dots represent gene which are highly up-regulated in biofilm cells and red dots represent gene which are highly down-regulated in biofilm cells which meet the cut-off criteria p-adj ≤0.01 and Log2 FC≥±2. Figure generated using Graphpad prism 9. Three outlier points (point 1 (log10= 15.8, Log2 (FC)= -2.6); point 2 (log10= 17, Log2 (FC)= -3.5) point 3((log10= 80, Log2 (FC)= 6) were removed from the volcano plot as it resulted in distortion of the other points.

5.2.4 Identification of differentially expressed genes between planktonic cells and attached biofilm cells

By comparing gene expression of pooled attached biofilm cells grown for 48 h against planktonic cells it was possible to identify and statistically validate the genes that are differentially expressed (144) between these two phenotypes (Table 5.1). The differentially expressed genes were grouped into seven categories (cell wall associated, physiological function (transport, DNA

repair, purine metabolism), transcription regulators, ribosomal proteins, resistance, hypothetical). Out of the differentially expressed genes, 107 were expressed higher in biofilm cells than in planktonic cells and 37 genes were expressed higher in planktonic cells than in biofilm cells (Figure 5.3). From the 144 DE genes 107 were expressed higher in biofilm cells than planktonic cells and 37 were expressed higher in planktonic cells than biofilm cells (Table 5.2). identification of the functional annotation was performed using the database for annotation visualisation and integrated discovery (DAVID) Bioinformatics software of these genes was identified using Kyoto Encyclopaedia of genes and Genomes (KEGG) pathways and analysed using the functional annotation tool.

5.2.4.1 DE genes involved in *S. aureus* Infection

Five differentially expressed genes (*clfA, clfB, VarX, sdrA, scn*) that contribute to *S. aureus* infection also play important roles in biofilm formation while two genes *(agrC, hld)* play more significant roles in biofilm dispersal. The majority of genes involved in *S. aureus* infection were down-regulated in biofilm cells, only *clfA, VarX* and *scn* were up-regulated. Some cellular functions and proteins play more significant role than others in biofilm formation in *S. aureus*, the first of these functions is attachment to surfaces which is mostly facilitated via cell wall associated proteins (Foster et al., 2014). Three genes (*clfA, clfB, agrC*) encoding cell wall associated proteins were differentially expressed (Table 5.2). Two of these genes (*clfA, clfB*) are directly involved in biofilm formation by facilitating attachment to surfaces via binding fibrinogen and fibronectin as well as binding aggregated platelets during the early stages of biofilm formation (Hartford et al., 2001, O'Brien et al., 2002). ClfA and ClfB are part of the MSCRAMMs family of proteins Some CWA proteins to bind host molecules such as fibrinogen and fibronectin, these typically include proteins which belong to the microbial surface component recognizing adhesive matrix molecules (MSCRAMMs) family of proteins (Foster et al., 2014). Although, ClfA and ClfB are major proteins that contribute to attachment to surfaces, interestingly, ClfA was up-regulated by 1.8-fold in biofilm cells while clfB was down-regulated by 2.2-fold (Table 5.2). A previous study which indicated that the expression level of *clfA* and *clfB* in *S. aureus* strain N315 biofilm peaks at

4 and 8-fold higher than planktonic cells after 16 h of growth then decreases after 48 h of growth but still remaining 3-fold higher than expression in planktonic cells (Resch et al., 2005). Since here only the expression of *clfA* was higher in biofilm cells than planktonic cells, this suggest that although both *clfA* and *clfB* contribute to attachment, *clfA* plays a more significant role in stabilisation of the biofilm and its expression is retained even in mature biofilm. This result validated the choice of ClfA as a candidate target to raise Affimers against (see Chapter 3). On another note, *agrC* which is a sensor histidine kinase component of the *agr* operon involved in biofilm dispersal through the quorum sensing mechanism in *S. aureus* was expressed 2-fold higher in planktonic cells compared to biofilm cells (Table 5.2) (Boles and Horswill, 2008). The expression of *agrC* is regulated by the production of autoinducing peptide (AIP) by *agrD* whose expression is regulated by other component of the *agr* operon; as other components of the *agr* operon were not differentially expressed the lower expression of *agrC* in biofilm cells is expected (Table 5.2) (Yarwood and Schlievert, 2003).

S. aureus genes *varX* (5.6-fold) and *scn* (8.3-fold) had higher levels of expression in biofilm cells than planktonic cells, amongst the genes contributing to *S. aureus* infection *varX* and *scn*, showed the highest fold change between planktonic cells and biofilm cells (Table 5.2). This indicates the important role that these genes in evasion of the host immune system during biofilm formation. Both VarX and Scn contribute to biofilm formation and cell survival by binding components of the complement pathway thereby inhibit complement activity (De Jong et al., 2018, Yan et al., 2017).

5.2.4.2 DE genes involved in Physiological processes

The differences in the expression pattern of some genes can reflect the importance of certain metabolic and physiological pathways that could be involved in biofilm formation and emergence of persister cells. Therefore, the expression of genes involved in purine metabolism, transport and DNA repair, were particularly important as they have been implicated in biofilm stability and conveying antibiotic tolerance via persister cells formation (Boles and Singh, 2008, Goncheva et al., 2019, Mok and Brynildsen, 2018, Yee et al.,

2015, Zhang, 2014). Several genes involved in DNA repair (*gyrA, uvrA, recO, DnaI*) and drug resistance (*EmrB*, *lyrA*, *fmhA*) were differentially expressed (Table 5.2). All genes involved in DNA repair were up-regulated in biofim cells, *DnaI* was amongst the top 20 up-regulated differentially expressed genes (Table 5.2). *EmrB*, *fmhA* were expressed 3-fold and 2.7-fold higher in biofilm cells respectively, while *lyrA* was expressed 2.3-fold higher in planktonic cells (Table 5.2). DNA repair and drug resistance have been implicated as contributors to the formation of persister cells within biofilms formed by many bacterial species including *Staphylococci* (Boles and Singh, 2008, Lewis, 2007, Wilmaerts et al., 2019). In which *S. aureus*, *P. aeruginosa* and *E. coli* persister cells were found to have an increased expression of genes which function in toxin production and DNA repair (Boles and Singh, 2008, Lewis, 2007, Wilmaerts et al., 2019). Furthermore, it has been reported that DNA repair genes contribute to survival of persister cells (Mok and Brynildsen, 2018). Although the main perception about persister cells is that they are dormant and therefore would not be affected by antibiotics that target active cells however, some studies have alluded to the fact that *E. coli* persister cells suffered DNA damage after treatment with fluoroquinolone antibiotics which inhibit DNA synthesis and cause damage to dsDNA(Mok and Brynildsen, 2018). As a result of DNA damage inflected by antibiotic treatment, persister cells undergo a recovery period which is thought to be crucial for persister cells survival that consists of DNA repair, DNA synthesis, and cell growth (Goneau et al., 2014, Mok and Brynildsen, 2018). Other reports also, allude that DNA repair may contribute to mutations that result in the emergence of variants in the persister cells populations within *P. aeruginosa* biofilm as a result of DNA damage during oxidative stress and starvation (Boles and Singh, 2008). This highlights the importance of DNA repair genes in biofilm formation and persister cell survival.

5.2.4.3 DE genes involved in Purine metabolism proteins

Further investigation into the expression pattern of differentially expressed genes indicated that genes involved in purine biosynthesis and transport proteins might play a significant role in biofilm formation and stability. Out of genes involved in purine metabolism, nine genes *purC, D, F, H, L, M, N, Q,S*

are part of the *purEKCSQLFMNHD* purine biosynthetic operon (Goncheva et al., 2019).The remaining four genes *rpoB,C* and *guaA,M* are involved in DNA repair and glutamine monophosphate (GMP) synthesis respectively (Aboshkiwa et al., 1992, Gillaspy et al., 2006). The importance of purine metabolism in biofilm formation is due to the fact that purines are important for the production of eDNA which is a part of *S. aureus* biofilm matrix, as well as inducing aggregation via fibrinogen and fibronectin binding which are both important factors that influence biofilm formation in *S. aureus* as well as other Gram-positive bacteria such as *B. subtilis* (Gélinas et al., 2020, Goncheva et al., 2019, Pisithkul et al., 2019). Furthermore, several studies have previously reported up-regulation of genes involved in purine metabolism in both Gram-positive and Gram-negative during biofilm formation (Goncheva et al., 2019, Sause et al., 2019, Shaffer et al., 2017, Yoshioka and Newell, 2016). This give confidence in the differential gene expression analysis conducted as it is in line with previous studies, here it was found that genes involved in purine metabolism such as guaA, guaB, *purN*, *purL*, *purQ*, *purH* and *purM* were ≥2.3-fold up-regulated in biofilm cells (Table 5.2). The importance in purine metabolism is further confirmed in a study indicated that deletion of genes involved in purine metabolism such as, *purN*, *purL*, *purQ*, *purH* and *purM* resulted in impairment of S. aureus biofilm formation (Gélinas et al., 2020). Another study also indicated the effect of overexpression of genes involved in purine metabolism results in increased clumping of *S. aureus* cells during biofilm formation in a fibrinogen and fibronectin dependent mechanism by increasing the expression of fnbA/B at low cell densities (Goncheva et al., 2019). However, both *fnb*A/B were not differentially expressed while *clfA* and *clfB* which induce clumping via fibrinogen binding were differentially expressed (Table 5.2). This further highlights the importance of purine metabolism in *S. aureus* biofilm formation is not just restricted to adaptation to environmental conditions by regulation of biosynthesis of IMP but induction of biofilm formation through aggregation. Furthermore, genes involved in purine biosynthesis have also been implicated in survival of persister cells within *S. aureus* biofilm and provides confirmation to the idea mentioned earlier that persister cells are not necessarily permanently dormant while

within a biofilm and that they could show some metabolic activity in order to undergo the recovery phase. Furthermore, purine biosynthesis has been implicated in increased tolerance to antibiotics particularly rifampicin in *S. aureus* USA300 persister cells (Yee et al., 2015). The study by Yee et. al, 2015 indicated that USA300 *pur* mutants were more susceptible to killing by rifampicin than the wild type (Yee et al., 2015). Similarly, to genes involved in toxin production and DNA repair, the importance of purine metabolism has been highlighted in several studies which have shown the involvement of purine biosynthesis in DNA repair and stress response pertaining to survival of persister cells in several organisms such as, *E. coli* and *P. aeruginosa* (Yee et al., 2015, Zhu et al., 2019).

5.2.4.4 DE genes involved in Thiamine metabolism

On the other hand, unlike genes involved in purine biosynthesis Differentially expressed genes (*thiE*, *thiM*, *thiD*) involved in thiamine metabolism were down regulated in biofilm cells as their expression was >2.5-fold higher in planktonic cells than biofilm cells (Table 5.2). Furthermore, *thiM* was amongst the top 20 down-regulated gene in biofilm cells (Table 5.3). This is in line with several studies that indicate that thiamine metabolism is down-regulated in *S.* aureus and *pseudomonas aeruginosa* (*P. aeruginosa*) biofilms (Gélinas et al., 2020, Kim et al., 2020, O'May et al., 2006). Thiamine pyrophosphate (TPP), the active form of thiamine is an important cofactor for many essential physiological processes in bacteria such as, carbohydrate, amino acid and lipid metabolism (Bunik et al., 2013, Singleton and Martin, 2001). Therefore, thiamine metabolism is essential to support planktonic cell growth for many organisms including *S. aureus* and *P. aeruginosa*, however its effect on biofilm growth is detrimental (Drebes et al., 2016, Kim et al., 2020). Foresentence, *pseudomonas aeruginosa* is known for biofilm formation under anaerobic growth conditions, in which limited oxygen and nutrition are available (O'May et al., 2006). However, under these conditions supplementation with vitamin B_{12} resulted in a reduction in biofilm formation (Lee et al., 2012). Therefore, it is expected that thiamine metabolism is up-regulated in planktonic cells and down-regulated in biofilm cells. Other downregulated genes include those involved in fatty acid metabolism such as, SAOUHSC_00963,

SAOUHSC_01709, SAOUHSC_01710 (Table 5.2). Similarly to thiamine metabolism, it has been reported that an increase in fatty acids result in decreased biofilm formation in *S. aureus* and other Gram-positive bacteria (Yuyama et al., 2020).

5.2.4.5 DE genes encoding Transport proteins

Furthermore, 21 genes encoding transport proteins were differentially expressed, the majority of these genes were up-regulated and only five were down-regulated (Table 5.2). ABC transporters are transmembrane proteins that are important for a variety of cellular functions including transport and translocation of important nutrients and molecules across the cell membrane such as adenosine triphosphate (ATP), amino acids, lipids and minerals (Davidson and Chen, 2004). Identification of the functional pathways of these genes using KEGG pathways indicated the presence of five genes (SAOUHSC_00133, SAOUHSC_00135, SAOUHSC_00136, SAOUHSC_00137, SAOUHSC_00138) in volved in Iron transport and three genes (*pstB*, *PstA*, *pstC*) involved in phosphate transport and two genes (*mnhC* and *mnhD*) part of the monovalent cation Na+/H+ antiporter system (Table 5.2). All differentially expressed genes were involved in iron transport and were up-regulated >2.9-fold higher in biofilm cells than planktonic cells (Table 5.2), SAOUHSC_00136, SAOUHSC_00138 were amongst the top 20 highest up-regulated differentially expressed genes in biofilm cells (Table 5.2). The importance of iron uptake in biofilm formation has been indicated for several bacterial species including *S. aureus* and *P. aeruginosa* (Kang and Kirienko, 2018, Lin et al., 2012). In which iron depravation resulted reduced biofilm formation of both *S. aureus* and *P. aeruginosa* (Kang and Kirienko, 2018, Lin et al., 2012). The differential expression of five genes involve in Iron transport which are highly expressed in biofilm cells further confirms involvement of iron in biofilm formation observed in previous studies (Kang and Kirienko, 2018, Lin et al., 2012). Similarly, all genes involved in iron transport, genes involved in phosphate transport were up-regulated >5-fold in biofilm cells (Table 5.2). The involvement of phosphate in biofilm formation

has been previously reported in several bacterial species including *S. aureus* and *E. coli* (Grillo-Puertas et al., 2012, Kelliher et al., 2018, Pereira et al., 2008).Several studies have reported that biofilm growth under phosphate limited conditions result in improved adherence to surfaces (Danhorn et al., 2004, Ghosh et al., 2019). Furthermore, *mnhC* and *mnhD* which are part of the *mnhABCDEFG* operon that is involved in the monovalent cation Na+/H+antiporter system were differentially expressed, the expressions of *mnhC* and *mnhD* were 1.9 and 2.1-fold higher in biofilm cells than planktonic cells (Table 5.2). Cation transporters are involved in maintaining pH during increased environmental stress levels (Vaish et al., 2018). This suggesting that these genes are important for biofilm maintenance (Wang, 2004). Another differentially expressed gene that encode transport proteins *thrE* which encodes a succinate transport protein was 2.9-fold up-regulated in biofilm cells. Succinate plays an important in the Tricarboxylic acid (TCA) cycle particularly the respiratory chain, it has been reported that genes involved in the TCA cycle are up-regulated in *S. aureus* and *S. epidermidis* biofilms (Resch et al., 2005, Sadykov et al., 2008). As an important part of the TCA cycle, increased succinate intake has been reported to increase biofilm formation, while deletion in genes involved with succinate oxidation such as succinate dehydrogenase decrease in *S. aureus* biofilm formation (Gaupp et al., 2010). Although biofilm cell are less metabolically active than planktonic cells, the importance of transporter genes enables the cells to utilise nutrients from the environment that are necessary for adaptation and physiological processes such as pH maintenance and protein synthesis needed to maintain the biofilm (Balasubramanian et al., 2017).The number of differentially expressed transport gene which are up-regulated in biofilm cells in this study was much higher that what was observed in a previous study (Resch et al., 2005). The study indicated that the number of genes encoding transport proteins that were expressed higher in *S. aureus* N315 biofilm cells was 16 genes after 8 h of growth and after 24 h of growth decreased to 1 gene (Resch et al., 2005). This could be attributed to strain differences or biofilm growth duration; on the other hand it could be due to the fact that they used DNA

microarray instead of RNA sequencing which is more accurate and reproducible than microarray (Kukurba and Montgomery, 2015).

5.2.4.6 DE genes encoding ribosomal proteins

Another group of differentially expressed genes included ribosomal proteins, ribosomal proteins are needed for proteins synthesis, an increased in their expression is indicative of cell replication (Doudna and Rath, 2002). Only, two gene (*rplL* and *rplW*) which encode ribosomal proteins were differentially expressed, the expression of *rplW* was up-regulated by 6.4-fold in biofilm cells while *rplL* was down-regulated by 2.2-fold in biofilm cells. It is unclear why only two genes encoding ribosomal proteins were differentially expressed considering the need for all ribosomal gene are needed for proteins synthesis (Doudna and Rath, 2002). However, this have been reported in several studies which indicate that a small number of genes encoding ribosomal proteins are expressed in mature biofilms (Resch et al., 2006, Resch et al., 2005). The study indicated that *S. aureus* biofilm grown for 8 h, 20 differentially expressed genes encoding ribosomal proteins were expressed >2-fold higher in biofilm cells than planktonic cells, however, only one DE gene encoding ribosomal protein was expressed at higher level in biofilm cells than planktonic cells after 16 h of growth and no genes were expressed at higher level in biofilm grown for 24 and 48 h (Resch et al., 2005).

5.2.4.7 DE genes encoding phage proteins

Nine genes encoding phage proteins were differentially expressed, all genes were expressed >4-fold higher in biofilm cells than planktonic cells (Table 5.2), five genes (SAOUHSC_02113, SAOUHSC_02178, SAOUHSC_02180, SAOUHSC_02181, SAOUHSC_02182) were amongst the top 20 up-regulated genes in biofilm cell between the differentially expressed genes (Table 5.3). The successful integration of phage genetic material into the genome of many bacterial species including *S. aureus* has been regarded as a competitive evolutionary advantage over phage sensitive bacterial strains (Fernández et al., 2018). Incorporation of phage genome in bacteria results in acquisition of genetic information that often convey virulence factors such as antibiotic resistance Panton-Valentine leucocidin (PVL), staphylokinase and

cell lysins. As activation of phage proteins can cause cell lysis thereby the intracellular contents of the lysed cells can be utilised as nutrients (Fernández et al., 2018). Furthermore, components of lysed cells such as, extracellular DNA (eDNA) which is a major structural component of both Gram-positive and Gram-negative bacterial biofilms such as *S. aureus* and *P. aeruginosa* (Montanaro et al., 2011, Quinn et al., 2019). The role eDNA plays in biofilm formation is not restricted to contribution to the structural integrity of the biofilm, eDNA also plays a significant role in protection from the host immune system via preventing phagocytosis (Devaraj et al., 2019, Montanaro et al., 2011). Moreover, phage proteins have also been implicated in *S. aureus* biofilm formation by inhibition of the expression of the *agr* operon thereby inducing the expression of *sigB* which is a major regulator of *S. aureus* biofilm formation (Bischoff et al., 2001, Fernández et al., 2018, Pané-Farré et al., 2009).

5.2.4.8 DE genes encoding hypothetical proteins

Furthermore, out of the differentially expressed genes, 48 genes encoding hypothetical proteins (Table 5.2). No information on the function or involvement in physiological pathways of these genes was identified by DAVI or KEGG pathways. However, the majority of these genes showed higher expression in biofilm cells in which 30 genes were up-regulated in biofilm cells, out of which were five genes (SAOUHSC_02176, SAOUHSC_02226, SAOUHSC_02227, SAOUHSC_02228, SAOUHSC_02596) were amongst the top 20 up-regulated differentially expressed genes in biofilm cells (Table 5.2). Furthermore, four genes (SAOUHSC_02225, SAOUHSC_02226, SAOUHSC_02227, SAOUHSC_02228) encoding hypothetical proteins were adjacent to each other indicating that they could contribute to the same physiological function and that they might play a significant role in biofilm formation since three of these genes were amongst the top 20 up-regulated differentially expressed genes in biofilm cells as mentioned above (Table 5.2). Moreover, 18 genes were down-regulated in biofilm cells, out of which 11 genes were amongst the highest down-regulated differentially expressed genes, indicating that they most likely do not contribute to biofilm formation (Table 5.2).

In conclusion differential expression analysis comparing expression in biofilm cell with planktonic cells revealed 144 genes that were differentially expressed (Table 5.2), out of these genes 107 were up-regulated in biofilm cells and 37 were down-regulated in biofilm cells (Figure 5.3). Several of the differentially expressed genes appeared to contribute to the same metabolic or physiological pathway such as purine biosynthesis or transport which indicated that some of these pathways might be important to biofilm formation. Further analysis regarding the involvement of different gene in each pathway revealed that the majority of metabolic and physiological pathways such as purine biosynthesis and DNA repair have been reported in the literature to be involved in persister cells formation in *S. aureus* biofilm and biofilm formed by other bacterial species such as *E. coli* and *P. fluorescens* (Balaban et al., 2004, Mok and Brynildsen, 2018, Yee et al., 2015, Yoshioka and Newell, 2016). Targeting the gene product of the highest expressed genes involved these pathways using Affimers could have some potential therapeutic effects that limit the formation of persister cells within the biofilm. For instance, several genes involved in purine biosynthesis such as, *rpoC*, *rpoB*, *puLI*, *purH* were expressed >-fold higher respectively than the Table 5.2). Targeting the purine biosynthesis pathways has been shown to inhibit biofilm formation in *Pseudomonas fluorescens*, this suggest that targeting proteins involved in purine metabolism using Affimers might be an effective strategy to prevent *S. aureus* biofilm formation (Yoshioka and Newell, 2016). For the most part the findings from differential expression analysis between planktonic cells and biofilm cells is in line with findings presented in other studies (Beenken et al., 2004, Resch et al., 2005). However, differences between the findings can be attributed to several factors such as, biofilm maturation stage, strain differences and method used for transcriptomic analysis.

Table 5.2 Differentially expressed genes between planktonic cells and attached biofilm cells

Differentially expressed genes between planktonic cells and attached biofilm cells

Locus tag	UNIPROT & Annotation	Product/ Function	log2(FC)	Adjusted P-value	Fold change
***S. aureus* infection**					-
SAOUHSC_02167*	*Scn*	Inhibits opsonisation, complement inhibitor	-3.05401	0.001256	8.31↑
SAOUHSC_00561	*VarX*	Complement inhibitor	-2.50367	0.005143	5.67↑
SAOUHSC_02260$^{\Delta}$	*Hld*	Delta-hemolysin	2.069537	9.36E-10	4.20 ↓
SAOUHSC_02963	*clfB*	Clumping factor B	1.157399	0.003646	2.23↓
SAOUHSC_01175$^{\Delta}$	*sdrA*	Fibrinogen-binding protein A-like protein	1.141657	0.007551	2.21↓
SAOUHSC_02264	*agrC*	Accessory gene regulator protein C	1.025298	0.002566	2.04↓
SAOUHSC_00812	*clfA*	Clumping factor A	-0.91444	0.000842	1.88 ↑
Physiological process and cellular metabolism					
SAOUHSC_01576*		Exonuclease	-3.84489	1.40E-05	14.37↑
SAOUHSC_00773*		LysM domain-containing protein	-3.54053	4.48E-18	11.64↑
SAOUHSC_02173*		Amidase	-3.33277	0.000304	10.08↑
SAOUHSC_01612$^{\Delta}$		2-oxoisovalerate dehydrogenase component subunit beta	3.169299	0.000842	9.00↓
SAOUHSC_00422*		Trans-sulfuration enzyme family protein	-3.15667	8.65E-06	8.92↑
SAOUHSC_02653*		Selenocompound metabolism	-3.02987	1.54E-06	8.17↑
SAOUHSC_02019*	*lytO*	Autolysin	-3.01301	0.001303	8.07↑

SAOUHSC_00174		M23/M37 peptidase	-2.46864	0.006787	5.54↑
SAOUHSC_01761a		Membrane protein	-2.44862	0.009868	5.46↑
SAOUHSC_02737		Epimerase	-2.42888	0.00474	5.38↑
SAOUHSC_00421		Amino acid synthesis	-2.41654	2.35E-05	5.34↑
SAOUHSC_00577	*mvaK1*	Mevalonate kinase	-2.30566	0.000418	4.94↑
SAOUHSC_02452	*lacD*	Tagatose 1,6-diphosphate aldolase	-2.10802	0.00054	4.31↑
SAOUHSC_01709$^{\Delta}$		Acetyl-CoA carboxylase	2.015579	0.00026	4.04↓
SAOUHSC_01710$^{\Delta}$		Acetyl-CoA carboxylase biotin carboxyl carrier protein subunit	1.964845	0.001153	3.90↓
SAOUHSC_02455	*lacA*	Galactose-6-phosphate isomerase subunit LacA	-1.83867	0.004658	3.58↑
SAOUHSC_00118	*CapE*	Capsular polysaccharide biosynthesis protein Cap5E	-1.6767	0.008697	3.20↑
SAOUHSC_00119	*CapF*	Capsular polysaccharide biosynthesis protein Cap8F	-1.63636	0.001232	3.11↑
SAOUHSC_01748	*Tgt*	Queuine tRNA-ribosyltransferase	-1.62757	0.001582	3.09↑
SAOUHSC_01666	*glyQS*	Glycyl-tRNA synthetase	-1.60821	0.000304	3.05↑
SAOUHSC_02371	*coaW, coaA*	Pantothenate kinase	-1.59962	0.002566	3.03↑
SAOUHSC_02654		Selenocompound metabolism	-1.56704	0.004551	2.96↑
SAOUHSC_01499		Selenocompound metabolism	-1.41862	0.000476	2.67↑
SAOUHSC_00129		UDP-*N*-acetylglucosamine 2-epimerase	-1.40141	0.000327	2.64↑
SAOUHSC_00142		Formate dehydrogenase	-1.389	0.002149	2.62↑
SAOUHSC_02808		Gluconate kinase	-1.32435	0.008697	2.50↑
SAOUHSC_02875		D-lactate dehydrogenase	-1.2251	0.00915	2.34↑
SAOUHSC_02363		Aldehyde dehydrogenase	-1.09197	0.009872	2.13↑
SAOUHSC_02374		Aminobenzoyl-glutamate utilisation protein B	-1.07424	0.002149	2.11↑
SAOUHSC_00849		Selenocompound metabolism	-1.03853	0.001441	2.05↑
SAOUHSC_00756		Amino acid metabolism	-1.00359	0.006787	2.00↑
SAOUHSC_00771	*prfB*	Peptide chain release factor 2	-0.99265	0.000213	1.99↑

SAOUHSC_00963		Lipoyltransferase and lipoate-protein ligase	0.975214	0.006447	1.97↓
Purine metabolism					
SAOUHSC_01013	*purL*	Phosphoribosylformylglycinamidine synthase II	-2.04375	0.001005	4.12↑
SAOUHSC_01015	*purM*	Phosphoribosylaminoimidazole synthetase	-2.00166	0.001836	4.00↑
SAOUHSC_01016	*purN*	Phosphoribosylglycinamide formyltransferase	-1.99166	0.001586	3.98↑
SAOUHSC_01014	*purF*	Amidophosphoribosyltransferase	-1.98695	0.001836	3.96↑
SAOUHSC_01012	*purQ*	Phosphoribosylformylglycinamidine synthase I	-1.81369	0.000797	3.52↑
SAOUHSC_01017	*purH*	Bifunctional phosphoribosylaminoimidazolecarboxamide formyltransferase/IMP cyclohydrolase	-1.7789	0.003886	3.43↑
SAOUHSC_01018	*purD*	Phosphoribosylamine--glycine ligase	-1.72982	0.004228	3.32↑
SAOUHSC_00525	*rpoC*	DNA-directed RNA polymerase subunit beta'	-1.71141	0.006812	3.27↑
SAOUHSC_00524	*rpoB*	DNA-directed RNA polymerase subunit beta	-1.6776	0.006787	3.20↑
SAOUHSC_01011	*purS*	Phosphoribosylformylglycinamidine synthase PurS	-1.50746	0.006812	2.84↑
SAOUHSC_01010	*purC*	Phosphoribosylaminoimidazole-succinocarboxamide synthase	-1.47412	0.005847	2.78↑
SAOUHSC_00374	*guaB*	Inosine-5'-monophosphate dehydrogenase	-1.30357	8.63E-06	2.47↑
SAOUHSC_00375	*guaA*	GMP synthase	-1.26199	4.17E-05	2.40↑
Thiamine metabolism					
SAOUHSC_02329$^{\Delta}$	*thiM*	Hydroxyethylthiazole kinase	1.437913	0.00117	2.71↓
SAOUHSC_02330	*thiD*	Phosphomethylpyrimidine kinase	1.402502	0.001256	2.64↓
SAOUHSC_02328	*thiE*	Thiamine-phosphate pyrophosphorylase	1.311751	0.000773	2.48↓
ABC transporter					
SAOUHSC_01379	*oppC2, opp-2C*	oligopeptide transporter permease	-2.73305	0.00026	6.65↑
SAOUHSC_02270		Ammonium transporter	-2.43328	0.003974	5.40↑
SAOUHSC_02874	*copZ*	Cation transporter E1-E2 family ATPase	-2.42451	1.82E-05	5.37↑
SAOUHSC_02729$^{\Delta}$		ABC transporter-like protein	1.987741	1.54E-06	3.97↓

SAOUHSC_01991$^{\Delta}$		ABC transporter permease	1.862208	0.00026	3.64↓
SAOUHSC_00571	*thrE*	succinate transport	-1.56163	0.006682	2.95↑
SAOUHSC_00667$^{\Delta}$		ABC transporter ATP-binding protein	1.524684	0.005143	2.88↓
SAOUHSC_00927$^{\Delta}$		ABC transporter substrate-binding protein	1.494259	0.001024	2.82↓
SAOUHSC_00071	*sirC*	Lipoprotein SirC	-1.46789	1.47E-05	2.77↑
SAOUHSC_00668		ABC transporter permease	1.412614	0.001024	2.66↓
SAOUHSC_00628	*mnhD*	Monovalent cation antiporter subunit D	-1.12054	0.001005	2.17↑
SAOUHSC_00747		ABC transporter permease	-1.06375	0.006862	2.09↑
SAOUHSC_00627	*mnhC*	Monovalent cation/H+ antiporter subunit C	-0.98251	0.005244	1.98↑
Iron transport					
SAOUHSC_00138*		Iron transport	-3.58147	2.18E-10	11.97↑
SAOUHSC_00136*		Iron transport	-3.4956	1.95E-07	11.28↑
SAOUHSC_00133		Iron transport	-2.72696	0.000112	6.62↑
SAOUHSC_00135		Iron transport	-2.59674	1.17E-15	6.05↑
SAOUHSC_00137		Iron transport	-1.56946	0.006787	2.97↑
Phosphate transport					
SAOUHSC_01385	*pstB*	Transporter ATP-binding protein	-2.57543	0.004551	5.96↑
SAOUHSC_01387	*pstC*	Phosphate transport system permease protein; Part of the binding-protein-dependent transport system for phosphate; probably responsible for the translocation of the substrate across the membrane	-2.52736	0.006787	5.77↑
SAOUHSC_01386	*PstA*	ABC transporter permease	-2.50637	0.006787	5.68↑
DNA synthesis/ repair					
SAOUHSC_01791*	*DnaI*	Primosomal protein	-3.98542	4.17E-06	15.84↑
SAOUHSC_00006	*gyrA*	DNA gyrase subunit A	-2.00277	0.000488	4.01↑
SAOUHSC_01667	*recO*	DNA repair	-1.5649	0.000816	2.96↑

SAOUHSC_00780	*uvrA*	Excinuclease ABC subunit A	-1.05144	0.001296	2.07↑
Phage protein					
SAOUHSC_02182*		Tail length tape measure protein	-3.40531	0.00026	10.59↑
SAOUHSC_02178*		phi PVL orf 22-like protein	-3.18448	0.000747	9.09↑
SAOUHSC_02180*		phage minor structural protein	-3.1766	0.000776	9.04↑
SAOUHSC_02181*		phi PVL orfs 18-19-like protein	-3.09631	0.001067	8.55↑
SAOUHSC_02113*	*rumA*	RNA methyltransferase	-2.82006	0.000743	7.06↑
SAOUHSC_02239		Integrase	-2.72935	0.004731	6.63↑
SAOUHSC_02060		phi PVL orf 51-like protein	-2.64926	0.006812	6.27↑
SAOUHSC_01580		phi PVL ORF 30-like protein	-2.57627	0.006962	5.96↑
SAOUHSC_02250		Phage terminase subunit	-2.25328	0.005705	4.77↑
Drug resistance					
SAOUHSC_02629	*EmrB*	EmrB/QacA family drug resistance transporter	-1.65878	0.000488	3.16↑
SAOUHSC_02696	*FmhA*	Methicillin resistance determinant protein FmhA	-1.47115	0.002513	2.77↑
SAOUHSC_02611	*lyrA*	Lysostaphin resistance protein A	1.201688	1.80E-05	2.30↓
Ribosomal proteins					
SAOUHSC_02510	*rplW*	50S ribosomal protein L23	-2.68596	0.005847	6.44↑
SAOUHSC_00521	*rplL*	50S ribosomal protein L7/L12	1.175901	0.002097	2.26↓
Other					
SAOUHSC_01361	*msrR*	Transcriptional regulator	-1.66345	0.000441	3.17↑
Hypothetical					
SAOUHSC_02674$^{\Delta}$		hypothetical protein	4.382399	2.19E-08	20.86↓
SAOUHSC_02596*		hypothetical protein	-3.31328	8.19E-05	9.94↑
SAOUHSC_02227*		hypothetical protein	-3.20658	0.00069	9.23↑
SAOUHSC_02228*		hypothetical protein	-3.13489	0.000866	8.78↑
SAOUHSC_02226*		hypothetical protein	-3.03685	0.001315	8.21↑

SAOUHSC_02176*	hypothetical protein	-3.00015	0.001604	8.00↑
SAOUHSC_01573	hypothetical protein	-2.78897	0.003886	6.91↑
SAOUHSC_01388	hypothetical protein	-2.76665	0.002566	6.81↑
SAOUHSC_02225	hypothetical protein	-2.67974	0.006484	6.41↑
SAOUHSC_00401	hypothetical protein	-2.67125	0.003933	6.37↑
SAOUHSC_02531	hypothetical protein	-2.43918	0.000488	5.42↑
SAOUHSC_01712$^{\Delta}$	hypothetical protein	2.332083	7.05E-05	5.04↓
SAOUHSC_02294	hypothetical protein	-2.31003	0.006061	4.96↑
SAOUHSC_00659	hypothetical protein	-2.26522	0.004071	4.81↑
SAOUHSC_00596$^{\Delta}$	hypothetical protein	2.162799	3.45E-05	4.48↓
SAOUHSC_02756$^{\Delta}$	hypothetical protein	2.135078	0.000102	4.39↓
SAOUHSC_01711$^{\Delta}$	hypothetical protein	2.117482	0.000309	4.34↓
SAOUHSC_01707$^{\Delta}$	hypothetical protein	2.019059	0.000118	4.05↓
SAOUHSC_00569	hypothetical protein	-1.99171	0.000647	3.98↑
SAOUHSC_02757$^{\Delta}$	hypothetical protein	1.927891	0.004062	3.80↓
SAOUHSC_01034	hypothetical protein	-1.87963	0.002526	3.68↑
SAOUHSC_03035	hypothetical protein	-1.86936	2.12E-06	3.65↑
SAOUHSC_02686	hypothetical protein	-1.82567	0.009925	3.54↑
SAOUHSC_00682	hypothetical protein	-1.77815	0.000788	3.43↑
SAOUHSC_00598$^{\Delta}$	hypothetical protein	1.700895	0.006812	3.25↓
SAOUHSC_02630	hypothetical protein	-1.62612	3.69E-06	3.09↑
SAOUHSC_00400$^{\Delta}$	hypothetical protein	1.612281	0.008697	3.06↓
SAOUHSC_01763	hypothetical protein	-1.59592	0.000278	3.02↑
SAOUHSC_00830$^{\Delta}$	hypothetical protein	1.497898	0.002013	2.82↑
SAOUHSC_01021$^{\Delta}$	hypothetical protein	1.479411	0.002566	2.79↓

SAOUHSC_01019	hypothetical protein	1.42769	0.009643	2.69↓
SAOUHSC_01508	hypothetical protein	1.429514	0.005846	2.69↓
SAOUHSC_00851	hypothetical protein	-1.4219	0.00014	2.68↑
SAOUHSC_01878	hypothetical protein	-1.42191	1.76E-05	2.68↑
SAOUHSC_01630	hypothetical protein	-1.41168	0.006862	2.66↑
SAOUHSC_02994	hypothetical protein	-1.3917	0.007185	2.62↑
SAOUHSC_00327	hypothetical protein	-1.38075	0.001315	2.60↑
SAOUHSC_03041	hypothetical protein	1.353154	0.003974	2.55↓
SAOUHSC_02551	hypothetical protein	-1.33706	0.004989	2.53↑
SAOUHSC_00531	hypothetical protein	-1.26205	0.007166	2.40↑
SAOUHSC_01877	hypothetical protein	-1.26283	0.001153	2.40↑
SAOUHSC_02670	hypothetical protein	1.187181	0.005847	2.28↓
SAOUHSC_02626	hypothetical protein	1.18077	0.002312	2.27↓
SAOUHSC_00850	hypothetical protein	-1.18103	0.004726	2.27↑
SAOUHSC_01847	hypothetical protein	0.939829	0.000768	1.92↓
SAOUHSC_01074	hypothetical protein	0.928047	0.005847	1.90↓
SAOUHSC_01070	hypothetical protein	-0.88436	0.009316	1.85↑
SAOUHSC_00939	hypothetical protein	0.767404	0.009872	1.70↓

-Genes arranged by fold change, Arrows indicate up-regulation (↑) or down-regulation (↓) in attached biofilm cells
-Top 20 up-regulated genes marked with (*)
-Top 20 down-regulated genes marked with (∆)

5.2.5 Gene expression of cell wall associated proteins in biofilms

Successful targeting using Affimers and other targeting molecules is improved when the target is easily accessible and more abundant, based on that proteins that are surface exposed can be considered good candidates to use as targets for Affimers (Tiede et al., 2014). To determine which proteins would be the most suitable candidates to raise Affimers against, based on information gathered from literature and protein function databases such as Uniprot (https://www.uniprot.org), a list of 25 genes encoding CWA proteins which are expected to be expressed in *S. aureus* biofilms was compiled (Table 5.3). Furthermore, CWA proteins play several significant roles in *S. aureus* biofilm formation and pathogenicity, such as attachment, antibiotic resistance and evasion of the immune system (Archer et al., 2011, Arciola et al., 2015, Corrigan et al., 2009). Eleven genes were expressed>1.3-fold higher than the average level of gene expression in biofilm cells however 14 genes were expressed<1-fold lower than the average level of gene expression between biofilm cells

To identify the most suitable candidates within the list of *S. aureus* CWA proteins, the gene expression profile of these genes in biofilm cells was compared to their expression relative to their gene expression in planktonic cells. Along with the gene expression, CWA proteins were also judged based on their relative expression (RE) (i.e. expression level relative to the average of the total level of gene expression of all protein coding genes in biofilm cells). Analysis of the gene expression levels and RE revealed that the gene expression levels are directly proportional to the RE. This is evident from previous gene expression analysis studies on *S. aureus* biofilms which indicate that there is a noticeable decrease in gene expression of certain genes particularly those which encode surface exposed proteins such as, *clfB*, *icaD* and *prop* as a biofilm matures (Beenken et al., 2004, Resch et al., 2005). The genes encoding CWA proteins that showed gene expression levels greater than the average level of gene expression in biofilm cells were *clfA*,

pbp2, *spa*, *isaA*, *ebpS*, *ClfB*, *pbp1*, *sdrC*, *sraP*, *sdrC* and *agrC* respectively. Amongst these gene *ClfA*, *pbp2* and *pbp1* were also expressed >1-fold higher in biofilm cells than planktonic cells, indicating that the expression of these genes is retained as a biofilm matures. While the other genes such as *capD*, and *capM*) that also showed >1-fold GE levels in biofilm cells compared to planktonic cells, were expressed <1-fold lower than the average level of gene expression in biofilm cells. Suggesting that the fold difference in gene expression between biofilm cells and planktonic cells does not necessarily dictate higher expression in biofilm cells, which could be explained by the presence of persister cells and small colony variants which make up about 1% of as some of the cell population within the biofilm (Archer et al., 2011, Lewis, 2010).

Several genes encoding CWA proteins selected shared common functions that contribute to *S. aureus* pathogenicity and biofilm formation by facilitating attachment to surfaces by interaction with host components. From the list of genes encoding CWA proteins six genes (*clfA*, *clfB*, *fnbA*, *fnbB*, *sdrC*, *sdrD*, *sarP*, *ebpS*) were identified from the literature to encode proteins that are known to interact with host components to enable attachment to surfaces (Kwiecinski et al., 2014). (Table 5.3). Although the expression of the majority of these gene was higher in planktonic cells than biofilm cells the RE of *clfA*, *clfB*, *sdrC*, *sdrD*, *sarP*, *ebpS* was >1-fold higher than the average of biofilm cells, while the RE of *fnbA* and *fnbB* was <1-fold higher than the average expression of biofilm cells (Table 5.3). Since these gene encode proteins that bind different host components such as fibrinogen (*clfA*, *clfB*, *sdrC*, *sdrD*), fibronectin (*fnbA*, *fnbB*), platlets (*sarP*) and elastin (*ebpS*) the rate at which they are expressed is expected to be different (Begum et al., 2011, Kwiecinski et al., 2014, O'Brien et al., 2002, Paharik and Horswill, 2016, Wann et al., 2000). For instance, the expression of four genes that bind fibrinogen of which the RE of *clfA* and *clfB* was 21 and 2.7-fold respectively higher than the average of other biofilm cells, indicate that fibrinogen binding is an essential factor that affects biofilm formation and maturation; as opposed to only two genes which bind fibronectin (Table 5.3). Furthermore, the importance of expression of genes involved in fibrinogen binding is confirmed in a study

which indicates that the expressions of *clfA*, *clfB* and *sdrC* were 3-fold higher in biofilm grown for 16, 24 and 48 h than planktonic cells (Resch et al., 2005). Since proteins involved in attachment to surfaces are expressed in planktonic cells and at early stages of biofilm formation, they would be sensible candidates to choose to raise Affimers against. However, the abundance and expression of the proteins might be influenced by their function as was observed in the gene expression of *clfA* and *clfB* (Table 5.3). Furthermore, the continued expression of these genes after 48 h of growth is another factor to consider. Based on the gene expression *clfA* and *ebpS* were expressed 21 and 3-fold higher respectively than the average level of gene expression in biofilm cells and were also reported in other studies to be expressed in biofilm cells at higher levels than planktonic cells at different stages of biofilm formation suggesting that they would be more suitable candidates to raise Affimers against (Resch et al., 2005).

As biofilm matrix production is the next step in biofilm formation, genes that influence the composition of the biofilm matrix are an important factor to consider when attempting targeting of a biofilm. For this reason, the gene products of genes involved in the production of the biofilm matrix were selected to investigate as potential candidates for Affimer targeting. These genes include *icaA*, *icaC* and *icaD* which are part of the *ica* operon which is responsible for production of PIA which is the major component of the biofilm matrix in most *S. aureus* strains (Fitzpatrick et al., 2005, Namvar et al., 2013). All three genes were expressed at >1-fold higher in planktonic cells than in biofilm cells. This was not surprising since PIA production typically would occur during early stages of biofilm formation (Arciola et al., 2015). The gene expression pattern noticed with *icaA*, *icaC* and *icaD* is in line with their gene expression pattern noticed in a previous study which showed between 3 to 8-fold higher gene expression levels in biofilm cells compared to planktonic cells for *S. aureus* strain N315 biofilm cells than in planktonic cells for biofilms grown for 6-8 h compared to biofilm grown for 24-48 h where their expression was lower than planktonic cells (Resch et al., 2005). Originally PIA was thought to be the most important component of the *S. aureus* and *S. epidermidis* biofilm matrix and that it is essential for biofilm formation (Arciola

et al., 2015). However, several reports contradict how essential PIA is in biofilm formation in both *S. aureus* and *S. epidermidis* suggesting that PIA production is strain dependent and may be influenced by environmental factors and global gene regulators (Beenken et al., 2004, Rohde et al., 2001, Toledo-Arana et al., 2005). The ability of *S. aureus* to form biofilm in an *ica*-dependent manner was examined in *S. aureus* strain UAMS-1 in which, UAMS-1 *ica* mutants were still able to form biofilms independently of PIA production, suggesting that biofilm formation is an adaptive process and that *S. aureus* possesses several mechanisms alternative to PIA production that allow biofilm formation(Beenken et al., 2004). Since PIA production is strain dependent, it would be sensible to conclude that targeting of icaA, icaC, icaD using Affimers would not be practical.

Within the list of genes encoding CWA proteins the gene products of a group of genes (*capM***,** *capD*, *capJ*, *capK*, *spa*, *sbi*, *isaA*) that play an important role in interaction of *S. aureus* with the host immune system by limiting opsonization were selected as potential targets for Affimers. Although these genes encode proteins with similar functions their expression was different between biofilm cells and planktonic cells in which *capJ*, *capK*, *spa*, *sbi*, *isaA* were expressed >1-fold higher in planktonic cells than biofilm cell however, *capD***,** *capM* were expressed 2.3 and 1.3-fold respectively higher in *S. aureus* biofilm cells than planktonic cells (Table 5.3). the expression level of *capD* is in line with a previous study which indicates that the expression *capD* was 3-fold higher in biofilm cells compared to planktonic cells (Beenken et al., 2004). Also, the expression of *isaA* was observed to be higher in *S. aureus* biofilms than planktonic cells by 3-fold after 8 h of growth, while the other genes involved in protection or evasion of the host immune system were not expressed at high levels in biofilm after biofilm formation compared to planktonic cells (Resch et al., 2005). This suggest that a higher number of genes that encode proteins that protect from the host immune system are needed for planktonic cells since the cells are more vulnerable, however, once the biofilm is matured, less genes need to be expressed. Although *spa* and *isaA* were expressed higher in planktonic cells their expression in biofilm cells was >5-fold higher than the average level of gene expression compared to

other genes in biofilm cells, however the expression of *capD* and *capM* was amongst the lowest relative to the average level of gene expression in biofilm cells (Table 5.3). The products of these genes may share a similar function and some are part of the same operon but the mechanism they use is different for instance, *capM***,** *capD*, *capJ*, *capK* are part of the cap operon which is responsible for the production of capsular polysaccharide (CP); CP is present in the extracellular surface of *S. aureus* cells and serves to encapsulate them, resulting in masking of surface proteins from components of the host immune system thereby limiting phagocytosis (Visansirikul et al., 2020). CP is produced by many bacterial species such as, *P. aeruginosa* and *E. coli* and contributes the increase in their pathogenicity (Corbett and Roberts, 2008, Franklin et al., 2011). However, Spa and sbi prevent opsonisation by binding the Fc region of IgG, furthermore spa plays an important role in biofilm formation in which it is able to promote cell-to-cell adherence (Gao and Stewart, 2004, Gonzalez et al., 2015). Targeting of the protein products of these gene would certainly be useful either for diagnostic or therapeutic purposes as evasion of the immune system is one of the most effective methods that increase the pathogenicity of *S. aureus* and aid in biofilm formation (Visansirikul et al., 2020, Willis and Whitfield, 2013). Based on the RE of these genes, *spa* and *isaA* were expressed 6.5 and 5.4-fold respectively higher than the average level of gene expression in biofilm cell making spa and isaA more suitable candidates than other proteins in this group (Table 5.3).

The gene products of another group of genes include *pbp1*, *pbp2*, *pbp3* which are involved in resistance to antibiotic particularly β-lactam class of antimicrobials were amongst the CWA proteins selected for targeting using Affimers (Table 5.3) (Kim et al., 2018, Kylväjä et al., 2016, Łeski and Tomasz, 2005). Amongst these genes *pbp1* and *pbp2* showed >1-fold higher gene expression levels in biofilm cells compared to planktonic cells, while *pbp3* showed 1.5-fold higher gene expression in planktonic cells compared to biofilm cells (Table5.3). Furthermore, *pbp1* and *pbp2* were expressed 2.6 and 8-fold respectively higher than the average of gene expression of all biofilm cells (Table 5.3). The fact that *pbp1* and *pbp2* were amongst gene with the

highest RE between the genes encoding CWA proteins suggests that although these gene might not be essential for biofilm formation, they are certainly important factors that contribute to the pathogenicity of *S. aureus* by contributing to the tolerance of the biofilm to antimicrobials. Therefore, targeting gene products of these genes particularly *pbp2* which was expressed >8-fold higher relative to other biofilm cells using Affimers in an effort to disrupt their activity could potentially be useful for treatment of *S. aureus* biofilm infections at early stages of biofilm formation.

Furthermore, the gene products of two genes (*agrB* and *agrC*) encoding CWA proteins that are part of the *agr* operon were selected as potential candidates for Affimer targeting. The *agr* operon is the most important factor that regulates biofilm dispersal by QS in *S. aureus* (Boles and Horswill, 2008). Although QS is mostly involved in biofilm dispersal, QS can also be indirectly involved in biofilm formation in which the expression of the *agr* operon triggers the switch from a dormant state to planktonic cells state thereby allowing colonisation of different surfaces in the host body (Boles and Horswill, 2008). The *agr* operon is under the regulation of several global regulators such as *sarA*, *codY* and *sigB* that increase the expression of virulence factors such as CWA proteins and toxins (Bischoff et al., 2001, Cheung et al., 2001, Tan et al., 2018). The expression of both *agrB* and *agrC* were 2.9-fold higher in planktonic cells than biofilm cells, furthermore, *agrC* was one of the genes that were differentially expressed when comparing expression between Bf cells and planktonic cells (Table 5.3). AgrB and agrC proteins are the surface exposed components of the *agr* operon in which agrB exports the effector molecule of the *agr* operon auto inducing peptide (AIP) and agrC is a sensor histidine kinase that is activated in response to the accumulation of AIP past a certain threshold (Novick and Geisinger, 2008). Although their expression level was different in biofilm cells, the observed fold difference in the expression of *agrB* and *agrC* between biofilm cell and planktonic cells could indicate that the expression of *agrC* is proportional to *agrB* since the expression of *agrC* is reliant on sensing AIP (Novick and Geisinger, 2008).

Table 5.3 Gene expression of cell wall associated proteins.

Gene expression of cell wall associated proteins

Locus tag	UNIPROT & Annotation	Product	Comment	average level of gene expression of Biofilm cells (n=4)	Biofilm cells relative expression*	Reference
SAOUHSC_00812	*clf*A*	clumping factor	Implicated in virulence; Fibrinogen attachment and biofilm formation; Promotes bacterial clumping; Induces human platelet aggregation and	126926.75	21.32	(Dominiecki and Weiss, 1999, Hartford et al., 2001)

			decreased phagocytosis.			
SAOUHSC_01467	*pbp*2	penicillin-binding protein 2	penicillin binding; biosysntheysis of peptidoglycan, glycosyltransferase activity	49221.75	8.27	(Łeski and Tomasz, 2005)
SAOUHSC_00069	*spa*	protein A	prevents opsonization, Immunoglobulin (IgG) bindng; cell-cell adhesion, attachment to coated surfaces by binding Von Willbrand Factor, biofilm formation; promote cytokine	39164.50	6.58	(Gao and Stewart, 2004, Zhu et al., 2019)

			release via binding to tumour necrosis factor (TNF) receptor 1			
SAOUHSC_02887	isaA	immunodominant antigen A		32217.50	5.41	(Resch et al., 2005)
SAOUHSC_01501	*ebp*S	elastin binding protein	promotes binding of soluble elastin and tropoelastin; may be involved in environment sensing or nutrient transport	20216.75	3.40	(Gillaspy et al., 2006)
SAOUHSC_02963	*clfB**	clumping factor B	Cell surface-associated protein, binds fibrinogen, induce bacterial clumps formation;	16251.50	2.73	(Hartford et al., 2001)

			Binds cultured keratinocytes.			
SAOUHSC_01145	*pbp*1, *pbp*A	penicillin-binding protein 1	penicillin binding; biosynthesis of peptidoglycan, glycosyltransferase activity	15576.00	2.62	(Kim et al., 2018)
SAOUHSC_00544	*sdr*C	fibrinogen-binding protein SdrC	cell adhesion, surface attachment; may bind calcium	7952.50	1.34	(Dedent et al., 2008, Josefsson et al., 1998)
SAOUHSC_02990	*sra*P, *sas*A		platlet binding; calcium binding	7736.75	1.30	(Mazmanian et al., 2001, Siboo et al., 2001)
SAOUHSC_00545	*sdr*D	fibrinogen-binding protein SdrD	cell adhesion to surfaces,fibrinogen-binding, calcium binding	7691.75	1.29	(Dedent et al., 2008, Josefsson et al., 1998)

SAOUHSC_02264	*agr*C*	Accessory gene regulator protein C	Biofilm dispersal	7573.25	1.27	(Queck et al., 2008)
SAOUHSC_02261	*agr*B	Accessory gene regulator protein B	Biofilm dispersal	4779.25	0.80	(Queck et al., 2008)
SAOUHSC_01652	PBP3	penicillin-binding protein 3	penicillin binding	4454.75	0.75	(Kylväjä et al., 2016)
SAOUHSC_00117	*cap*D	capsular polysaccharide biosynthesis protein CapD	capsular polysaccharide biosynthesis	1568.25	0.26	(Gillaspy et al., 2006)
SAOUHSC_02803	*fnb*A	fibronectin-binding protein	binding fibronectin; attachment to surfaces coated with immobilised elastin peptides or human tropoelastin; platelets aggregation, biofilm formation.	1371.50	0.23	(Hartford et al., 2001)

SAOUHSC_00114	*cap*A	capsular polysaccharide biosynthesis protein CapA	capsular polysaccharide biosynthesis	848.50	0.14	(Hartford et al., 2001)
SAOUHSC_02802	*fnb*B	fibronectin binding protein B	fibronectin binding; cell adhesion	647.00	0.11	(Hartford et al., 2001)
SAOUHSC_02706	*sbi*	immunoglobulin G-binding protein Sbi	involved in defence agsint host immune system, binds IgG	613.50	0.10	(Gonzalez et al., 2015)
SAOUHSC_00816	*emp*	extracellular matrix and plasma binding protein	Adhesin that binds to the host cell extracellular matrix proteins fibronectin, fibrinogen, collagen, and vitronectin	387.00	0.07	(Hussain et al., 2001)
SAOUHSC_00123	*cap*J	capsular polysaccharide biosynthesis protein CapJ	capsular polysaccharide biosynthesis	326.75	0.05	(Gillaspy et al., 2006)

SAOUHSC_00124	*cap*K	Capsular polysaccharide biosynthesis protein CapK	capsular polysaccharide biosynthesis	269.00	0.05	(Namvar et al., 2013)
SAOUHSC_03005	*ica*C	intercellular adhesion protein C	involved in PIA synthesis	166.00	0.03	(Namvar et al., 2013)
SAOUHSC_03002	*ica*A	*N*-glycosyltransferase	PIA production	24.50	0.00	(Namvar et al., 2013)
SAOUHSC_00126	*cap*M	Capsular polysaccharide biosynthesis protein CapM	capsular polysaccharide biosynthesis	7.25	0.00	(Gillaspy et al., 2006)
SAOUHSC_03003	*ica*D	intercellular adhesion protein D	involved in PIA synthesis	6.25	0.00	(Namvar et al., 2013)

- Note: Genes are arranged from highest to lowest gene expression in biofilm cells.
- Relative expression: gene expression relative to the average to total gene expression for all genes*.

In conclusion, differential expression analysis was useful in identifying metabolic and physiological pathways that could be important in biofilm formation in S. aureus biofilm. However, due to the limitation associated with data collected from mature biofilm, monitoring the change in gene expression of these pathways is not possible. Further expansion of the analysis should include RNA-seq data for biofilm at deferent growth stages. The same can be concluded regarding the expression of CWA proteins. Regardless of this limitation several gene encoding CWA proteins exhibited signs that they could be suitable candidates to raise Affimers against their encoded proteins. These gene include *clfA*, *pbp2*, *spa*, *isaA*, *ebpS*, *clfB*, although only *clfA* and *clfB* were differentially expressed, their RE was >7-fold higher than the average level of gene expression in biofilm cells, indicating that they would be suitable targets to raise Affimers against.

5.3 Discussion

Affimers have been successfully raised against *S. aureus* Protein A and ClfA and biofilm components and their binding has been confirmed in previous chapters. Since the identity of the targets of the Affimers raised against biofilm components was unknown further characterisation of the Affimers was needed. In this chapter, a candidate approach was taken to identify potential proteins that would be good candidates to raise Affimers against based on their gene expression in *S. aureus* biofilm cells. Furthermore, using differential expression analysis to gain a sense of the physiological differences that *S. aureus* planktonic cells undergo when switching to a biofilm phenotype. This was done by sequencing RNA extracted from planktonic cells and attached and detached biofilm cells to identify differentially expressed genes in planktonic cells compared to biofilm cells.

Although differential gene expression analysis of biofilm cells compared to planktonic cells revealed the involvement of several genes and pathways to be important in biofilm formation. Differential gene expression analysis indicated that gene components involved in several physiological processed

were up-regulated in biofilm cells, such as components of purine, iron and phosphate metabolism. Targeting the purine synthetic pathway was previously observed to inhibit biofilm formation in *Pseudomonas fluorescens* (Yoshioka and Newell, 2016). Therefore, it is sensible to investigate this using Affimers against *S. aureus* biofilm. However, there are limitations in the approach used in this thesis in which the biofilm used was a mature biofilm grown for 48 h. Limiting the biofilm samples to mature biofilms would represent gene expression of cells in mature biofilms but not cells at early stages of biofilm formation. For example, the genes part of the *ica* operon which is responsible for PIA production which is the main component of the biofilm matrix in some *S. aureus* strains were not differentially expressed (Fitzpatrick et al., 2005). PIA is produced by cells once the cells are attached to a surface and have established the formation of microcolonies, therefore gene components of the *ica* operon would not be expected to be expressed at high level in a mature biofilm rather they would be expressed at higher levels at early stages of biofilm formation. The expression of components of the *ica* operon in *S. aureus* has been reported in previous studies which indicated that *icaD*, *icaC*, and *icaA* were expressed at higher level in biofilm cells than planktonic cells in biofilm grown for 6-8 h (Resch et al., 2005). Therefore, further investigation in the expression pattern of the *ica* operon is needed to establish the possibility of including protein product of these genes as part of the candidates to raise Affimers against.

On another note, the gene expression profiles of 25 genes encoding CWA proteins were compared in order to select candidates for Affimer production (Table 5.3). CWA proteins are important virulence factors involved in infection and facilitate biofilm formation in *S. aureus* and other organisms; furthermore, the accessibility of CWA proteins makes them ideal candidates to targeting for imaging and therapeutic applications (Jan-Roblero et al., 2017, Tiede et al., 2017). Based on the importance of the contribution of CWA proteins in infection and biofilm formation, several genes encoding cell wall associated proteins were expected to be differentially expressed particularly *spa*, *FnbA* and *FnbB*. However, only 3 genes (*clfA*, *clfB* and *agrC*) encoding CWA proteins were differentially expressed (Table 5.2).

While the majority of genes encoding CWA proteins were not differentially expressed, this suggesting that the gene expression of most CWA proteins decreases as biofilms mature. This indicates that their expression is probably dependent on the biofilm growth stage, suggesting that they might play a more significant role during the initial stages of biofilm formation and a lesser role in biofilm maturity (Beenken et al., 2004, Resch et al., 2005). The expression pattern found in this study confirms the observations in other studies in which the majority of the selected genes encoding CWA proteins were expressed at higher level in planktonic cells than biofilm cells (Beenken et al., 2004, Resch et al., 2005). However, differences were found in the expression pattern of *clfA* and *clfB* between this study and other studies, here the expression of *clfB* was observed to be 2.2-fold higher in planktonic cells rather than biofilm cells while the expression of *clfA* was 1.8-fold higher in biofilm than planktonic cells suggesting that clfA plays a more significant role in biofilm formation and maintenance while *clfB* may contribute more to biofilm formation during the attachment stage (Table 5.3). However other studies show that the expression of *clfA* and *clfB* were higher in *S. aureus* N315 and UAMB-1 biofilm cells than planktonic cells throughout the biofilm formation process until maturation (Beenken et al., 2004, Resch et al., 2005). This suggest that *clfA* and *clfB* might play similar role in biofilm formation and maintenance and that results obtained here could be attributed to strain differences or to technical variation within replicates. Furthermore, in this study the expression of the majority of genes encoding cell wall associated proteins in a mature biofilm was down regulated suggesting that they are not essential for the maintenance or survival of cells within the biofilm. This indicates that when selecting protein targets to raise Affimers against, the expression pattern of these proteins should be taken into consideration in which the selected proteins should be expressed at high level throughout the biofilm formation process. Based on that, the most suitable candidates that would be cell wall associated proteins which are expressed at all stages of biofilm formation, based on the gene expression profile of the cell wall associated proteins the expression of six genes (*clfA*, *pbp2*, *spa*, *isaA*, *ebpS*, *clfB*) fit this criterion (Table 5.3). Although only *clfA* and *pbp2* were expressed at higher levels in biofilm cells than

planktonic cells, all of these genes were expressed >21 and 8-fold respectively higher than the average level of gene expression of other biofilm cells (Table 5.3).

Furthermore, in this study only genes with known function were investigated, however several hypothetical proteins were differentially expressed and were up-regulated in biofilm cells (Table 5.2). As an extension to this study, the function of genes encoding hypothetical can be inferred using sequence homology with known genes from other *S. aureus* strains or other bacteria and the gene products can be purified. Highly up-regulated hypothetical genes in biofilm cells were highly expressed compared to other differentially expressed genes that are known to be involved in biofilm formation such as *clfA* Therefore, investigation of the expression profile of these highly up-regulated gene at early stages of biofilm formation could reveal that these gene are essential for biofilm formation which means they would be excellent candidates to raise Affimers against.

There are several aspects of this study that can be modified to obtain a better understanding of biofilm formation that can be useful when selecting targets to raise Affimers against. To improve this study, differential expression analysis of *S. aureus* biofilm should include RNA samples from biofilm grown for 6, 8, 12, 16, 24 h as well as 48 h to get a complete scope of the gene expression profile of genes that are known to be involved in biofilm formation such as those involved in attachment such as, *spa* and *clfA* and potentially identify the involvement of other gene that were not previously known to be involved in biofilm formation or stability in *S. aureus*. Also, incorporation of RNA-seq data for other *S. aureus* strains such as USA300 and UAMS-1 to provide a much broader view of potential similarities and differences between *S. aureus* biofilm. Work in that front has already been done, RNA samples extracted from USA300 and UAMS-1 mature biofilm have already been sequenced, however due to time restrictions the data has not been fully analysed thus it was not included and the analysis was limited only to strain SH1000.

Another aspect to consider in the expansion of this study would be investigation of Clinical isolates isolated from patients with IE. Since there is not much literature regarding the gene expression of clinical isolates during IE, using RNA-seq to examine the gene expression of *S. aureus* clinical isolates would be useful since it would reflect gene expression under constant threat of the host immune system. Furthermore, it would help identify highly expressed genes which encode proteins that are highly expressed during infection to be targeted by Affimers.

Along with investigation of gene expression of *S. aureus* clinical isolates, this study could be further expanded to investigate differences in gene expression using different growth conditions such changing the growth media or duration of biofilm growth (Beenken et al., 2004). Furthermore, it is well known that biofilm formation and dispersal are influenced greatly by environmental conditions, of these conditions nutrient availability and changes in pH can greatly influence changes in gene expression between planktonic cells and biofilm cells (Chen et al., 2012, Kennedy and O'Gara, 2004). In Chapter 4, it was observed that changes in growth conditions can effect biofilm formation, this was observed when *S. aureus* biofilm grown on peptone NaCl agar (PNG) media produced biofilm with less biomass than those grown in rich media such as brain heart infusion agar (BHI) or tryptone soy agar (TSA). This further indicates that a difference in gene expression of decrease or increase in expression of cell wall associated proteins and pathways involved in biofilm formation will most likely occur as a result of nutrient availability. These changes could potentially affect the ability of Affimers to bind their targets depending on the effect the change in growth conditions will have on biofilm formation. The effect of growth conditions have been alluded to in several studies which indicated that supplementation and depletion of nutrients result in positive or negative effects on *S. aureus* biofilm (Wijesinghe et al., 2019). For example, supplementation of growth media with an iron chelator such as, 1,2,3,4,6-penta-O-galloyl-b-D-glucopyranose (PGG) inhibits biofilm formation and causes increased expression of genes involved in iron regulation such as the *isd* operon and *srtB* that are usually expressed under iron deprived conditions; however, supplementing the same medium with $FeSO_4$ results in

restoration of biofilm formation in *S. aureus* SA113 (Lin et al., 2012). Another study suggests that supplementation of media with 1 M NaCl and glucose result in decreasing the transcription of RNAIII causing a decrease in the expression of *agr* operon thereby increasing biofilm formation (Cheung and Zhang, 2002). Therefore, it would be interesting to expand this study by investigating the effect of different growth media on the gene expression of biofilm cells and how it could affect expression of genes encoding the proteins target to which the Affimers described in Chapter 4 bind.

Chapter 6: Concluding remarks and future perspective

6.1. Discussion and future work

This thesis successfully describes raising and characterisation of Affimers against *S. aureus* protein A (spA) and clumping factor A (ClfA), these Affimers were further charicterised and confirmed to specifically recognise their perspective target (Chapter 3). It also describes successfully raising Affimers against components of *S. aureus* biofilms formed by strains SH1000, USA300 and UAMS-1 (Chapter 4). Some of these Affimers were confirmed to significantly recognise biofilm components when tested for binding against these strains in an *in vitro* double-blind screening. Furthermore, analysis of transcriptomic data provided insight into the physiology of the cell within biofilms grown using the cellulose disk method (Chapter 5). When comparing gene expression between planktonic cells and biofilm cells using differential expression analysis indicated the presence of genes and group of genes involved in different physiological processes such as, purine metabolism, persister cell formation and heme scavenging that are important for biofilm formation (Sause et al., 2019, Torres et al., 2006, Yoshioka and Newell, 2016). Also, transcriptomic analysis enabled identification of the gene expression levels of surface exposed proteins that could be used as candidates to raise Affimers against, some of which are documented in the literature to be directly or indirectly involved in *S. aureus* biofilm formation (Corrigan et al., 2009, Foster et al., 2014, Jan-Roblero et al., 2017). The significant findings pertaining to each section have been discussed within each chapter and improvements and modifications to progress the study of the interaction of Affimers with *S. aureus* biofilm for diagnostic and therapeutic purposes. In this final chapter, consideration is given to widening the scope of targeting *S. aureus* biofilm for diagnostic and therapeutic purposes.

Since this study commenced there is still a need to be able to detect *S. aureus* biofilm formation associated within Infective Endocarditis (IE); the economic strain and deteriorating patient quality of life due to complications associated

with IE is continuing to be a problem worldwide (Cahill and Prendergast, 2016, Sunil et al., 2019); as the number of deaths associated with IE continues to increase due to the limitation of current diagnostic and therapeutic means available for biofilm detection and treatment (Baddour et al., 2015, DeSimone and Sohail, 2018, Liesman et al., 2017). This prompts haste to develop more efficient and rapid diagnostic and therapeutic solutions to decrease the complications associated with IE due to biofilm formation.

In this thesis the potential use of Affimers in the clinical setting as tools for monitoring and diagnosis of IE is explored. The ability of Affimers to recognise biofilms in vitro suggests that the Affimers demonstrate the first of many attributes necessary for them to be used as a potential platform to establish a method for detection of *S. aureus* biofilm in vivo via different imaging applications such as Fluorescent and ultrasound imaging. In the past decade the utilisation of ultrasound contrast agents (UCAs) have been used in several imaging and therapeutic applications. The use of ultrasound has gained popularity over the years in diagnostic and therapeutic applications due to the safety of application, the ability of deep tissue penetration and its non-invasiveness (Cai et al., 2020).

One of the several detection and imaging methods have been developed in the past decade that enable in vitro or in vivo detection of molecules in patient samples or in the host body such as ultrasound contrast agents (UCAs) (Lindner, 2004). In this thesis the potential use of Affimers in the clinical setting as tools for monitoring and diagnosis of IE is explored, as Affimers that recognise *S. aureus* biofilm in vitro have the potential to be used in as delivery vehicles to guide ultrasound contrast agents (UCAs) such as microbubbles or nanoparticles to the sight of *S. aureus* biofilm in IE patients and used for diagnosis of IE by in vivo imaging of *S. aureus* biofilm.

Up to this point echocardiography is still the relied upon method for detection of biofilm formation in IE patients as an essential part of the Duke criteria for diagnosis of IE (Durack et al., 1994, Topan et al., 2015). However, the limitations associated with relying on echocardiography for the diagnostic imaging of biofilm in IE is that their low sensitivity and poor image quality

furthermore, the presence of blood clots at the sight of infected heart valves which are indistinguishable from biofilms (Evangelista, 2004).

Several points were taken into consideration such as, the ability of Affimers to recognise clinical samples and the immunogenicity of the Affimers and identification of ligands that the Affimers are binding to in the biofilm. To address these concerns several strategies can be applied that would lead to in vivo investigation of the clinical application of Affimers for detection of *S. aureus* biofilm in IE.

For a long time, antibodies have been relied upon for detection and treatment. Here it has been recognise that human antibodies are good alternatives to Affimers. However, since antibodies are much more expensive to produce and develop and are less stable than Affimers, it would be more efficient and economically sensible to use Affimers instead of antibodies. Furthermore, Affimers are 150-fold smaller than antibodies which could allow for better tissue penetration and identifying epitopes unaccusable to antibodies due to the size difference (Tiede et al., 2017). To fully realise this goal several factors must first be addressed begpre considering using Affimer in the clinical setting; it is essential that the selected Affimer(s) would be able to recognise *S. aureus* biofilm components expressed in most if not all *S. aureus* biofilm. Therefore, Affimers can be screened against a panel of different *S. aureus* strains and clinical isolates with different clonal complexes and transposon mutants compiled in strain libraries such as Nebraska Transposon Mutant Library (NTML) (http://app1.unmc .edu/fgx/) (Fey et al., 2013).

The ability of some Affimers identified in this thesis to recognize *S. aureus* biofilm in vitro demonstrates that they possess the first of many attributes necessary for them to be considered as a platform to drive the development of an Affimer-MB conjugate for *S. aureus* biofilm detection *in vivo*.

6.2 Clinical applications of Affimers

Affimers confirmed to bind *S. aureus* biofilm components *in vivo* and *in vitro* has the potential to be used for diagnostic and therapeutic applications. Several detection and imaging methods have been developed in the past

decade that enable detection of molecules in patient samples or in the host body such as microbubbles.

The successful incorporation of Affimers with Microbubbles for in vivo biofilm imaging can be further exploited to be used for targeted treatment of *S. aureus* biofilm infection as a targeted drug delivery system to *S. aureus* biofilms at the infection sight. Since Affimers recognise specific biofilm components, the incorporation of Affimers would provide a higher level of specificity and localisation of the therapeutic agent. The use of MB and other UCAs have been previously exploited for their ability to deliver therapeutics in cancer research (Cai et al., 2019). Several examples of ultra sound responsive materials such as microbubbles and liposomes used for drug delivery are in clinical trials for treatment of Colorectal Cancer National Clinical Trial number (NCT) 03458975, hepatocellular Carcinoma NCT 03199274; (Cai et al., 2019) (https://clinicaltrials.gov/). Furthermore, the use of microbubble loaded with doxorubin resulted in improved bone healing in osteosarcoma patients (Lee et al., 2016). Several *in vitro* and *in vivo* studies have suggested that the use of UCAs such as microbubbles can easily penetrate through biofilm matrix while carrying the therapeutic agents. This is possible with the application of ultrasound to the sight of the biofilm growth. Increasing the frequency of the ultrasound results in increase in the vibration of the microbubbles thereby making crakes and loosening the biofilm matrix allowing therapeutic agents to reach the cells within the biofilm (Sharma et al., 2016, Zhurauski et al., 2018). Several studies have shown an increase in the effectiveness of antimicrobials when used in conjugation with microbubbles and ultrasound application. For instance, the effectiveness of vancomycin in killing *Staphylococcus epidermidis* (*S. epidermidis*) cells within the biofilms grown for 12h and 24h increased with the application of ultrasound compared to without ultrasound application (Sharma et al., 2016, Zhurauski et al., 2018). Another study also showed increased permeability of microbubbles in combination with ultrasound, vancomycin loaded microbubbles resulted in increased permeability of *S. epidermidis* biofilm grown for 12h and 24h resulting in a higher cell death (He et al., 2011). Although, this approach was successful for *S. epidermidis* biofilm, other studies indicate that this might not be the case

for all biofilms. The use of microbubbles with gentamicin has been reported for treatment of *Escherichia coli* (*E. coli*) and *Pseudomonas aeruginosa* (*P. aeruginosa*) biofilm (He et al., 2011). Treatment of 24h and 48h *E. coli* biofilm with the use of ultrasound on microbubbles loaded with gentamicin resulted in complete eradication of viable cells in 24h biofilms and partial eradication of viable cells in 48h biofilms (He et al., 2011). However, no effect on cell viability was observed for *P. aeruginosa* 24 h or 48 h biofilms (He et al., 2011). Therefore, the use of microbubble can be quite limited as the effectiveness of the ultrasound in damaging of the biofilm is dependent of the biofilm stage of growth, as mature biofilms tend to be more resilient and less susceptible to permeation and sheer force exerted by the microbubbles. Never the less the use of UCA can be tested against mature *S. aureus* biofilm in vivo using a mouse IE model to determine the extent of damage to the heart valves and surrounding tissue as a result of vibration of the UCA used (Gibson et al., 2007).

6.3 Detection of *S. aureus* biofilm in animal models

The application of protein scaffolds in molecule recognition has been increasing and getting recognition as a viable approach for *in vitro* targeting applications. The ability of these molecules to recognise their targets *in vitro* however is not enough for progression in their development as the possibility of these molecules to produce an immunogenic response is a problem that would render them unsuitable for clinical use. The ability of Affimers developed in this thesis to recognise *S. aureus* biofilm *in vitro* is an important first step as a proof of principle to confirm their specificity that could lead to further investigation of their immunogenicity using animal models. The use of *in vivo* animal models is a useful approach that will allow better understanding of the potential host response to Affimers. To take full advantage of this approach, transgenic animal models could be used, such as knockin (KI) mice, which are transgenic mice with the substitution of a mouse genes with a human gene using the CRISPR/Cas9 system to produce human antibodies (Doyle et al., 2012, Jin and Li, 2016). This would enable the presentation of *S. aureus* antigens to the animal model which would elicit the human immune

response resulting in the production of human monoclonal antibodies against specific *S. aureus* antigens. Affimers can be tested against biofilms grown in transgenic animal models and their immunogenicity can be evaluated using *in vivo* induced antigen technology (IVIAT). IVAIT enables detection of host antigens during infection but not during laboratory growth conditions (Rollins et al., 2005).

During bacterial biofilm infection, bacteria can sense environmental conditions such as nutrient availability and detection of components of the host immune system, thereby, biofilms grown *in vitro* are presented with sufficient amount of nutrients and a suitable growth conditions thereby certain virulence genes might not be expressed at the same level as *in vivo* (Gu et al., 2009). Therefore, selection of an appropriate animal model that accurately elicits the human immune response to IE is crucial (Kim et al., 2014). Studies have demonstrated that a challenge with using of animal models is that they often do not elicit the host immune system response to infection (Kim et al., 2014). For example, during infection *S. aureus* secretes toxins that neutralize components of the human immune system, however, these components are not part of the mouse immune system (Kim et al., 2014, Spaan et al., 2013). To resolve such an issue, the use of transgenic mice could be considered as they will more accurately elicit the same human response to *S. aureus* antigens (Shultz et al., 2007). The use of transgenic mice has been proven successful in mouse models in which *S. aureus* infected mice that were transgenic for human hemoglobin were able to produce an *isdB*-heme scavenging response to human haemoglobin (Pishchany et al., 2010). The *isdB* gene is one of the major promoters of heme-iron scavenging during *S. aureus* infection (Torres et al., 2006). The use of a mouse model in clinical studies provides the advantage that the model is relatively cheaper and easier to work with than other models (Wiles et al., 2006). However, due to the small size of the mouse carotid artery, the use of a IE mouse model could present some challenges, a rabbit or rat model might be a less challenging choice to consider (Kim et al., 2014).

The approaches described throughout this chapter open new ventures that would allow identification of *S. aureus* biofilm targets for imaging and vaccine development though using the most resent and up to date methods that could lead to more efficient methods in diagnosis and treatment of IE. Similarly, these same approaches can be utilised to uncover target for imaging and vaccine development for other species biofilms particularly those associated with colonisation of indwelling medical devices.

References

ABOSHKIWA, M., AL-ANI, B., COLEMAN, G. & ROWLAND, G. 1992. Cloning and physical mapping of the Staphylococcus aureus rplL, rpoB and rpoC genes, encoding ribosomal protein L7/L12 and RNA polymerase subunits and '. 138**,** 1875-1880.

ARCHER, N. K., MAZAITIS, M. J., COSTERTON, J. W., LEID, J. G., POWERS, M. E. & SHIRTLIFF, M. E. 2011. Staphylococcus aureusbiofilms. *Virulence,* 2**,** 445-459.

ARCIOLA, C. R., CAMPOCCIA, D., RAVAIOLI, S. & MONTANARO, L. 2015. Polysaccharide intercellular adhesin in biofilm: structural and regulatory aspects. *Frontiers in Cellular and Infection Microbiology,* 5.

BADDOUR, L. M., WILSON, W. R., BAYER, A. S., FOWLER, V. G., TLEYJEH, I. M., RYBAK, M. J., BARSIC, B., LOCKHART, P. B., GEWITZ, M. H., LEVISON, M. E., BOLGER, A. F., STECKELBERG, J. M., BALTIMORE, R. S., FINK, A. M., O'GARA, P. & TAUBERT, K. A. 2015. Infective Endocarditis in Adults: Diagnosis, Antimicrobial Therapy, and Management of Complications. *Circulation,* 132**,** 1435-1486.

BALABAN, N. Q., MERRIN, J., CHAIT, R., KOWALIK, L. & LEIBLER, S. 2004. Bacterial Persistence as a Phenotypic Switch. *Science,* 305**,** 1622-1625.

BALASUBRAMANIAN, D., HARPER, L., SHOPSIN, B. & TORRES, V. J. 2017. Staphylococcus aureus pathogenesis in diverse host environments. *Pathogens and Disease***,** ftx005.

BEENKEN, K. E., DUNMAN, P. M., MCALEESE, F., MACAPAGAL, D., MURPHY, E., PROJAN, S. J., BLEVINS, J. S. & SMELTZER, M. S. 2004. Global Gene Expression in Staphylococcus aureus Biofilms. *Journal of Bacteriology,* 186**,** 4665-4684.

BEGUM, A., DREBES, J., PERBANDT, M., WRENGER, C. & BETZEL, C. 2011. Purification, crystallization and preliminary X-ray diffraction analysis of the thiaminase type II from Staphylococcus aureus. *Acta crystallographica. Section F, Structural biology and crystallization communications,* 67**,** 51-53.

BENJAMINI, Y. & HOCHBERG, Y. 1995. Controlling the False Discovery Rate: A Practical and Powerful Approach to Multiple Testing. *Journal of the Royal Statistical Society. Series B (Methodological),* 57**,** 289-300.

BISCHOFF, M., ENTENZA, J. M. & GIACHINO, P. 2001. Influence of a Functional sigB Operon on the Global Regulators sar and agr in Staphylococcus aureus. 183**,** 5171-5179.

BJARNSHOLT, T. 2013. The role of bacterial biofilms in chronic infections. *APMIS,* 121**,** 1-58.

BOLES, B. R. & HORSWILL, A. R. 2008. agr-Mediated Dispersal of Staphylococcus aureus Biofilms. *PLoS Pathogens,* 4**,** e1000052.

BOLES, B. R. & SINGH, P. K. 2008. Endogenous oxidative stress produces diversity and adaptability in biofilm communities. *Proceedings of the*

National Academy of Sciences of the United States of America, 105**,** 12503-12508.
BOLGER, A. M., LOHSE, M. & USADEL, B. 2014. Trimmomatic: a flexible trimmer for Illumina sequence data. *Bioinformatics,* 30**,** 2114-2120.
BOR, D. H., WOOLHANDLER, S., NARDIN, R., BRUSCH, J. & HIMMELSTEIN, D. U. 2013. Infective endocarditis in the U.S., 1998-2009: a nationwide study. *PLoS One,* 8**,** e60033.
BRACKMAN, G., DE MEYER, L., NELIS, H. J. & COENYE, T. 2013. Biofilm inhibitory and eradicating activity of wound care products against Staphylococcus aureus and Staphylococcus epidermidis biofilms in an in vitro chronic wound model. *Journal of Applied Microbiology,* 114**,** 1833-1842.
BUNIK, V. I., TYLICKI, A. & LUKASHEV, N. V. 2013. Thiamin diphosphate-dependent enzymes: from enzymology to metabolic regulation, drug design and disease models. *FEBS Journal,* 280**,** 6412-6442.
CAHILL, T. J. & PRENDERGAST, B. D. 2016. Infective endocarditis. *Lancet,* 387**,** 882-93.
CAI, X., JIANG, Y., LIN, M., ZHANG, J., GUO, H., YANG, F., LEUNG, W. & XU, C. 2019. Ultrasound-Responsive Materials for Drug/Gene Delivery. *Front Pharmacol,* 10**,** 1650.
CAI, X., JIANG, Y., LIN, M., ZHANG, J., GUO, H., YANG, F., LEUNG, W. & XU, C. 2020. Ultrasound-Responsive Materials for Drug/Gene Delivery. *Frontiers in Pharmacology,* 10.
CESCUTTI, P., TOFFANIN, R., FETT, W. F., OSMAN, S. F., POLLESELLO, P. & PAOLETTI, S. 1998. Structural investigation of the exopolysaccharide produced by Pseudomonas flavescens strain B62 . Degradation by a fungal cellulase and isolation of the oligosaccharide repeating unit. 251**,** 971-979.
CHEN, P., ABERCROMBIE, J. J., JEFFREY, N. R. & LEUNG, K. P. 2012. An improved medium for growing Staphylococcus aureus biofilm. *J Microbiol Methods,* 90**,** 115-8.
CHEUNG, A. L., SCHMIDT, K., BATEMAN, B. & MANNA, A. C. 2001. SarS, a SarA Homolog Repressible by agr, Is an Activator of Protein A Synthesis in Staphylococcus aureus. *Infection and Immunity,* 69**,** 2448-2455.
CHEUNG, A. L. & ZHANG, G. 2002. Global regulation of virulence determinants in Staphylococcus aureus by the SarA protein family. *Front Biosci,* 7**,** d1825-42.
CHOE, W., DURGANNAVAR, T. A. & CHUNG, S. J. 2016. Fc-Binding Ligands of Immunoglobulin G: An Overview of High Affinity Proteins and Peptides. *Materials (Basel, Switzerland),* 9**,** 994.
CORBETT, D. & ROBERTS, I. S. 2008. Capsular polysaccharides in Escherichia coli. *Adv Appl Microbiol,* 65**,** 1-26.
CORRIGAN, R. M., MIAJLOVIC, H. & FOSTER, T. J. 2009. Surface proteins that promote adherence of Staphylococcus aureus to human desquamated nasal epithelial cells. *BMC microbiology,* 9**,** 22-22.
DANHORN, T., HENTZER, M., GIVSKOV, M., PARSEK, M. R. & FUQUA, C. 2004. Phosphorus Limitation Enhances Biofilm Formation of the Plant

Pathogen Agrobacterium tumefaciens through the PhoR-PhoB Regulatory System. *Journal of Bacteriology,* 186**,** 4492-4501.
DAVIDSON, A. L. & CHEN, J. 2004. ATP-Binding Cassette Transporters in Bacteria. *Annual Review of Biochemistry,* 73**,** 241-268.
DE JONG, N. W. M., VRIELING, M., GARCIA, B. L., KOOP, G., BRETTMANN, M., AERTS, P. C., RUYKEN, M., VAN STRIJP, J. A. G., HOLMES, M., HARRISON, E. M., GEISBRECHT, B. V. & ROOIJAKKERS, S. H. M. 2018. Identification of a staphylococcal complement inhibitor with broad host specificity in equidStaphylococcus aureusstrains. *Journal of Biological Chemistry,* 293**,** 4468-4477.
DEDENT, A., BAE, T., MISSIAKAS, D. M. & SCHNEEWIND, O. 2008. Signal peptides direct surface proteins to two distinct envelope locations of Staphylococcus aureus. *The EMBO Journal,* 27**,** 2656-2668.
DEL POZO, J. L. & PATEL, R. 2007. The challenge of treating biofilm-associated bacterial infections. *Clinical Pharmacology and Therapeutics,* 82**,** 204-209.
DESIMONE, D. C. & SOHAIL, M. R. 2018. Approach to Diagnosis of Cardiovascular Implantable-Electronic-Device Infection. *Journal of Clinical Microbiology,* 56.
DEVARAJ, A., BUZZO, J. R., MASHBURN-WARREN, L., GLOAG, E. S., NOVOTNY, L. A., STOODLEY, P., BAKALETZ, L. O. & GOODMAN, S. D. 2019. The extracellular DNA lattice of bacterial biofilms is structurally related to Holliday junction recombination intermediates. *Proceedings of the National Academy of Sciences,* 116**,** 25068-25077.
DOMINIECKI, M. E. & WEISS, J. 1999. Antibacterial action of extracellular mammalian group IIA phospholipase A2 against grossly clumped Staphylococcus aureus. *Infection and immunity,* 67**,** 2299-2305.
DOUDNA, J. A. & RATH, V. L. 2002. Structure and Function of the Eukaryotic Ribosome. *Cell,* 109**,** 153-156.
DOYLE, A., MCGARRY, M. P., LEE, N. A. & LEE, J. J. 2012. The construction of transgenic and gene knockout/knockin mouse models of human disease. *Transgenic research,* 21**,** 327-349.
DREBES, J., KÜNZ, M., WINDSHÜGEL, B., KIKHNEY, A. G., MÜLLER, I. B., EBERLE, R. J., OBERTHÜR, D., CANG, H., SVERGUN, D. I., PERBANDT, M., BETZEL, C. & WRENGER, C. 2016. Structure of ThiM from Vitamin B1 biosynthetic pathway of Staphylococcus aureus – Insights into a novel pro-drug approach addressing MRSA infections. *Scientific Reports,* 6**,** 22871.
DURACK, D. T., LUKES, A. S. & BRIGHT, D. K. 1994. New criteria for diagnosis of infective endocarditis: utilization of specific echocardiographic findings. Duke Endocarditis Service. *Am J Med,* 96**,** 200-9.
ETTER, D., CORTI, S., SPIRIG, S., CERNELA, N., STEPHAN, R. & JOHLER, S. 2020. Staphylococcus aureus Population Structure and Genomic Profiles in Asymptomatic Carriers in Switzerland. *Frontiers in Microbiology,* 11.

EVANGELISTA, A. 2004. Echocardiography in infective endocarditis. *Heart,* 90**,** 614-617.
FERNANDEZ GUERRERO, M. L., GONZALEZ LOPEZ, J. J., GOYENECHEA, A., FRAILE, J. & DE GORGOLAS, M. 2009. Endocarditis caused by Staphylococcus aureus: A reappraisal of the epidemiologic, clinical, and pathologic manifestations with analysis of factors determining outcome. *Medicine (Baltimore),* 88**,** 1-22.
FERNÁNDEZ, L., GONZÁLEZ, S., QUILES-PUCHALT, N., GUTIÉRREZ, D., PENADÉS, J. R., GARCÍA, P. & RODRÍGUEZ, A. 2018. Lysogenization of Staphylococcus aureus RN450 by phages ϕ11 and ϕ80α leads to the activation of the SigB regulon. *Scientific Reports,* 8.
FEY, P. D., ENDRES, J. L., YAJJALA, V. K., WIDHELM, T. J., BOISSY, R. J., BOSE, J. L. & BAYLES, K. W. 2013. A Genetic Resource for Rapid and Comprehensive Phenotype Screening of Nonessential Staphylococcus aureus Genes. *mBio,* 4**,** e00537-12-e00537.
FITZPATRICK, F., HUMPHREYS, H. & O'GARA, J. P. 2005. Evidence for icaADBC-independent biofilm development mechanism in methicillin-resistant Staphylococcus aureus clinical isolates. *Journal of clinical microbiology,* 43**,** 1973-1976.
FOSTER, T. J., GEOGHEGAN, J. A., GANESH, V. K. & HÖÖK, M. 2014. Adhesion, invasion and evasion: the many functions of the surface proteins of Staphylococcus aureus. *Nature Reviews Microbiology,* 12**,** 49-62.
FRANKLIN, M. J., NIVENS, D. E., WEADGE, J. T. & HOWELL, P. L. 2011. Biosynthesis of the Pseudomonas aeruginosa Extracellular Polysaccharides, Alginate, Pel, and Psl. *Frontiers in microbiology,* 2**,** 167-167.
GAO, J. & STEWART, G. C. 2004. Regulatory elements of the Staphylococcus aureus protein A (Spa) promoter. *Journal of bacteriology,* 186**,** 3738-3748.
GAUPP, R., SCHLAG, S., LIEBEKE, M., LALK, M. & GÖTZ, F. 2010. Advantage of Upregulation of Succinate Dehydrogenase in Staphylococcus aureus Biofilms. *Journal of Bacteriology,* 192**,** 2385-2394.
GÉLINAS, M., MUSEAU, L., MILOT, A. & BEAUREGARD, P. B. 2020. Cellular adaptation and the importance of the purine biosynthesis pathway during biofilm formation in Gram-positive pathogens. Cold Spring Harbor Laboratory.
GHOSH, R., BARMAN, S. & MANDAL, N. C. 2019. Phosphate deficiency induced biofilm formation of Burkholderia on insoluble phosphate granules plays a pivotal role for maximum release of soluble phosphate. *Scientific Reports,* 9.
GIBSON, G. W., KREUSER, S. C., RILEY, J. M., ROSEBURY-SMITH, W. S., COURTNEY, C. L., JUNEAU, P. L., HOLLEMBAEK, J. M., ZHU, T., HUBAND, M. D., BRAMMER, D. W., BRIELAND, J. K. & SULAVIK, M. C. 2007. Development of a mouse model of induced Staphylococcus aureus infective endocarditis. *Comp Med,* 57**,** 563-9.
GILLASPY, A. F., WORRELL, V., ORVIS, J., ROE, B. A., DYER, D. W. & IANDOLO, J. J. 2006. The Staphylococcus aureus NCTC 8325

Genome. *Gram-Positive Pathogens, Second Edition.* American Society of Microbiology.
GONCHEVA, M. I., FLANNAGAN, R. S., STERLING, B. E., LAAKSO, H. A., FRIEDRICH, N. C., KAISER, J. C., WATSON, D. W., WILSON, C. H., SHELDON, J. R., MCGAVIN, M. J., KISER, P. K. & HEINRICHS, D. E. 2019. Stress-induced inactivation of the Staphylococcus aureus purine biosynthesis repressor leads to hypervirulence. *Nature Communications,* 10.
GONEAU, L. W., YEOH, N. S., MACDONALD, K. W., CADIEUX, P. A., BURTON, J. P., RAZVI, H. & REID, G. 2014. Selective Target Inactivation Rather than Global Metabolic Dormancy Causes Antibiotic Tolerance in Uropathogens. 58**,** 2089-2097.
GONZALEZ, C. D., LEDO, C., GIAI, C., GARÓFALO, A. & GÓMEZ, M. I. 2015. The Sbi Protein Contributes to Staphylococcus aureus Inflammatory Response during Systemic Infection. *PLoS One,* 10**,** e0131879.
GRILLO-PUERTAS, M., VILLEGAS, J. M., RINTOUL, M. R. & RAPISARDA, V. A. 2012. Polyphosphate Degradation in Stationary Phase Triggers Biofilm Formation via LuxS Quorum Sensing System in Escherichia coli. *PLoS ONE,* 7**,** e50368.
GU, H., ZHU, H. & LU, C. 2009. Use of in vivo-induced antigen technology (IVIAT) for the identification of Streptococcus suis serotype 2 in vivo-induced bacterial protein antigens. *BMC microbiology,* 9**,** 201-201.
HALL-STOODLEY, L., STOODLEY, P., KATHJU, S., HØIBY, N., MOSER, C., WILLIAM COSTERTON, J., MOTER, A. & BJARNSHOLT, T. 2012. Towards diagnostic guidelines for biofilm-associated infections. *FEMS Immunology & Medical Microbiology,* 65**,** 127-145.
HARRO, J. M., SHIRTLIFF, M. E., ARNOLD, W., KOFONOW, J. M., DAMMLING, C., ACHERMANN, Y., BRAO, K., PARVIZI, J. & LEID, J. G. 2020a. Development of a Novel and Rapid Antibody-Based Diagnostic for Chronic Staphylococcus aureus Infections Based on Biofilm Antigens. *J Clin Microbiol,* 58.
HARRO, J. M., SHIRTLIFF, M. E., ARNOLD, W., KOFONOW, J. M., DAMMLING, C., ACHERMANN, Y., BRAO, K., PARVIZI, J. & LEID, J. G. 2020b. Development of a Novel and Rapid Antibody-Based Diagnostic for Chronic Staphylococcus aureus Infections Based on Biofilm Antigens. *Journal of clinical microbiology,* 58**,** e01414-19.
HARTFORD, O. M., WANN, E. R., HOOK, M. & FOSTER, T. J. 2001. Identification of Residues in the Staphylococcus aureus Fibrinogen-binding MSCRAMM Clumping Factor A (ClfA) That Are Important for Ligand Binding. 276**,** 2466-2473.
HE, N., HU, J., LIU, H., ZHU, T., HUANG, B., WANG, X., WU, Y., WANG, W. & QU, D. 2011. Enhancement of vancomycin activity against biofilms by using ultrasound-targeted microbubble destruction. *Antimicrobial agents and chemotherapy,* 55**,** 5331-5337.
HOEN, B., ALLA, F., SELTON-SUTY, C., BÉGUINOT, I., BOUVET, A., BRIANÇON, S., CASALTA, J.-P., DANCHIN, N., DELAHAYE, F., ETIENNE, J., LE MOING, V., LEPORT, C., MAINARDI, J.-L., RUIMY, R., VANDENESCH, F. & GROUP, F. T. A. P. L. E. E. L. P. D. L. E. I.

S. 2002. Changing Profile of Infective EndocarditisResults of a 1-Year Survey in France. *JAMA,* 288**,** 75-81.
HØIBY, N., BJARNSHOLT, T., MOSER, C., BASSI, G. L., COENYE, T., DONELLI, G., HALL-STOODLEY, L., HOLÁ, V., IMBERT, C., KIRKETERP-MØLLER, K., LEBEAUX, D., OLIVER, A., ULLMANN, A. J. & WILLIAMS, C. 2015. ESCMID∗ guideline for the diagnosis and treatment of biofilm infections 2014. *Clinical Microbiology and Infection,* 21**,** S1-S25.
HORSBURGH, M. J., AISH, J. L., WHITE, I. J., SHAW, L., LITHGOW, J. K. & FOSTER, S. J. 2002. sigmaB modulates virulence determinant expression and stress resistance: characterization of a functional rsbU strain derived from Staphylococcus aureus 8325-4. *Journal of bacteriology,* 184**,** 5457-5467.
HUSSAIN, M., BECKER, K., VON EIFF, C., SCHRENZEL, J., PETERS, G. & HERRMANN, M. 2001. Identification and Characterization of a Novel 38.5-Kilodalton Cell Surface Protein of Staphylococcus aureus with Extended-Spectrum Binding Activity for Extracellular Matrix and Plasma Proteins. 183**,** 6778-6786.
J.F, S. & RUSSELL, D. 2001. *Molecular Cloning: A Laboratory Manual (3-Volume Set)*.
JAN-ROBLERO, J., GARCÍA-GÓMEZ, E., RODRÍGUEZ-MARTÍNEZ, S., CANCINO-DIAZ, M. E. & CANCINO-DIAZ, J. C. 2017. Surface Proteins of Staphylococcus aureus. InTech.
JENKINS, C. & BOGEMA, D. R. 2016. Factors associated with seroconversion to the major piroplasm surface protein of the bovine haemoparasite Theileria orientalis. *Parasit Vectors,* 9**,** 106.
JIN, L.-F. & LI, J.-S. 2016. Generation of genetically modified mice using CRISPR/Cas9 and haploid embryonic stem cell systems. *Dong wu xue yan jiu = Zoological research,* 37**,** 205-213.
JOHNSON, A., SONG, Q., KO FERRIGNO, P., BUENO, P. R. & DAVIS, J. J. 2012. Sensitive Affimer and Antibody Based Impedimetric Label-Free Assays for C-Reactive Protein. 84**,** 6553-6560.
JOSEFSSON, E., MCCREA, K. W., EIDHIN, D. N., O'CONNELL, D., COX, J., HOOK, M. & FOSTER, T. J. 1998. Three new members of the serine-aspartate repeat protein multigene family of Staphylococcus aureus. 144**,** 3387-3395.
KANG, D. & KIRIENKO, N. V. 2018. Interdependence between iron acquisition and biofilm formation in Pseudomonas aeruginosa. *Journal of Microbiology,* 56**,** 449-457.
KELLIHER, J. L., RADIN, J. N. & KEHL-FIE, T. E. 2018. PhoPR Contributes to Staphylococcus aureus Growth during Phosphate Starvation and Pathogenesis in an Environment-Specific Manner. *Infection and immunity,* 86**,** e00371-18.
KENNEDY, C. A. & O'GARA, J. P. 2004. Contribution of culture media and chemical properties of polystyrene tissue culture plates to biofilm development by Staphylococcus aureus. *J Med Microbiol,* 53**,** 1171-3.
KIESER, T., BIBB, M. J., BUTTNER, M. J., CHATER, K. F. & HOPWOOD, D. A. 2000. *Practical Streptomyces genetics,* Norwich, The John Innes Foundation.

KIM, H. J., LEE, H., LEE, Y., CHOI, I., KO, Y., LEE, S. & JANG, S. 2020. The ThiL enzyme is a valid antibacterial target essential for both thiamine biosynthesis and salvage pathways in Pseudomonas aeruginosa. *Journal of Biological Chemistry***,** jbc.RA120.01329.
KIM, H. K., MISSIAKAS, D. & SCHNEEWIND, O. 2014. Mouse models for infectious diseases caused by Staphylococcus aureus. *Journal of immunological methods,* 410**,** 88-99.
KIM, S., CHEN, J., CHENG, T., GINDULYTE, A., HE, J., HE, S., LI, Q., SHOEMAKER, B. A., THIESSEN, P. A., YU, B., ZASLAVSKY, L., ZHANG, J. & BOLTON, E. E. 2018. PubChem 2019 update: improved access to chemical data. *Nucleic Acids Research,* 47**,** D1102-D1109.
KIRMUSAOLU, S. 2017. MRSA and MSSA: The Mechanism of Methicillin Resistance and the Influence of Methicillin Resistance on Biofilm Phenotype of Staphylococcus aureus. InTech.
KONG, C., CHEE, C.-F., RICHTER, K., THOMAS, N., ABD. RAHMAN, N. & NATHAN, S. 2018. Suppression of Staphylococcus aureus biofilm formation and virulence by a benzimidazole derivative, UM-C162. *Scientific Reports,* 8**,** 2758.
KOSTAKIOTI, M., HADJIFRANGISKOU, M. & HULTGREN, S. J. 2013. Bacterial Biofilms: Development, Dispersal, and Therapeutic Strategies in the Dawn of the Postantibiotic Era. *Cold Spring Harbor Perspectives in Medicine,* 3.
KOUTSOUMPELI, E., TIEDE, C., MURRAY, J., TANG, A., BON, R. S., TOMLINSON, D. C. & JOHNSON, S. 2017. Antibody Mimetics for the Detection of Small Organic Compounds Using a Quartz Crystal Microbalance. 89**,** 3051-3058.
KUJUNDZIC, E., CRISTINA FONSECA, A., EVANS, E. A., PETERSON, M., GREENBERG, A. R. & HERNANDEZ, M. 2007. Ultrasonic monitoring of early-stage biofilm growth on polymeric surfaces. *Journal of Microbiological Methods,* 68**,** 458-467.
KUKURBA, K. R. & MONTGOMERY, S. B. 2015. RNA Sequencing and Analysis. *Cold Spring Harbor Protocols,* 2015**,** pdb.top084970.
KWIECINSKI, J., JIN, T. & JOSEFSSON, E. 2014. Surface proteins of Staphylococcus aureus play an important role in experimental skin infection. *Apmis,* 122**,** 1240-50.
KYLVÄJÄ, R., OJALEHTO, T., KAINULAINEN, V., VIRKOLA, R. & WESTERLUND-WIKSTRÖM, B. 2016. Penicillin binding protein 3 of Staphylococcus aureus NCTC 8325-4 binds and activates human plasminogen. *BMC Research Notes,* 9.
LADE, H., PARK, J. H., CHUNG, S. H., KIM, I. H., KIM, J.-M., JOO, H.-S. & KIM, J.-S. 2019. Biofilm Formation by Staphylococcus aureus Clinical Isolates is Differentially Affected by Glucose and Sodium Chloride Supplemented Culture Media. *Journal of clinical medicine,* 8**,** 1853.
LAI, Y. 2017. A statistical method for the conservative adjustment of false discovery rate (q-value). *BMC Bioinformatics,* 18**,** 69.
LANGMEAD, B. & SALZBERG, S. L. 2012. Fast gapped-read alignment with Bowtie 2. *Nat Methods,* 9**,** 357-9.
LEE, K.-M., GO, J., YOON, M. Y., PARK, Y., KIM, S. C., YONG, D. E. & YOON, S. S. 2012. Vitamin B12-Mediated Restoration of Defective

Anaerobic Growth Leads to Reduced Biofilm Formation in Pseudomonas aeruginosa. *Infection and Immunity,* 80**,** 1639-1649.
LEE, W. Y., LI, N., LIN, S., WANG, B., LAN, H. Y. & LI, G. 2016. miRNA-29b improves bone healing in mouse fracture model. *Molecular and Cellular Endocrinology,* 430**,** 97-107.
ŁESKI, T. A. & TOMASZ, A. 2005. Role of penicillin-binding protein 2 (PBP2) in the antibiotic susceptibility and cell wall cross-linking of Staphylococcus aureus: evidence for the cooperative functioning of PBP2, PBP4, and PBP2A. *Journal of bacteriology,* 187**,** 1815-1824.
LEWIS, K. 2007. Persister cells, dormancy and infectious disease. *Nature Reviews Microbiology,* 5**,** 48-56.
LEWIS, K. 2010. Persister cells. *Annu Rev Microbiol,* 64**,** 357-72.
LIESMAN, R. M., PRITT, B. S., MALESZEWSKI, J. J. & PATEL, R. 2017. Laboratory Diagnosis of Infective Endocarditis. *Journal of Clinical Microbiology,* 55**,** 2599-2608.
LIN, M.-H., SHU, J.-C., HUANG, H.-Y. & CHENG, Y.-C. 2012. Involvement of Iron in Biofilm Formation by Staphylococcus aureus. *PLoS ONE,* 7**,** e34388.
LINDNER, J. R. 2004. Microbubbles in medical imaging: current applications and future directions. *Nature Reviews Drug Discovery,* 3**,** 527-533.
LISTER, J. L. & HORSWILL, A. R. 2014. Staphylococcus aureus biofilms: recent developments in biofilm dispersal. *Frontiers in Cellular and Infection Microbiology,* 4.
LOISELLE, M. & ANDERSON, K. W. 2003. The Use of Cellulase in Inhibiting Biofilm Formation from Organisms Commonly Found on Medical Implants. *Biofouling,* 19**,** 77-85.
LOPATA, A., HUGHES, R., TIEDE, C., HEISSLER, S. M., SELLERS, J. R., KNIGHT, P. J., TOMLINSON, D. & PECKHAM, M. 2018. Affimer proteins for F-actin: novel affinity reagents that label F-actin in live and fixed cells. *Scientific Reports,* 8.
LOSS, G., SIMÕES, P. M., VALOUR, F., CORTÊS, M. F., GONZAGA, L., BERGOT, M., TROUILLET-ASSANT, S., JOSSE, J., DIOT, A., RICCI, E., VASCONCELOS, A. T. & LAURENT, F. 2019. Staphylococcus aureus Small Colony Variants (SCVs): News From a Chronic Prosthetic Joint Infection. *Frontiers in Cellular and Infection Microbiology,* 9.
LOVE, M. I., HUBER, W. & ANDERS, S. 2014. Moderated estimation of fold change and dispersion for RNA-seq data with DESeq2. *Genome Biology,* 15.
MÄDER, U., NICOLAS, P., DEPKE, M., PANÉ-FARRÉ, J., DEBARBOUILLE, M., VAN DER KOOI-POL, M. M., GUÉRIN, C., DÉROZIER, S., HIRON, A., JARMER, H., LEDUC, A., MICHALIK, S., REILMAN, E., SCHAFFER, M., SCHMIDT, F., BESSIÈRES, P., NOIROT, P., HECKER, M., MSADEK, T., VÖLKER, U. & VAN DIJL, J. M. 2016. Staphylococcus aureus Transcriptome Architecture: From Laboratory to Infection-Mimicking Conditions. 12**,** e1005962.
MAH, T. F. & O'TOOLE, G. A. 2001. Mechanisms of biofilm resistance to antimicrobial agents. *Trends Microbiol,* 9**,** 34-9.

MANNER, S., GOERES, D. M., SKOGMAN, M., VUORELA, P. & FALLARERO, A. 2017. Prevention of Staphylococcus aureus biofilm formation by antibiotics in 96-Microtiter Well Plates and Drip Flow Reactors: critical factors influencing outcomes. *Scientific Reports,* 7**,** 43854.

MARTIN, F. J., GOMEZ, M. I., WETZEL, D. M., MEMMI, G., O'SEAGHDHA, M., SOONG, G., SCHINDLER, C. & PRINCE, A. 2009. Staphylococcus aureus activates type I IFN signaling in mice and humans through the Xr repeated sequences of protein A.

MAZMANIAN, S. K., TON-THAT, H. & SCHNEEWIND, O. 2001. Sortase-catalysed anchoring of surface proteins to the cell wall of Staphylococcus aureus. *Molecular Microbiology,* 40**,** 1049-1057.

MOK, W. W. K. & BRYNILDSEN, M. P. 2018. Timing of DNA damage responses impacts persistence to fluoroquinolones. *Proceedings of the National Academy of Sciences***,** 201804218.

MONTANARO, L., POGGI, A., VISAI, L., RAVAIOLI, S., CAMPOCCIA, D., SPEZIALE, P. & ARCIOLA, C. R. 2011. Extracellular DNA in Biofilms. *The International Journal of Artificial Organs,* 34**,** 824-831.

MOORMEIER, D. E. & BAYLES, K. W. 2017. Staphylococcus aureusbiofilm: a complex developmental organism. *Molecular Microbiology,* 104**,** 365-376.

NAMVAR, A. E., ASGHARI, B., EZZATIFAR, F., AZIZI, G. & LARI, A. R. 2013. Detection of the intercellular adhesion gene cluster (ica) in clinical Staphylococcus aureus isolates. *GMS hygiene and infection control,* 8**,** Doc03-Doc03.

NEOPANE, P., NEPAL, H. P., SHRESTHA, R., UEHARA, O. & ABIKO, Y. 2018. In vitro biofilm formation by Staphylococcus aureus isolated from wounds of hospital-admitted patients and their association with antimicrobial resistance. *International Journal of General Medicine,* Volume 11**,** 25-32.

NHS. 2019. *National health service UK, Endocardities overview* [Online]. Available: https://www.nhs.uk/conditions/endocarditis/ [Accessed March 10 2019].

NOVICK, R. P. & GEISINGER, E. 2008. Quorum Sensing in Staphylococci. *Annual Review of Genetics,* 42**,** 541-564.

O'BRIEN, L. M., WALSH, E. J., MASSEY, R. C., PEACOCK, S. J. & FOSTER, T. J. 2002. Staphylococcus aureus clumping factor B (ClfB) promotes adherence to human type I cytokeratin 10: implications for nasal colonization. *Cellular microbiology,* 4**,** 759-770.

O'MAY, C. Y., REID, D. W. & KIROV, S. M. 2006. Anaerobic culture conditions favor biofilm-like phenotypes in Pseudomonas aeruginosa isolates from patients with cystic fibrosis. *FEMS Immunol Med Microbiol,* 48**,** 373-80.

OTTO, M. 2013. Staphylococcal Infections: Mechanisms of Biofilm Maturation and Detachment as Critical Determinants of Pathogenicity*. 64**,** 175-188.

OTTO, M. 2018. Staphylococcal Biofilms. *Microbiology spectrum,* 6**,** 10.1128/microbiolspec.GPP3-0023-2018.

PAHARIK, A. E. & HORSWILL, A. R. 2016. The Staphylococcal Biofilm: Adhesins, Regulation, and Host Response. *Microbiology spectrum,* 4**,** 10.1128/microbiolspec.VMBF-0022-2015.

PANÉ-FARRÉ, J., JONAS, B., HARDWICK, S. W., GRONAU, K., LEWIS, R. J., HECKER, M. & ENGELMANN, S. 2009. Role of RsbU in Controlling SigB Activity in Staphylococcus aureus following Alkaline Stress. *Journal of Bacteriology,* 191**,** 2561.

PANT, S., PATEL, N. J., DESHMUKH, A., GOLWALA, H., PATEL, N., BADHEKA, A., HIRSCH, G. A. & MEHTA, J. L. 2015. Trends in infective endocarditis incidence, microbiology, and valve replacement in the United States from 2000 to 2011. *J Am Coll Cardiol,* 65**,** 2070-6.

PEREIRA, M. P., D'ELIA, M. A., TROCZYNSKA, J. & BROWN, E. D. 2008. Duplication of Teichoic Acid Biosynthetic Genes in Staphylococcus aureus Leads to Functionally Redundant Poly(Ribitol Phosphate) Polymerases. 190**,** 5642-5649.

PERSHAD, K., PAVLOVIC, J. D., GRÄSLUND, S., NILSSON, P., COLWILL, K., KARATT-VELLATT, A., SCHOFIELD, D. J., DYSON, M. R., PAWSON, T., KAY, B. K. & MCCAFFERTY, J. 2010. Generating a panel of highly specific antibodies to 20 human SH2 domains by phage display. *Protein Eng Des Sel,* 23**,** 279-88.

PERTEA, M., PERTEA, G. M., ANTONESCU, C. M., CHANG, T.-C., MENDELL, J. T. & SALZBERG, S. L. 2015. StringTie enables improved reconstruction of a transcriptome from RNA-seq reads. *Nature Biotechnology,* 33**,** 290-295.

PISHCHANY, G., MCCOY, A. L., TORRES, V. J., KRAUSE, J. C., CROWE, J. E., JR., FABRY, M. E. & SKAAR, E. P. 2010. Specificity for human hemoglobin enhances Staphylococcus aureus infection. *Cell Host Microbe,* 8**,** 544-50.

PISITHKUL, T., SCHROEDER, J. W., TRUJILLO, E. A., YEESIN, P., STEVENSON, D. M., CHAIAMARIT, T., COON, J. J., WANG, J. D. & AMADOR-NOGUEZ, D. 2019. Metabolic Remodeling during Biofilm Development ofBacillus subtilis. *mBio,* 10.

QUECK, S. Y., JAMESON-LEE, M., VILLARUZ, A. E., BACH, T.-H. L., KHAN, B. A., STURDEVANT, D. E., RICKLEFS, S. M., LI, M. & OTTO, M. 2008. RNAIII-Independent Target Gene Control by the agr Quorum-Sensing System: Insight into the Evolution of Virulence Regulation in Staphylococcus aureus. *Molecular Cell,* 32**,** 150-158.

QUINN, L., BARROS, C., VITALE, S. & CASEY, E. 2019. Extraction and identification of components of the biofilm matrix in Pseudomonas species biofilms. *Access Microbiology,* 1.

REDDY, P. N., SRIRAMA, K. & DIRISALA, V. R. 2017. An Update on Clinical Burden, Diagnostic Tools, and Therapeutic Options of Staphylococcus aureus. *Infect Dis (Auckl),* 10**,** 1179916117703999.

RESCH, A., LEICHT, S., SARIC, M., PÁSZTOR, L., JAKOB, A., GÖTZ, F. & NORDHEIM, A. 2006. Comparative proteome analysis ofStaphylococcus aureus biofilm and planktonic cells and correlation with transcriptome profiling. *PROTEOMICS,* 6**,** 1867-1877.

RESCH, A., ROSENSTEIN, R., NERZ, C. & GÖTZ, F. 2005. Differential gene expression profiling of Staphylococcus aureus cultivated under biofilm and planktonic conditions. *Applied and environmental microbiology,* 71**,** 2663-2676.

RISPENS, T. & VIDARSSON, G. 2014. Chapter 9 - Human IgG Subclasses. *In:* ACKERMAN, M. E. & NIMMERJAHN, F. (eds.) *Antibody Fc.* Boston: Academic Press.

ROBINSON, J. I., BAXTER, E. W., OWEN, R. L., THOMSEN, M., TOMLINSON, D. C., WATERHOUSE, M. P., WIN, S. J., NETTLESHIP, J. E., TIEDE, C., FOSTER, R. J., OWENS, R. J., FISHWICK, C. W. G., HARRIS, S. A., GOLDMAN, A., MCPHERSON, M. J. & MORGAN, A. W. 2018. Affimer proteins inhibit immune complex binding to FcγRIIIa with high specificity through competitive and allosteric modes of action. *Proc Natl Acad Sci U S A,* 115**,** E72-e81.

ROHDE, H., KNOBLOCH, J. K., HORSTKOTTE, M. A. & MACK, D. 2001. Correlation of biofilm expression types of Staphylococcus epidermidis with polysaccharide intercellular adhesin synthesis: evidence for involvement of icaADBC genotype-independent factors. *Med Microbiol Immunol,* 190**,** 105-12.

ROLLINS, S. M., PEPPERCORN, A., HANG, L., HILLMAN, J. D., CALDERWOOD, S. B., HANDFIELD, M. & RYAN, E. T. 2005. In vivo induced antigen technology (IVIAT). *Cell Microbiol,* 7**,** 1-9.

RYDER, V. J., CHOPRA, I. & O'NEILL, A. J. 2012. Increased Mutability of Staphylococci in Biofilms as a Consequence of Oxidative Stress. *PLoS ONE,* 7**,** e47695.

SADYKOV, M. R., OLSON, M. E., HALOUSKA, S., ZHU, Y., FEY, P. D., POWERS, R. & SOMERVILLE, G. A. 2008. Tricarboxylic Acid Cycle-Dependent Regulation of Staphylococcus epidermidis Polysaccharide Intercellular Adhesin Synthesis. *Journal of Bacteriology,* 190**,** 7621-7632.

SAUSE, W. E., BALASUBRAMANIAN, D., IRNOV, I., COPIN, R., SULLIVAN, M. J., SOMMERFIELD, A., CHAN, R., DHABARIA, A., ASKENAZI, M., UEBERHEIDE, B., SHOPSIN, B., VAN BAKEL, H. & TORRES, V. J. 2019. The purine biosynthesis regulator PurR moonlights as a virulence regulator in Staphylococcus aureus. *Proceedings of the National Academy of Sciences,* 116**,** 13563-13572.

SCHWARTZ, K., SYED, A. K., STEPHENSON, R. E., RICKARD, A. H. & BOLES, B. R. 2012. Functional amyloids composed of phenol soluble modulins stabilize Staphylococcus aureus biofilms. *PLoS pathogens,* 8**,** e1002744-e1002744.

SHAFFER, C. L., ZHANG, E. W., DUDLEY, A. G., DIXON, B. R. E. A., GUCKES, K. R., BRELAND, E. J., FLOYD, K. A., CASELLA, D. P., ALGOOD, H. M. S., CLAYTON, D. B. & HADJIFRANGISKOU, M. 2017. Purine Biosynthesis Metabolically Constrains Intracellular Survival of Uropathogenic Escherichia coli. *Infection and Immunity,* 85**,** IAI.00471-16.

SHARMA, R., DEACON, S. E., NOWAK, D., GEORGE, S. E., SZYMONIK, M. P., TANG, A. A. S., TOMLINSON, D. C., DAVIES, A. G., MCPHERSON, M. J. & WÄLTI, C. 2016. Label-free electrochemical impedance biosensor to detect human interleukin-8 in serum with sub-pg/ml sensitivity. *Biosensors & bioelectronics,* 80**,** 607-613.
SHULTZ, L. D., ISHIKAWA, F. & GREINER, D. L. 2007. Humanized mice in translational biomedical research. *Nature Reviews Immunology,* 7**,** 118-130.
SIBOO, I. R., CHEUNG, A. L., BAYER, A. S. & SULLAM, P. M. 2001. Clumping factor A mediates binding of Staphylococcus aureus to human platelets. *Infection and Immunity,* 69**,** 3120-3127.
SINGH, R., RAY, P., DAS, A. & SHARMA, M. 2009. Role of persisters and small-colony variants in antibiotic resistance of planktonic and biofilm-associated Staphylococcus aureus: an in vitro study. *Journal of Medical Microbiology,* 58**,** 1067-1073.
SINGLETON, C. K. & MARTIN, P. R. 2001. Molecular mechanisms of thiamine utilization. *Curr Mol Med,* 1**,** 197-207.
SIRSI, S. & BORDEN, M. 2009. Microbubble compositions, properties and biomedical applications. *Bubble Science, Engineering & Technology,* 1**,** 3-17.
SPAAN, A. N., SUREWAARD, B. G., NIJLAND, R. & VAN STRIJP, J. A. 2013. Neutrophils versus Staphylococcus aureus: a biological tug of war. *Annu Rev Microbiol,* 67**,** 629-50.
SPEZIALE, P., PIETROCOLA, G., FOSTER, T. J. & GEOGHEGAN, J. A. 2014. Protein-based biofilm matrices in Staphylococci. *Frontiers in cellular and infection microbiology,* 4**,** 171-171.
STENBERG, E., PERSSON, B., ROOS, H. & URBANICZKY, C. 1991. Quantitative determination of surface concentration of protein with surface plasmon resonance using radiolabeled proteins. *Journal of Colloid and Interface Science,* 143**,** 513-526.
SUN, Y., DOWD, S. E., SMITH, E., RHOADS, D. D. & WOLCOTT, R. D. 2008. In vitro multispecies Lubbock chronic wound biofilm model. *Wound Repair Regen,* 16**,** 805-13.
SUNIL, M., HIEU, H. Q., ARJAN SINGH, R. S., PONNAMPALAVANAR, S., SIEW, K. S. W. & LOCH, A. 2019. Evolving trends in infective endocarditis in a developing country: a consequence of medical progress? *Annals of Clinical Microbiology and Antimicrobials,* 18**,** 43.
SZABADOS, F., TIX, H., ANDERS, A., KAASE, M., GATERMANN, S. & GEIS, G. 2012. Evaluation of species-specific score cutoff values of routinely isolated clinically relevant bacteria using a direct smear preparation for matrix-assisted laser desorption/ionization time-of-flight mass spectrometry-based bacterial identification. *European journal of clinical microbiology & infectious diseases,* 31**,** 1109-1119.
TAN, L., LI, S. R., JIANG, B., HU, X. M. & LI, S. 2018. Therapeutic Targeting of the Staphylococcus aureus Accessory Gene Regulator (agr) System. *Frontiers in Microbiology,* 9.
TIEDE, C., BEDFORD, R., HESELTINE, S. J., SMITH, G., WIJETUNGA, I., ROSS, R., ALQALLAF, D., ROBERTS, A. P., BALLS, A., CURD, A., HUGHES, R. E., MARTIN, H., NEEDHAM, S. R., ZANETTI-

DOMINGUES, L. C., SADIGH, Y., PEACOCK, T. P., TANG, A. A., GIBSON, N., KYLE, H., PLATT, G. W., INGRAM, N., TAYLOR, T., COLETTA, L. P., MANFIELD, I., KNOWLES, M., BELL, S., ESTEVES, F., MAQBOOL, A., PRASAD, R. K., DRINKHILL, M., BON, R. S., PATEL, V., GOODCHILD, S. A., MARTIN-FERNANDEZ, M., OWENS, R. J., NETTLESHIP, J. E., WEBB, M. E., HARRISON, M., LIPPIAT, J. D., PONNAMBALAM, S., PECKHAM, M., SMITH, A., FERRIGNO, P. K., JOHNSON, M., MCPHERSON, M. J. & TOMLINSON, D. C. 2017. Affimer proteins are versatile and renewable affinity reagents. *eLife,* 6.

TIEDE, C., TANG, A. A., DEACON, S. E., MANDAL, U., NETTLESHIP, J. E., OWEN, R. L., GEORGE, S. E., HARRISON, D. J., OWENS, R. J., TOMLINSON, D. C. & MCPHERSON, M. J. 2014. Adhiron: a stable and versatile peptide display scaffold for molecular recognition applications. *Protein Eng Des Sel,* 27**,** 145-55.

TOLEDO-ARANA, A., MERINO, N., VERGARA-IRIGARAY, M., DÉBARBOUILLÉ, M., PENADÉS, J. R. & LASA, I. 2005. Staphylococcus aureus Develops an Alternative, ica-Independent Biofilm in the Absence of the arlRS Two-Component System. *Journal of Bacteriology,* 187**,** 5318-5329.

TOPAN, A., CARSTINA, D., SLAVCOVICI, A., RANCEA, R., CAPALNEANU, R. & LUPSE, M. 2015. Assesment of the Duke criteria for the diagnosis of infective endocarditis after twenty-years. An analysis of 241 cases. 88**,** 321.

TORRES, V. J., PISHCHANY, G., HUMAYUN, M., SCHNEEWIND, O. & SKAAR, E. P. 2006. Staphylococcus aureus IsdB is a hemoglobin receptor required for heme iron utilization. *J Bacteriol,* 188**,** 8421-9.

TRAN, P. L., HAMMOND, A. A., MOSLEY, T., CORTEZ, J., GRAY, T., COLMER-HAMOOD, J. A., SHASHTRI, M., SPALLHOLZ, J. E., HAMOOD, A. N. & REID, T. W. 2009. Organoselenium Coating on Cellulose Inhibits the Formation of Biofilms by Pseudomonas aeruginosa and Staphylococcus aureus. *Applied and Environmental Microbiology,* 75**,** 3586-3592.

VAISH, M., PRICE-WHELAN, A., REYES-ROBLES, T., LIU, J., JEREEN, A., CHRISTIE, S., ALONZO, F., 3RD, BENSON, M. A., TORRES, V. J. & KRULWICH, T. A. 2018. Roles of Staphylococcus aureus Mnh1 and Mnh2 Antiporters in Salt Tolerance, Alkali Tolerance, and Pathogenesis. *Journal of bacteriology,* 200**,** e00611-17.

VAZQUEZ-LOMBARDI, R., PHAN, T. G., ZIMMERMANN, C., LOWE, D., JERMUTUS, L. & CHRIST, D. 2015. Challenges and opportunities for non-antibody scaffold drugs. *Drug Discovery Today,* 20**,** 1271-1283.

VISANSIRIKUL, S., KOLODZIEJ, S. A. & DEMCHENKO, A. V. 2020. Staphylococcus aureus capsular polysaccharides: a structural and synthetic perspective. *Organic & Biomolecular Chemistry*.

VOYICH, J. M., BRAUGHTON, K. R., STURDEVANT, D. E., WHITNEY, A. R., SAÏD-SALIM, B., PORCELLA, S. F., LONG, R. D., DORWARD, D. W., GARDNER, D. J., KREISWIRTH, B. N., MUSSER, J. M. & DELEO, F. R. 2005. Insights into Mechanisms Used by

Staphylococcus aureus to Avoid Destruction by Human Neutrophils. *The Journal of Immunology,* 175**,** 3907-3919.
WANG, L. 2004. Genome-wide operon prediction in Staphylococcus aureus. *Nucleic Acids Research,* 32**,** 3689-3702.
WANN, E. R., GURUSIDDAPPA, S. & HÖÖK, M. 2000. The Fibronectin-binding MSCRAMM FnbpA ofStaphylococcus aureusIs a Bifunctional Protein That Also Binds to Fibrinogen. *Journal of Biological Chemistry,* 275**,** 13863-13871.
WIJESINGHE, G., DILHARI, A., GAYANI, B., KOTTEGODA, N., SAMARANAYAKE, L. & WEERASEKERA, M. 2019. Influence of Laboratory Culture Media on in vitro Growth, Adhesion, and Biofilm Formation of Pseudomonas aeruginosa and Staphylococcus aureus. *Medical Principles and Practice,* 28**,** 28-35.
WILES, S., HANAGE, W. P., FRANKEL, G. & ROBERTSON, B. 2006. Modelling infectious disease - time to think outside the box? *Nat Rev Microbiol,* 4**,** 307-12.
WILLIS, L. M. & WHITFIELD, C. 2013. Structure, biosynthesis, and function of bacterial capsular polysaccharides synthesized by ABC transporter-dependent pathways. *Carbohydrate Research,* 378**,** 35-44.
WILMAERTS, D., WINDELS, E. M., VERSTRAETEN, N. & MICHIELS, J. 2019. General Mechanisms Leading to Persister Formation and Awakening. *Trends Genet,* 35**,** 401-411.
YAN, J., HAN, D., LIU, C., GAO, Y., LI, D., LIU, Y. & YANG, G. 2017. Staphylococcus aureus VraX specifically inhibits the classical pathway of complement by binding to C1q. *Molecular Immunology,* 88**,** 38-44.
YANG, L., BISWAS, M. E. & CHEN, P. 2003. Study of binding between protein a and Immunoglobulin G using a surface tension probe. *Biophysical Journal,* 84**,** 509-522.
YARWOOD, J. M. & SCHLIEVERT, P. M. 2003. Quorum sensing in Staphylococcus infections. 112**,** 1620-1625.
YEE, R., CUI, P., SHI, W., FENG, J. & ZHANG, Y. 2015. Genetic Screen Reveals the Role of Purine Metabolism in Staphylococcus aureus Persistence to Rifampicin. *Antibiotics (Basel, Switzerland),* 4**,** 627-642.
YOSHIOKA, S. & NEWELL, P. D. 2016. Disruption of de novo purine biosynthesis in Pseudomonas fluorescens Pf0-1 leads to reduced biofilm formation and a reduction in cell size of surface-attached but not planktonic cells. 4**,** e1543.
YUYAMA, K. T., ROHDE, M., MOLINARI, G., STADLER, M. & ABRAHAM, W.-R. 2020. Unsaturated Fatty Acids Control Biofilm Formation of Staphylococcus aureus and Other Gram-Positive Bacteria. *Antibiotics,* 9**,** 788.
ZHANG, Y. 2014. Persisters, persistent infections and the Yin-Yang model. *Emerging microbes & infections,* 3**,** e3-e3.
ZHAO, W., HE, X., HOADLEY, K. A., PARKER, J. S., HAYES, D. & PEROU, C. M. 2014. Comparison of RNA-Seq by poly (A) capture, ribosomal

RNA depletion, and DNA microarray for expression profiling. *BMC Genomics,* 15**,** 419.
ZHU, Q., WEN, W., WANG, W. & SUN, B. 2019. Transcriptional regulation of virulence factors Spa and ClfB by the SpoVG-Rot cascade in Staphylococcus aureus. *International Journal of Medical Microbiology,* 309**,** 39-53.
ZHURAUSKI, P., ARYA, S., JOLLY, P., TIEDE, C., TOMLINSON, D., KO FERRIGNO, P. & ESTRELA, P. 2018. Sensitive and selective Affimer-functionalised interdigitated electrode-based capacitive biosensor for Her4 protein tumour biomarker detection. *Biosensors and Bioelectronics,* 108.